

Chemical Engineering Report Series

Kemian laitetekniikan raporttisarja

Espoo 2010

No. 56

FROM EUCALYPT FIBER DISTRIBUTIONS TO TECHNICAL PROPERTIES OF PAPER

Iiro Pulkkinen

Chemical Engineering Report Series
Kemian laitetekniikan raporttisarja
Espoo 2010

No. 56

FROM EUCALYPT FIBER DISTRIBUTIONS TO TECHNICAL PROPERTIES OF PAPER

Iiro Pulkkinen

Doctoral dissertation for the degree of Doctor of Science in Technology to be presented with due permission of the Faculty of Chemistry and Materials Sciences for public examination and debate in Auditorium KE2 (Komppa Auditorium) at the Aalto University School of Science and Technology (Espoo, Finland) on the 17th of September 2010 at 12 noon.

Aalto University
School of Science and Technology
Faculty of Chemistry and Material Sciences
Department of Biotechnology and Chemical Technology

Aalto-yliopisto
Teknillinen korkeakoulu
Kemian ja materiaalitieteiden tiedekunta
Biotekniikan ja kemian tekniikan laitos

Distribution:
Aalto University
School of Science and Technology
Chemical Engineering
P. O. Box 16100
FI-00076 AALTO
Tel. + 358-9-4702 2634
Fax. +358-9-4702 2694
E-mail: iiro.pulkkinen@tkk.fi

© Iiro Pulkkinen

ISBN 978-952-60-3290-0
ISSN 1236-875X

Multiprint Oy
Espoo 2010

"Las batallas de la vida no siempre favorece al hombre más fuerte o al más rápido, pero tarde o temprano el hombre que gana es el hombre que PIENSA QUE PUEDE!"

ABSTRACT

The objective of this thesis was to examine interfiber bonding and fiber segment activation as basic phenomena: how different raw material parameters and fiber property distributions affect bonding and activation, and in turn, how bonding and activation relate to end use properties of paper, especially to strength, structural and hygroexpansional properties. The raw materials for this study consisted of eucalypt fibers.

The findings of this thesis work confirm what has already been established about bonding: raw material parameters, fiber treatments and process parameters all play a significant role in bonding and bonding development. A new observation was the interdependence of interfiber bonding and fiber network activation for structural and strength properties and the link observed between hygroexpansion and fiber network activation.

Fiber size analyses were made with an optical analyzer that applies image analysis techniques on single fibers. The effects of fiber length, fiber width, fiber wall thickness, fines content and fiber curl distributions on the quality potential of eucalypt fibers were evaluated. The results of this work improved the understanding of the effects of fiber property distribution characteristics on paper technical properties.

Fiber curl and fiber wall thickness were found to be the most promising fiber parameters in the evaluation of eucalypt fiber quality potential. In the development of parameters derived from fiber property distributions, the variations in paper technical properties were most often explained with fiber curl and fiber wall thickness.

In addition to metafiber properties developed during this study (wet pressed density and activation parameter), more explicatory power was sought from the structure of fiber wall by means of simple water retention value and fiber saturation point measurements, differential scanning calorimetry, and by using solid-state cross-polarization/magic angle spinning (CP/MAS) ¹³C nuclear magnetic resonance measurements.

TIIVISTELMÄ

Tämän väitöskirjan tavoitteena oli tarkastella sitoutumista ja aktivaatiota paperin perusilmiönä: kuinka erilaiset raaka-aineparametrit ja raaka-aineen ominaisuusjakaumat vaikuttavat niihin ja kuinka niiden avulla voidaan ennustaa paperin loppuominaisuuksia, erityisesti lujuus- ja rakenneominaisuuksia sekä paperin kosteuslaajenemaa. Kuituraaka-aineena tässä työssä käytettiin eukalyptuskuituja.

Väitöskirjatyön tulokset vahvistavat käsityksiä kuitujen sitoutumisesta: raaka-aineparametrit, kuitujen käsittely sekä prosessimuuttujat vaikuttavat kaikki sitoutumiseen ja sen kehittymiseen. Uutena havaintona esitettiin teoria kuitujen välisen sitoutumisen ja kuituverkoston aktivaation keskinäiselle riippuvuussuhteelle lujuus- ja rakenneparametreille, sekä kuituverkoston aktivaation liittäminen myös paperin kosteuslaajenemaan.

Kuidunkokoanalyysit tehtiin konenäköä soveltavalla, yksittäisiä kuituja mittaavalla laitteella. Tutkimuksessa selvitettiin kuidunpituuden, kuidun leveyden, seinämävahvuuden, hienoaineen, ja kuidun kiharuuden jakaumien vaikutusta eukalyptuskuidusta valmistetun paperin laatuun. Työn tuloksena selvitettiin esimerkiksi kuidun jakaumaparametrien tuottama lisäarvo pelkkien keskiarvotulosten tarkastelun sijaan.

Konenäköön perustuvan kuituanalysointilaitteen antamista tuloksista kuidun kiharus ja kuidun seinämävahvuus osoittautuivat luotettavimmiksi eukalyptuksen laatupotentiaalin indikaattoreiksi. Kuitujen sitoutumista ja kuituverkoston aktivaatiota kuvaavia parametreja kehittäessä näiden jakaumat selittivätkin suurimman osan paperitekniikan ominaisuuksien vaihtelusta.

Tutkimuksessa kehitettyjen metakuituominaisuuksien (märkäpuristettu tiheys ja aktivaatioparametri) lisäksi kuituseinämän rakenteesta haettiin selitysvoimaa tukeutuen kuitujen vedenpoisto- ja saturaatiopistemittauksiin ja differentiaaliseen pyyhkäisykalorimetriaan, sekä käyttäen kiinteän aineen ydinmagneettisen resonanssin mittauksia.

PREFACE

This thesis work was carried out at Aalto University School of Science and Technology (TKK) in the research group of Chemical Engineering during 2005-2009. The work was funded by Oy Metsä-Botnia Ab.

I would like to thank all the people that have helped and supported me during my postgraduate studies and thesis work:

Docent Juhani Aittamaa and D.Sc. (Tech.) Kari Ala-Kaila, for giving me the opportunity to work with this fascinating subject and for their advice and encouragement in supervising the early parts of my thesis work. Professor Ville Alopaeus supervised me through the rest of this thesis work with youthful enthusiasm and deserves a big thank you. The instructor of my thesis, D.Sc. (Tech.) Juha Fiskari is acknowledged for his expertise in the field of pulp industry, for his valuable comments and advices, and for his contagious laughter. Co-author Stefan Antonsson is acknowledged for his input on my thesis. The researchers at the Universidade Federal de Viçosa are acknowledged for their inspiring and beautiful company during my few short but memorable visits to Brazil, while introducing me to the world of eucalypt.

All my research colleagues and the technical personnel at the Laboratory of Chemical Engineering: without them this work would have been much more difficult to conduct. A special Thank You should go to all of you who think my behavior has been too unorthodox for engineering purposes and still have managed to live through all my quirks.

The same story continues after this thesis work. All that needs to be done (wherever it may be) will be done with the enthusiasm and creativity of a small child (unfortunately trapped in a body that will get older). This makes me a great future candidate for upper level management positions.

Espoo, September 2010

LIST OF PUBLICATIONS

This thesis consists of a summary part and of seven individual scientific articles. The papers are denoted with Roman numbers I-VII and are quoted accordingly in the summary part.

- [I] **Pulkkinen, I.; Ala-Kaila, K.; Aittamaa, J. (2006).** Characterization of wood fibers using fiber property distributions. *Chemical Engineering and Processing* **45**(7): 546-554.
- [II] **Pulkkinen, I.; Fiskari, J.; Aittamaa, J. (2007).** The effect of refining on fiber transverse dimension distributions of eucalyptus pulp species. *O Papel* **68**(5):58- 66.
- [III] **Pulkkinen, I.; Fiskari, J.; Joutsimo, O; Alopaeus, V. (2008b).** The use of fiber wall thickness data to predict handsheet properties of eucalypt pulp fibers. *O Papel* **69**(10): 71-85.
- [IV] **Pulkkinen, I.; Fiskari, J.; Alopaeus, V. (2009a).** The effect of hardwood fiber morphology on the hygroexpansivity of paper. *BioResources* **4**(1):126-141.
- [V] **Pulkkinen, I.; Fiskari, J.; Alopaeus, V. (2009b).** The effect of sample size and shape on the hygroexpansion coefficient - A study made with advanced methods for hygroexpansion measurement. *Tappsa J.* (March): 26-33.
- [VI] **Pulkkinen, I.; Fiskari, J.; Alopaeus, V. (2010).** New model for tensile strength and density of eucalyptus hand sheets - An activation parameter based on fiber distribution characteristics. *Holzforschung* **64**(2):201-209.
- [VII] **Pulkkinen, I.; Fiskari, J.; Alopaeus, V. (2009c).** CPMAS ¹³C NMR Analysis and Differential Scanning Calorimetry of Fully Bleached Eucalypt Pulp Samples: Links to hand sheet hygroexpansivity and strength properties. *Journal of Applied Sciences* **9**(22):1-8.
- [VIII] **Antonsson, S.; Pulkkinen, I.; Fiskari, J.; Lindström, M.E.; Karlström, K. (2010).** The relationship between hygroexpansion, tensile stiffness, and mechano-sorptive creep in bleached hardwood kraft pulp samples. *Appita J.* **63**(3):225,231-234.

The research papers are included as appendices in the printed version of this thesis.

AUTHOR'S CONTRIBUTION

- [I]** The author wrote the paper, made the simulations and analysed the results.
- [II]** The author wrote the paper, made the simulations and analysed the results.
- [III]** The author wrote the paper, made the correlations and analysed the results.
- [IV]** The author wrote the paper, made the correlations and analysed the results.
- [V]** The author wrote the paper, made the correlations and analysed the results.
- [VI]** The author wrote the paper, made the simulations and analysed the results.
- [VII]** The author wrote the paper, made the correlations and analysed the results.
- [VIII]** The handling of experimental data, contribution to the results and contribution to conclusions part of the first version. The author wrote 25% of the second version of the paper and contributed to the analysis of the results.

1 INTRODUCTION.....	2
1.1 Background.....	2
1.2 Objectives.....	2
1.3 Structure of the thesis.....	3
2 INDIVIDUAL FIBER PROPERTIES RELATED TO BONDING	5
2.1 Ultrastructure of fibers	6
2.1.1 Cellulose I ^α and I ^β	7
2.1.2 Crystallinity index	8
2.1.3 Hemicelluloses	9
2.1.4 Microfibril angle.....	9
2.1.5 Fiber wall pore volume and structure	10
2.2 Fiber defects.....	11
2.3 Fiber dimension distributions	11
2.4 Industrial processes affecting fiber properties	12
2.4.1 Refining.....	12
2.4.2 Wet pressing	13
2.4.3 Drying	13
3 FIBER-TO-FIBER BONDING AND NETWORK PROPERTIES	14
3.1 Hygroexpansivity and mechanosorptive creep.....	14
3.2 Tensile strength.....	15
4 MATERIALS AND METHODS	18
4.1 Pulp samples and sample preparation	18
4.2 Measurement of the ultra-structure of the fiber wall.....	19
4.2.1 (CP/MAS) ¹³ C NMR.....	19
4.2.2 SilviScan®.....	20
4.3 Methods to characterize fiber-water interactions	20
4.3.1 Water retention value.....	20
4.3.2 Fiber saturation point	21
4.3.3 Differential scanning calorimetry	21
4.4 FiberLab® analyzer	21
4.5 SEM.....	23
4.6 Hygroexpansivity measurements	24
4.6.1 OPTIDIM hygroexpansivity measurement apparatus (IV, V).....	24
4.6.2 Laser measurement apparatus (V, VIII).....	25
4.6.3 The Creep Measurements (VIII)	25
5 MATHEMATICAL ANALYSIS	26
5.1 Calculation of distribution moments	26
5.2 Weighting of distributions.....	26
5.3 Statistical analysis.....	28
5.3.1 Correlation analysis	28
5.3.2 Factor analysis.....	28
5.4 The wet-pressed density	28
5.5 The activation parameter	29
6 RESULTS	32
6.1 Changes in distributions induced by refining (II)	32
6.2 The drying shrinkage and cell wall thickness (III, VI).....	34
6.3 Correlations between variables (III).....	34
6.4 Principal Component Analysis and Factor Analysis (VI).....	36
6.5 Parameters developed (III, VI)	37
6.5.1 Wet-pressed density and paper technical properties (III)	37

6.5.2 Activation parameter and paper technical properties (VI).....	39
6.6 Dimensional stability (IV, V, VIII)	43
6.6.1 The effect of fiber transverse dimension distributions on hygroexpansivity (IV)	43
6.6.2 Laser measurement and OPTIDIM apparatus.....	46
6.6.3 The effect of sample size measured with the OPTIDIM apparatus.....	49
6.7 Mechanosorptive creep (VIII).....	49
6.8 Raw material and fiber network parameters affecting hygroexpansivity and mechano-sorptive creep	51
6.9 Changes in fiber wall thickness distributions due to moisture	52
6.10 The degree of crystallinity and handsheet properties (VII)	54
6.11 Pore size distribution measurements: links to hygroexpansion and activation (VII).....	57
7 OPTIMAL FIBER DISTRIBUTION AND PAPER PROPERTIES (I-VIII).....	60
8 CONCLUSIONS	62
LIST OF ABBREVIATIONS AND SYMBOLS	64
REFERENCES.....	65
ERRATA	75

1 INTRODUCTION

1.1 Background

Wood and fiber raw material with uniform, suitable and predictable properties are very important for competitive production of pulp and paper. More recently, chemical pulp fiber potential for commercial use has been evaluated based on the mean values of the evaluated properties, e.g. fiber dimensions (fiber length, fiber wall thickness etc.) or other morphological factors (micro fibril angle, internal fibrillation, external fibrillation, fiber curl, chemical composition etc.) for both hardwoods and softwoods (Htun and de Ruvo 1978; Mohlin and Hornatowska 2006; Paavilainen 1989, 2000; Retulainen et al. 1998; Santos et al. 2006; Wimmer et al. 2002). These all have an affect on how paper properties develop. Single fiber strength is considered to be very important to paper and paperboard strength (Van Den Akker et al. 1958). Also fibers' abilities to swell and form inter-fiber bonds are important for the strength of paper and paperboard. There is still a lot of information, readily obtainable with the off-line fiber analysers that are not used in full potential. Fiber property distributions with similar mean values can have other fiber characteristics that vary considerably. This can be a major factor contributing to structural- and strength properties of ready-made paper or packaging product.

The mechanical properties of paper, and the strength of the fiber network, have been thought to arise from inter-fiber bonding- the strength of individual bonds and all the bonds within the fiber network--and from the axial strength of individual papermaking fibers (Retulainen et al. 1998). The models to predict strength of paper are normally based on both, individual fiber strength and inter-fiber bond strength. The same applies to hygroexpansion of the paper, although in this case, the hygroexpansivity of fiber network is mainly controlled by the transverse shrinkage of the fibers.

Nowadays the paper machines are running record speeds, requiring paper webs to be increasingly stronger. At the same time, paper makers want their paper to have high bulk and still meet the strength requirements. This is only possible, if the process is optimized. High bulk results in easier water removal and good bonding ability and high network activation results in higher tensile strengths.

Because of this delicate relationship, it is crucial to understand the interactions between different pulp fibers and the role of different factors that may have an influence on paper properties. With eucalypt fibers, or hardwood fibers in general, fiber length does not determine the structural and strength properties of paper. More emphasis was placed on studying the transverse dimension distributions of the fibers and the structure of fiber wall as their importance on handsheet properties of softwoods and hardwoods have been suggested in several studies. The geometrical shape of the fiber also has to be considered as it is an important factor for fiber network activation.

The starting point of this study was to investigate, if analyser based information can be used to gain additional information for quality control and provoke ideas on how to improve the on-line quality control. The relevant information was screened by investigating fiber size and shape parameters and distribution together with the structural features obtained with the analysis of fiber ultra-structure and sheet cross-sections.

1.2 Objectives

This thesis work was started with a clear goal of investigating various fiber property distributions and their links to phenomena affecting sheet structure, strength and hygroexpansion. The objective of all this was to gain an understanding of an "optimal" fiber distributions for a given end use. As the starting point of this Thesis work, fiber property distributions were taken as the most significant factor for the development of tensile, hygroexpansional and structural properties. By utilizing this approach, new parameters were sought to describe fiber bonding and network activation and which could be used to describe the effects of fiber properties in a clear and logical way, by offering means to apply them also in the case of real paper furnishes.

A simplified chart of the factors affecting paper properties, shown in Figure 1, was used as a starting point for this work. It shows the paper properties concerned, including strength-, structural- and hygroexpansional properties.

In addition to “metafiber” properties developed during this study (wet pressed density and activation parameter), more explicated power was sought from the structure of fiber wall by the means of simple water retention value (WRV), fiber saturation point (FSP) measurements and differential scanning calorimetry (DSC) to characterise fiber-water interactions, X-ray diffractometer to determine the microfibril angle (MFA), and solid-state cross-polarization/magic angle spinning (CP/MAS) ¹³C nuclear magnetic resonance (NMR) measurements to determine the fiber ultrastructure.

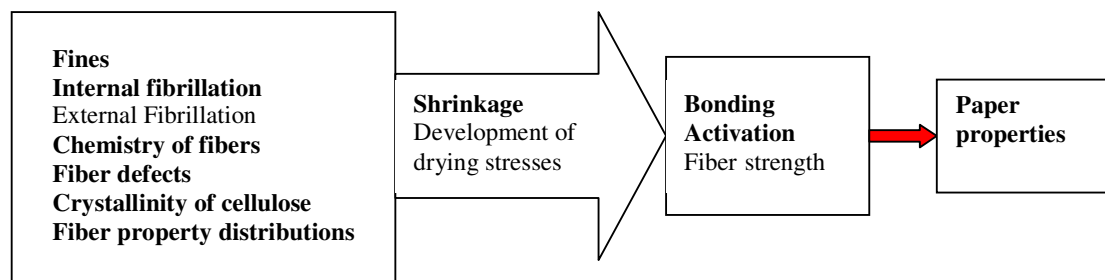


Figure 1. The factors affecting paper properties. Properties studied in this work are marked as darker text.

When the objective is the optimal and homogeneous quality of the product a huge amount of information is needed of the properties of fibers and fiber suspensions. This information is already available in the form of the measurement results of modern fiber analysers. The most common way of expressing the results is to use mean values, even though most of the time furnish consist of various distributions of properties that are sometimes very heterogeneous. In this study, the fiber property distributions were investigated and analysed in order to include all the fibers inside a given distribution. A proper analysis of the distributions give more tools to improve the quality potential of a given pulp mixture.

Combining the information obtained with the measurements of individual fibers and fiber mixtures including fiber dimension and shape (curl) distributions, chemical and structural features of fibers, together with the use of proper statistical tools, give valuable information concerning raw material choices for different end-use purposes.

1.3 Structure of the thesis

The results are reviewed critically and discussed in relation to other published papers, keeping in mind the above hypothesis and objective.

Chapter 2 contains a short survey of what is known about the use of fiber property distributions as predictors of paper technical properties and how activation of the paper is affected by distributions. It also examines all the raw material variables that affect this phenomenon. Chapter 3 contains a brief introduction to investigated raw material dependent network properties, hygroexpansion and mechano-sorptive creep and tensile strength. Chapter 4 describes the raw materials, their treatment and the experimental methods used in this study. The measurement of hygroexpansion is described in detail, together with the calculation of parameters used to characterize paper technical properties.

Chapter 5 presents the mathematical distributions and tools used throughout this Thesis, including an introduction to new parameters used to describe the bonding and activation potential.

The results of this work are presented in Chapter 6, starting from the examination of the changes in distributions when fibers are refined (6.1). The study progress in to explaining paper technical properties and hygroexpansion based on parameters (activation parameter and wet-pressed apparent density) created

based on FiberLab measurement data and their distributions: fiber wall thickness as a predictor of paper technical properties (6.5), activation coefficient as a predictor of strength properties and hand sheet density (6.5) and the effect of fiber wall thickness on hygroexpansion (6.6). Comparison between two alternative methods to characterize hygroexpansion used in this study was made in Chapter 6.6. Effect of fiber parameters and hygroexpansion on mechano-sorptive creep is presented in Chapter 6.7. The supermolecular structure of the fiber wall was characterized with (CP/MAS) ^{13}C NMR to link the ultrastructural features of fiber wall to fiber network properties (Chapter 6.10). Chapter 6.11 discusses the effect of pore size (measured with DSC) on fiber ultrastructure and fiber network properties. The rest of the Thesis concentrates on summing up the properties and property distributions which are most important in determining the quality of an end-use product (Chapter 7).

2 INDIVIDUAL FIBER PROPERTIES RELATED TO BONDING

The aim of sample characterization, whether laboratory-made un-dried *E. grandis* clone samples (II, V) or mill made once-dried ECF bleached commercial grade samples (I,II,IV,VI-VIII) were involved was the same. To determine the most important raw material factors affecting fiber-to-fiber bonding and network activation. The basic analyses throughout the study were performed with FiberLab® analyzer that utilizes measurement principles and analytics make it an excellent choice for rapid measurement of fiber property distributions. Individual fiber structure was characterized with (CP/MAS) ¹³C nuclear magnetic resonance measurements. The ultrastructure of fibers affects a range of network properties (e.g. strength and hygroexpansion) due to the characteristics of xylan/cellulose-matrix. In this Thesis, evidence supporting a linkage between the ultrastructural properties of fibers and fiber analyzer results was also found. This is convincing evidence that encourage the use of fiber property distributions in handsheet property simulations. Mechanical properties of pulps are usually evaluated by measurements on handsheets made in a standardized way from pulps beaten to different degrees in a laboratory refiner. Most handsheet properties depend on several factors, which complicate the evaluation of differences in fiber properties between different pulp grades or types. In the following sections, the relations between the fiber properties and handsheet properties are discussed.

Fiber-to-fiber bonding:

Not only fiber strength but also bonding strength between fibers is important and the mechanical properties of fibers in a network are therefore related to inter-fiber bonds (Retulainen 1997; Retulainen et al. 1998). Dependent of the paper property investigated, whether tensile strength or dimensional stability of the paper under changing humidity conditions, the basic principle remains the same. During the drying process, fibers shrink laterally, causing shear stresses in the bonded area, originating from the anisotropic shrinkage of fibers in lateral and longitudinal direction. The amount of shrinkage depends on the swelling degree of the wet fiber wall, which in turn is affected by the internal fibrillation and chemical composition of the fiber wall. Shrinkage stresses generate axial compressive forces on the crossing fibers and may cause deformations in bonded fiber segments also with sheets dried in restraint.

The structure of inter-fiber bonds is influenced by refining, wet-pressing and drying. Material parameters that influence bond structure include, for example, fiber morphology, pulping procedure and drying of the sheets. As the specific bond strength cannot be reliably measured from paper, rapid and simple methods to characterize fiber-to-fiber bonding have to be applied. The bonding potential of fibers was characterized with WRV. Effect of fiber dimensions on bonding of the eucalypt handsheets was studied with scanning electron microscope (SEM) at varying humidity conditions. The effect of microscopic properties of fibers on fiber-to-fiber bonding, i.e. fibrils and fibril aggregates on strength and hygroexpansional properties were studied with (CP/MAS) ¹³C nuclear magnetic resonance (NMR).

Activation:

Activation is one of the relevant properties of fibers within a network. Activation means that originally kinky, curly or otherwise deformed fiber segments, unable to carry load in the network, can be modified into active components of the network. Activation of the network occurs during drying, when lateral shrinkage of fibers is transmitted to axial shrinkage of the neighboring fibers at bonded areas. If drying is restrained, the free segments dry under stress and are therefore removed of their slackness (Giertz 1964; Giertz and Roedland 1979). The level of slackness removal depends on numerous things. For example good inter-fiber bonding is a prerequisite for activation. The amount of drying stress needed to activate free fiber segments depends on the morphology of the fibers (Retulainen 1997). This makes the accurate and reliable characterization of fiber dimension distributions and fiber curl very important. In this thesis, fiber network activation on a macro scale has been studied by using an activation coefficient model consisting of fiber wall thickness- and fiber curl distributions (to describe the activation potential of a given furnace), and of WRV to describe the shrinkage potential of the fibers. The ultra structure of fibers is also important as the activation of free segments may increase the structural order of cellulose and hemicelluloses inside the fibrils and decrease fibril angle.

2.1 Ultrastructure of fibers

Typically eucalypt fibers used in papermaking are about 1mm long and roughly 10-30 μm wide. The thickness of the cell wall is around 2-4 μm . These dimensions are not homogeneous, and depending on the property can vary considerably. The main constituents in a fiber wall are cellulose, hemicelluloses and lignin. Fiber cell wall is formed by the primary and secondary wall, and the latter is divided in S1, S2 and S3 layers (Fengel and Wegener, 1984). Secondary wall layers are composed of lamellae of spiraling cellulose fibrils, which are surrounded by hemicelluloses and lignin. In S2-layer the spiraling angle, the microfibrillar angle (MFA), is 10° to 30° for gymnosperms (Boyd 1980). For angiosperms (including the genus *Eucalyptus*) the MFA ranges from about 5° to 20° . This is clearly lower than for the other two layers (S1 and S3), but as S2 layer is by far the thickest of the layers some authors have discussed the possibility of all variation of MFA to be due to the S2 layer (Brändström et al. 2003). Figure 2 presents the structural organization of the cell wall.

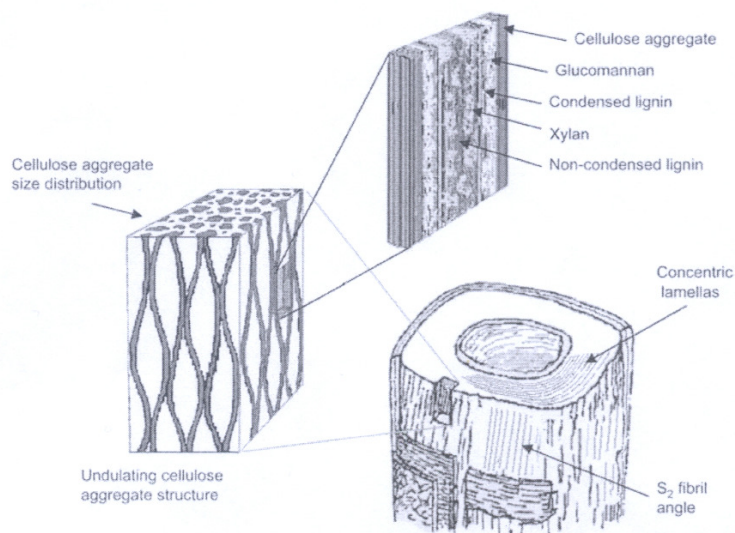


Figure 2. Schematic picture of the cell wall of a softwood fiber (tracheid) indicating the cellulose microfibrillar angle (MFA) of the secondary wall (S₂), the concentric lamellar arrangement of cellulose aggregates interspaced by matrix lamella, the lenticular undulating structure and the variability of cellulose aggregate sizes, as well as the arrangement of matrix components from glucomannan (non-substituted xylan in hardwoods) closest to the cellulose microfibrils that outwards associates to a condensed type of lignin followed by the xylan (more highly substituted xylan in hardwoods) associated to a more non-condensed type of lignin (Salmén and Burgert, 2009).

The arrangement of chemical components and the number and size of the structural units in fibers is not entirely known yet, even though a significant amount of research has been conducted on the topic. The native structure of hardwoods is shown in Figure 3. Ruel et al. (2009) studied the spatio-temporal relationships occurring between hemicelluloses, lignin and cellulose microfibrils during the secondary wall development. Their study indicates that xylans with less substituted polymer chains would be more directly interacting with cellulose microfibrils than those with higher substitution patterns. They also suggest that lignin molecules of the non-condensed type have a function in bringing cohesion between the lamellae of cellulose microfibrils. Bardage et al. (2004) determined the spacing between the undulating aggregates with a tangential diameter between 3 and 14 nm. This is consistent with the arrangement shown in Figure 2. In general, hardwood structure is more complex than softwood structure, and varies considerably between species.

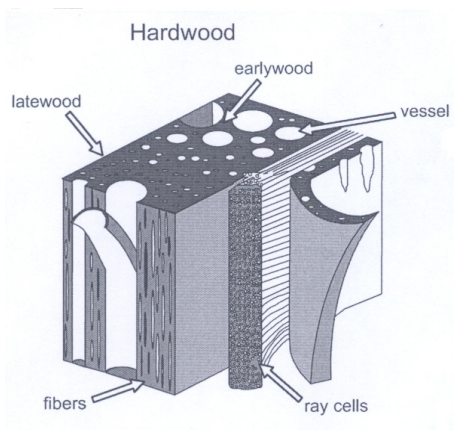


Figure 3. Native hardwood fiber (Taiz and Zeiger 2002).

2.1.1 Cellulose I^α and I^β

Cellulose is the main structural and load bearing element in fibers. It is a linear polymer consisting of glucose units joined together by β -1,4-glycosidic bonds (Figure 4). Cellulose possesses a high tendency for intra-and interfibrillar hydrogen bonding, leading to formation of microfibrils. Cellulose microfibrils exhibit excellent mechanical properties.

There are two different crystalline forms of native cellulose, cellulose I, designated as I^α and I^β (Atalla and VanderHart 1984).

The next larger structural unit from single cellulose chains is microfibril, which consist of 30-40 parallel cellulose chains. Microfibrils again aggregate into what are called fibril aggregates with the size of about 20 nm. The aggregates have also been shown to be able to take up moisture and thus change laterally their dimensions quite substantially (Salmén and Fahlén, 2003).

Kraft cooking alters the amounts of different forms of cellulose I^α and I^β and the size of the fibril aggregates. In two NMR studies conducted by Hult. et al. (2001, 2004) it was observed that the small initial amount of cellulose I^α is converted to cellulose I^β during the kraft cooking, causing a minor decrease in cellulose crystallinity. This was also observed by Åkerholm and Salmén (2002, 2004), who their two studies using dynamic FT-IR reported the conversion of cellulose I^α to cellulose I^β. It is probable that this is due to the thermodynamically more stable cellulose I^β and that a conversion from cellulose I^α to cellulose I^β thus occurs at the high temperature and high alkalinity prevailing during the kraft process (Åkerholm and Salmén, 2004). In terms of this thesis work, it is interesting to recognize that hardwood samples have a higher amount of cellulose I^β than softwood samples (Newman, 1994). The increase in fibril aggregate dimensions during kraft cook is attributed to an increased contact between cellulose fibril surfaces as a result of the removal of hemicellulose and lignin (Hult et al. 2001; Duchesne et al. 2001).

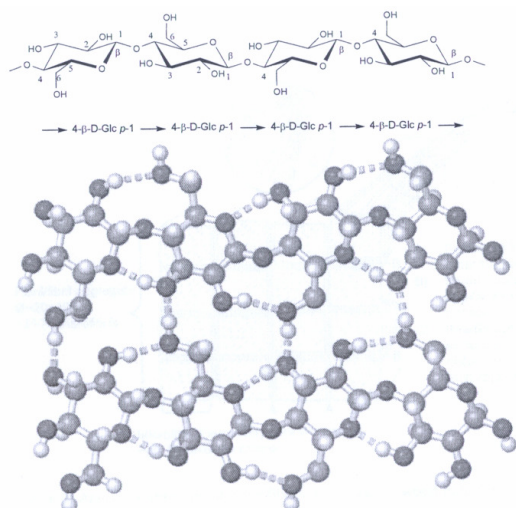


Figure 4. Chemical structure of cellulose and the hydrogen bonding pattern of cellulose I α (Horton et al. 2001).

2.1.2 Crystallinity index

Various methods of assessing the crystallinity index are available, namely X-ray diffraction (Segal et al. 1959), CP/MAS ^{13}C solid-state NMR (Atalla and VanderHart 1984), and Fourier transform IR-spectroscopy (Nelson and O'Connor 1964). Even though results from these different techniques show a good correlation (Evans et al. 1995), the values obtained can vary significantly depending on the instrument and data analysis technique (Thygesen et al. 2005). The crystallinity index of native cellulose can be lowered and changes the nature of crystalline cellulose induced by refining (Newman and Hemmingson 1994). Also, the hydration of celluloses has been seen to increase their crystallinity indexes by approximately 5% due to an increase in cellulose order (Park et al. 2009).

The fairly sharp signals from 86 to 92 ppm of (CP/MAS) ^{13}C NMR spectrum is corresponding to C-4 carbons from crystalline forms together with para-crystalline (ordered) domains, whereas the broader upfield resonance line from 79 to 86 ppm is assigned to C-4 carbons in the amorphous (disordered) domain (Figure 5).

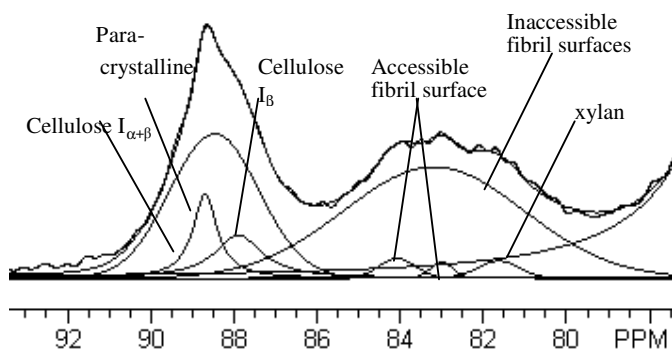


Figure 5. Spectral fitting for the C-4 region of the CP/MAS ^{13}C NMR spectrum of a birch kraft pulp sample (unpublished data).

The crystallinity index of each pulp samples was calculated as the percentage of area of 86-92 ppm in the C-4 signal cluster of 79-92 ppm. Spectral fitting was performed according to the model for the spectral C4-region of the CP/MAS ^{13}C NMR spectra of pure cellulose I fibrils consisting of seven distinct lines: three Lorentzian lines for the signals from the crystalline cellulose I allomorph (i.e. cellulose I α , I $_{\alpha+\beta}$), and

I_β), and four Gaussian lines for the remaining signals attributed to non-crystalline cellulose forms (i.e. para-crystalline cellulose, two accessible fibril surfaces and one inaccessible fibril surfaces) (Hult et al. 2000). In addition to the determination of the ordering of cellulose chains, CP/MAS ¹³C NMR can be used to determine the amount of structured xylan in the samples (Wickholm et al. 1998). The xylan signal is seen also in the spectrum shown in Figure 5.

2.1.3 Hemicelluloses

Hemicelluloses constitute about 15-25 % of eucalypt wood material. Hemicelluloses are polysaccharides with a degree of polymerization (DP) of 50-300. Hemicelluloses in hardwoods are different from those found in the softwoods. The major hardwood hemicellulose is a partially acetylated 4-O-Methylglucurono xylan with a minor proportion of glucomannan present.

The contribution of hemicelluloses to fiber strength has been widely discussed and is not entirely clear. Un-dried fibers with low hemicellulose contents have also seen to behave almost like dried fibers, showing high tear strength maximum and low maximum tensile strength (Duchesne et al. 2001; Neagu et al. 2006).

Surface hemicelluloses seem to affect significantly the formation of inter-fiber bonding. Schönberg et al. (2001) studied the role of xylan in spruce kraft pulp fibers. The location and the charge of xylan greatly influenced the formation of inter-fiber bonds. The amount of surface hemicelluloses and pulp handsheet strength has also been seen to correlate (Sjöberg et al. 2004), but not with the amount of internal hemicelluloses and handsheet tensile properties.

Swelling of the individual fibers is mainly due to the hydroxyl groups in hemicelluloses. Swelling itself is likely to internally organize a fiber favorably, but the main effect comes when a wet fiber network is dried. Hemicelluloses in fibers allow fibrils to flow and organize more favorably when fibers are dried (Kim et al. 1975). This reduces fibrillar angle and straightens dislocations and other potential weak parts of the fiber. Swollen fibers shrink during drying, and fiber transverse shrinkage at inter-fiber bonds causes an elongation of free fiber segments (Giertz 1964; Giertz and Roedland 1979), which in turn is proportional to the swelling ability of the fibers. This has a favorable effect on fiber network strength properties, and the more fibers swell, the more fiber network is activated after drying.

Higher hemicellulose content of kraft pulps may also lead to a more porous surface structure of kraft pulp fibers (Duschesne et al. 2001). Our recent study (Pulkkinen et al. 2009c) suggests that eucalypt fibers with higher xylan content has a larger mean pore size than fibers with low xylan content. This can be due to the closer association of cellulose fibril surfaces for fibers with low xylan content.

The total hemicellulose content was measured with standard carbohydrate analysis (Tappi T 249-cm00)(III-VIII) and the ordered xylan content with (CP/MAS) ¹³C NMR (VII).

2.1.4 Microfibril angle

Since S2-layer constitutes most of the fiber and contains the largest amount of cellulose, its microfibrillar angle (MFA) has a great influence on the mechanical properties of the fibers. If the S1 layer is relatively intact after pulping and subsequent operations, fibers' mechanical properties are not solely dominated by the S2-layer (Mark 2002). The lower the MFA, the stronger and stiffer the fiber is (Williams 1994; Wakelin et al. 1994). When MFA is low, the cellulose chains are loaded in the axial direction. When the MFA increases, the fibrils are loaded more in the cross-direction of the fiber that have inferior mechanical properties compared to the chain direction. The microfibril angle is the average angle between the direction of the helical windings of cellulose microfibrils in the secondary cell wall of fibres and tracheids and the long axis of cell (Figure 6).

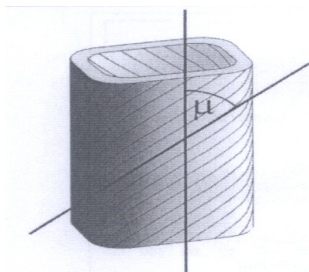


Figure 6. Microfibril angle for the S2 layer in a short section of fiber (Evans et al. 1999).

The fibrillar angle varies between fibers from the same tree. Latewood fibers usually have slightly lower MFA than earlywood fibers (Bonham and Barnett 2001) measured for birch fibers. MFA also varies within the growth rings (Bonham and Barnett 2001; French et al. 2000). The fibril angle was generally higher for the inner segments close to the pith of the studied eucalypt trees (French et al. 2000), but the differences were insignificant. Similar results were obtained for *E. urograndis* clones growing in four different sites in Brazil (Lima et al. 2004). Based on these studies it seems that the fibril angle in eucalypt had a negligible effect on fiber and sheet mechanical properties.

One could argue that it is sufficient to only look at the fiber wall thickness values, as MFA is a function of fiber wall thickness in pulpwood. For example Pulkkinen et al. (2008b) have discussed this issue. The opposite findings have been presented by Bergander et al. (2002) and Anagnost et al. (2000). Maceration of softwood material has been seen to cause narrowing in the MFA distribution (Peura 2007). This has to be considered when examining the measured MFA of the macerated eucalypt samples in this thesis work in relation to other properties. The samples used represented the earlywood and latewood of juvenile wood with varying density, cell wall dimensions, chemical composition and crystallite dimensions.

Studies by Uesaka and Moss (1997) and Courchene et al. (2007) have indicated that low microfibril angle (MFA) of wood fibers is beneficial to dimensional stability, but it could be that this becomes attenuated by the papermaking process (pulping, bleaching, beating and drying).

2.1.5 Fiber wall pore volume and structure

In wet state cellulosic fibers have porous structure (Stone and Scallan 1965; Scallan and Carles (1972)). The porosity has a large effect on fiber swelling, which is extremely important to fibers' ability to build strong networks. In chemical pulping material is removed from cell walls, resulting in fibers that have a more porous structure than the native fibers. Refining of the fibers also enhances pore formation.

The fiber wall porosity can be measured for example by means of thermoporosimetry using a differential scanning calorimeter (Maloney and Paulapuro 1998). The pore diameter is related to the temperature depression and the pore volume is proportional to the melting point of the water inside the pores. The amount of non-freezing water in a wet fiber can be quantified as the difference between the total water content, given by the weight measure, and the freezing water content (Hatakeyama 1987). It is concluded that the amount of bound water is a reflection only of the wood polymer composition of the fiber, whereas the pore water is affected by physical change of the fiber wall. Hornification does not influence the amount of bound water inside fiber wall (Salmén and Berthold 1997; Somwang et al. 2002).

The properties of papermaking fibers are influenced by the porous structure of the fiber wall. Initially, in the native fibers, the void volume in the fiber wall is around $0.02 \text{ cm}^3/\text{g}$ (Stone and Scallan 1965a) and when the fibers are liberated from wood by chemical treatment the void volume will increase to around $0.6 \text{ cm}^3/\text{g}$ at a yield of 47% (Kraft pulping), as determined by nitrogen adsorption of solvent exchanged pulps. This change is dramatic and when the last parts of the lignin in the fiber wall are removed by bleaching, the fiber wall will have a very open, porous structure as recently shown by Duschesne and Daniel (1999). The changes in structure will have a large influence on the ability of the fibers to conform towards each other during drying of the paper and hence also on the strength of papers formed from the

fibers. Also, the swelling of fibers (due to the remaining hemicelluloses in the fiber wall) has great impact on the softening of the fiber wall (Lindström 1986a).

2.2 Fiber defects

Wood fibers are submitted to very hard mechanical forces and stresses. During the cooking and bleaching processes, alkaline conditions favor the structural disorganization of the microfibril chains in the cell wall (Foelkel, 2007). The macropores created during the removal of wood constituents makes fiber walls more fragile and damaged in relation to its original organization in the wood. This cell wall fragility makes fibers more susceptible to mechanical damage.

The increase in curl, kinks and microcompression increase stretch but lowers the wet-web strength of the paper web. The increase in fiber curl makes the water removal easier (Page et al. 1985). High fiber curl leads to high stretch but low tensile strength (Trepanier 1998; Joutsimo et al. 2005). However, tear strength and light scattering are increased (Mohlin and Alfredsson 1990). The curliness of the fibers controls the extensibility of the wet-web (Trepanier 1998; Seth et al. 1984) which in turn determines the runnability of paper-web on open-draw machines (Seth et al. 1982).

Variables describing fiber deformations are for example the kink index (Kibblewhite and Brooks 1975) and the Jordan-Page curl index (Jordan and Page 1983). However, the fiber damage cannot always be recognized from the measurement of kinks and curl. The damage can be present as folded fiber (curl index value of 0.5), distorted regions of fiber wall, twist or microcompressed regions (Page et al. 1985). The identification of which is hard with the curl and kink measurements of modern fiber analyzers. However, fiber curl as a descriptive parameter for fiber shape is important in determining the extent of fiber network activation potential.

However, when modeling sheet properties based on fiber properties measured from laboratory made pulps, it is important to take into consideration that laboratory beating straightens the fibers (Mohlin 1991), whereas industrial refining does not. Considerable differences in refining responses between laboratory beaters and industrial refiners are to be expected. The strength potential of fibers is therefore reduced more during industrial processing than in the laboratory (MacLeod et al. 1987).

2.3 Fiber dimension distributions

End-use properties of paper products are dependent among other factors on fiber morphology and cross-section dimensions of fibers for both softwood and hardwood fibers (Santos et al. 2006; Paavilainen 1989, 2000). Eucalypt wood density varies with geographical locations, forest silvicultural practices, and positions within a tree (Downes et al. 2003; Evans et al. 1999a, 2000). The eucalypt fiber dimensions also vary with age (Downes et al. 2003).

Most of the original structure of papermaking fibers is preserved in the pulping and papermaking processes. Fiber properties will greatly determine the properties of paper. When considering the potential furnishes for different end-uses, the delicate balance between the strength properties and the structural properties (e.g. the bulk density) has to be considered. One of the main objectives of the genetic improvement programs of eucalypt has been to increase pulp production per cubic meter of wood, which is associated with the increase of wood paper density and pulp yield. The optimization efforts should also consider fiber characteristics such as fiber wall thickness, fiber width, and fiber length. Several papers were published recently concerning relationships between wood basic density and fiber and pulp characteristics for eucalypt (Downes et al. 2003; Kibblewhite 2003). The paper structure depends on the dimensions of the fibers and the mechanical properties of wet fibers. Mechanical properties of dry fibers are influenced by the stress under which drying takes place (Retulainen et al. 1998).

The mean values of fiber properties have been used to predict paper data, whereas the effect of heterogeneity has been studied to a lesser extent. Of the paper properties, non-uniformities in the raw material influence the formation by making it worse (Nazhad et al. 2003). It was concluded earlier in

studies conducted by Kärenlampi (1995, 1996) that short fibers with narrow fiber length distribution produced sheets with good formation and good strength properties.

Numerous models have been proposed to predict paper properties in terms of fiber and network properties (Cox 1952; Page 1969; Gurnagul et al. 1990). Page (1969) proposed a model to predict tensile strength from length, perimeter, density, shear tension and strength of the fibers, and relative bonded area of the handsheets. Clark (1985) simplified this model, by reducing the number of variables and adopting characteristics of easier evaluation.

The significant effects of cell wall thickness, length, coarseness and strength of the fiber upon paper properties have been confirmed in both theoretical models (Gurnagul et al. 1990) and overall evaluations of cause and effects (Seth 1990a, b; Gorres et al. 1989; Duffy and Kibblewhite 1989; Wimmer et al. 2002). The fibers with similar coarseness value can, however, differ greatly in their structural features. Therefore a model is only applicable if the parameters of the model take into account the whole mass distribution of the fiber furnish (Pulkkinen et al. 2008b, 2010).

Another approach, concerned with wood quality, has led to consideration of the effect of wood basic density as a basic predictor of paper quality (Duffy et al. 1989; Gurnagul et al. 1990; Wimmer et al. 2002; Santos et al. 2008). The results indicate that hardwoods in general (Gurnagul et al. 1990), and particularly eucalypts (Santos et al. 2008) display good relationships between wood basic density and fiber flexibility and conformability, which reflect on the consolidation of paper structure.

The wide natural variability of the fiber properties has to be implemented into any given model in order to make it more accurate. For example, two pulps with the same fiber wall thickness fraction and obtained from the same eucalypt wood raw material can have distinct fiber strength properties and paper performance (Foelkel 2007). A combination of fiber characteristics should be provided, which may be used to develop a model, based on parameters easy to measure and to control through breeding programs of eucalypt fibers.

2.4 Industrial processes affecting fiber properties

Several processes affect a number of fiber related properties, most importantly fiber-to-fiber bonding and fiber segment activation. Refining, wet pressing and drying regimens used in this study all have important role in paper property development. These are discussed in detail in the following chapters.

2.4.1 Refining

Fiber width, thickness, wall thickness, and wall area, as well cross sectional shapes can be very different depending on whether pulps are refined. Fibers can also respond to refining in different ways depending on whether the fibers have thin or thick walls (Kibblewhite 1989, 1993).

Actual cross-sectional wall areas of un-dried kraft fibers normally remain practically un-changed with increased refining whereas those of dried and rewetted fibers increase. For refined fibers, delaminated walls are envisaged as consisting of several concentrically oriented lamellae aggregates or coarse lamellae (wall substance + water) inter-dispersed with void space filled predominantly with water.

The distributions of fiber properties have been used little when examining the real effects of fiber furnaces on paper technical properties (Johnson 2004). The effect of refining has not, however, been the main topic of these studies.

The changes in fiber property distributions when fibers are refined have been mostly concentrating on the fiber length distributions, as the measurement of fiber length has been a standardized measurement for a long period of time (Anonymous 1991, 2000a), and is generally accepted to give reliable results (Trepanier 1998). Also, the effect of refining on the fiber wall thickness of eucalypt fibers has been a subject of numerous studies (Kibblewhite 1989; Hiltunen 2005; Pulkkinen et al. 2007).

When using the FiberLab® fiber analyzer, competing effects of delamination and fiber swelling may have an effect on the measurement results. These in turn are influenced by the hemicellulose content of the fibers, fibers containing more hemicellulose favoring fiber swelling and, consequently, increasing fiber dimensions. The analyzers based on polarized light (Pirainen 1985; Olson et al. 1995) are also influenced by the cellulose content and where in the fiber wall hemicellulose is located.

2.4.2 Wet pressing

The wet pressing can be described as to contribute to the strengthening of the paper web by bringing fibers and fiber cell walls into closer contact and by collapsing fibers, thereby enhancing the bonding potential (Pikulik et al. 1995). The effect of wet pressing on for example paper density and tensile properties will therefore depend upon the extent of fiber collapse. The type of furnish used will play a major role: if mechanical pulp is the dominant component of the furnish increases in density are only moderate with increasing wet pressing pressure. The tensile index increases with increasing wet pressing pressure (Pikulik et al. 1997). However, the major part of eucalypt fibers are already collapsed at the beginning of wet pressing, therefore reducing the effect of wet pressing to sheet properties.

2.4.3 Drying

The mechanical and hygroexpansional properties of fiber bonds and bonded segments are closely related to the drying stresses that act across interfiber bonds (Giertz 1964; Giertz and Roedland 1979; Lobben 1975; Retulainen 1997; Salmén et al. 1987). The main contributor to the drying shrinkage and drying stresses is the transverse shrinkage of fibers (Nanko et al. 1989). The shrinkage of individual fibers causes contraction of the whole fiber network and creates internal stresses in the paper (Salmén et al. 1987). The changes in mechanical properties caused by drying under load can be associated to two main mechanisms, the increase in crystallite orientation and more evenly distributed stresses among fibers (Kärelampi 1995; Retulainen 1997). Fiber network consisting of thin-walled fibers also have a narrow drying stress distribution, especially in the case of eucalypt fiber (Mohlin and Hornatowska, 2006; Pulkkinen et al. 2010), therefore resulting in an increased elastic modulus and tensile strength (Vainio 2007; Kärelampi 1995) when the sheet is dried. The fiber curl in freely dried sheets gives the sheet a higher shrinkage potential than straight fibers. The effect of original curliness is believed to disappear when sheets are dried in restraint (Salmén et al. 1987). This is due to a straightening of the free fiber segments between the fiber crossings postulated by Giertz (1964). This is a phenomenon what is generally known as fiber network activation. Inter-fiber bonding and shrinkage of fibers are the requisites for activation. The amount of drying stress needed to activate fiber segments depends on the morphology of the fibers (Retulainen 1997; Pulkkinen et al. 2010).

3 FIBER-TO-FIBER BONDING AND NETWORK PROPERTIES

3.1 Hygroexpansivity and mechanosorptive creep

Hygroexpansivity is the most basic paper property that determines various dimensional instability phenomena, such as curl, warp, twisting, wrinkle, coele, surface roughening etc., in the end-use. It is often said that reducing the degree of fiber-to-fiber bonding, for example by reducing refining energy, improves dimensional stability. This creates a conflict with other quality requirements, because many of the paper products require not only dimensional stability but also strength. To increase strength of fiber networks, refining is normally applied.

The effect of fiber-to-fiber bonding on hygroexpansivity is not as straightforward as on mechanical properties, as hygroexpansivity depends on various other factors than solely refining. Hygroexpansivity behaves rather abruptly as a function of refining. For example, Salmén et al. (1985) showed that the beaten long-fiber fraction has lower hygroexpansivity than the un-refined long fiber fraction. They also showed that wet pressing did not have an effect on sheets dried in restraint. In the literature, it has been reported that hygroexpansivity of restraint-dried sheets is not sensitive to changes in pulp types and refining (Salmén et al. 1986; Uesaka 2002).

Fiber morphology has a significant impact on hygroexpansivity of paper (Uesaka and Moss 1997). Increasing fiber length and decreasing fiber width have positive effects on dimensional stability. High fiber wall thickness (relative to fiber width) and smaller MFA (Uesaka and Moss 1997; Courchene et al. 2007) are also expected to improve dimensional stability. The fiber wall thickness and the fiber length are highly inter-correlated (Preston 1934; Dadswell 1958; Uesaka and Moss 1997; Wimmer et al. 2002; Pulkkinen et al. 2008b), so it is logical that both high fiber wall thickness (McMillin 1973; Megraw 1997; Pulkkinen et al. 2009a) and high fiber length (Uesaka and Moss 1997) result in a lower hygroexpansion coefficient. According to Vainio et al. (2007a), high MFA would suggest that there would be more drying shrinkage. However, the effects of MFA quite easily can be obscured by changes of other fiber properties (Watson and Dadswell 1964). Thin-walled fibers are generally believed to shrink more during drying (McIntosh 1961). The bonding ability of the fibers will determine how this translates into the hygroexpansivity of the fiber network. Together with the hemicellulose content of the fibers (Brecht et al. 1974; George 1958) fiber dimensions and MFA are the key raw material factors that strongly affect how your paper will behave in a chosen end-use. The fiber curl in freely dried sheets gives the sheet a higher shrinkage potential than straight fibers and thus give sheets with a higher hygroexpansivity. The effect of original curliness is believed to disappear when sheets are dried in restraint (Salmén et al. 1987). This may be due to a straightening of the free fiber segments between the fiber crossings postulated by Giertz (1964). This is a phenomenon what is generally known as fiber network activation.

The creep rate of paper is affected by moisture. The behavior of mechanical response of paper in a variable humidity climate is quite different from that in constant relative humidity. The creep rates of most hydrophilic materials increase greatly with moisture content. However, when these same materials are subjected to creep loads in cyclic humidity environments, they often exhibit much higher creep rates than in a constantly humid state. This is called accelerated creep (Byrd 1972). A mechano-sorptive effect is one arising from the interactions of the external forces on the paper structure with the ambient relative humidity as well as temperature.

It is important to know if furnish is more or less susceptible to moisture-accelerated creep and consequent dimensional stability. A second important issue is the influence of fiber network structure of paper on its response to variable relative humidity. The network structure can influence moisture-accelerated creep through the behavior of the inter-fiber bonds. Strain in the sheet may arise from the release of microcompressions (Haslach 2002). The pulp furnish affects the creep response of a sheet under variable humidity. Several scientists have observed that recycled fiber paper exhibits more moisture-accelerated creep than similar virgin fibers (Mark 2002). However, they were unable to connect it to the moisture absorbance rate (Mark 2002). More conformable fibers might be more likely to form microcompressions in their fiber-fiber bonds. The inter-fiber bonding is therefore important determinant in how mechano-sorptive creep will develop. After the inter-fiber bonding is at a sufficient level, i.e. fiber dimensions

become sufficiently small and fibers are relatively straight, fiber network activation has a bigger role in determining the development of network properties (Pulkkinen et al. 2010). The mechanisms governing the strength, dimensional stability and mechano-sorptive creep properties apparently are partially similar. A part of this thesis work was dedicated to investigate this phenomenon.

Comparisons of the mechano-sorptive creep stiffness behaviour of pulps made of different raw materials are not very common in the literature; the causes of tensile stiffness and hygroexpansion properties, though more investigated, are still not fully understood. Anisotropic hygroexpansion, which produces stress concentrations in fiber-fiber joints, is one factor that might explain mechano-sorptive creep behaviour (Alfthan et al. 2002). No experimental results, however, have been found in the literature showing a link between hygroexpansion and mechano-sorptive creep stiffness.

The results presented in the literature therefore indicate that the effects of fiber bonding, drying restraint, activation of the fiber network and fiber orientation are all crucial for these two properties. In order to achieve high strength, good dimensional stability and low mechano-sorptive creep of paper, the factors affecting fiber-to-fiber bonding need to be understood in detail.

3.2 Tensile strength

According to Mohlin (2001), fiber straightness and water retention value are enough to model the tensile strength development of commercial, dried bleached softwood kraft pulps. The same applies for commercial, dried bleached eucalypt kraft fibers. This is backed up by the results of this study. However, the activation model presented and used in this study to model tensile strength needs an additional parameter in terms of fiber wall thickness distribution. This is because fiber transverse shrinkage determines the extent of fiber straightening between free fiber segments. A requisite for this is sufficient amount bonding (high sheet density or highly refined fibers). This criterion varies depending on if the fibers are dried or not. Another important factor is that we get accurate enough information of the measured properties. As later discussed in Chapters 4.2 and 6.10, a factor that produces most of the model error is the measurement of fiber dimensions.

The strength of pulps consists of at least three components; single fiber strength, fiber-fiber bond strength per unit area and the total fiber-fiber bonded area (Johansson et al. 2001). Individual fiber strength properties are a direct result of the initial fiber strength in the original woodchips, and of the chemical and mechanical treatment in the mill. Once the pulp has left the process, it is not possible to improve individual fiber strength (Johansson et al. 2001). Furthermore, the detection of single fiber strength losses using conventional test methods is difficult. For example, in zero-span measurement, the fiber strength has to be calculated based on a number of assumptions, e.g. the fiber distribution, fiber network properties etc. (Johansson et al. 2001). The other two components, the bond strength and bonded area are considered to be less influenced by the process conditions, and these components can be influenced after the fibers have left the process.

There are several models trying to explain the correlation between the fiber properties in pulp and the tensile strength properties of the final paper. The Page model and the Shear-lag model are two of them (Page 1969; Calsson and Lindström 2005).

According to Page's theory (Page 1969) the tensile strength of a paper depends on the fraction of broken fibers in the zone of rupture, which depends on both the strength of individual fibers and the strength of the bonds between them. The model is based on two assumptions, where the first deals with the distribution of stress in a paper strip at the moment of tensile failure. The final form of the original Page equation is given as

$$\frac{1}{T} = \frac{9}{8Z} + \frac{12A\rho g}{\tau_b PL(RBA)} \quad (1)$$

Where the first term describes the individual fiber strength and the second term describes the strength of the bonds in a given fiber network.

Studies have shown that fibers can be pulled out intact even if the fiber-to-fiber bonds are strong, shear stress could be a limiting factor in paper strength properties. The Shear-lag model was developed for composites but can also be used in prediction of paper qualities (De Ruvo et al. 1986; Carlsson and Lindström 2005). A central idea in the model is the transfer of load from the matrix into the fiber. The shear stress is assumed to be constant along the fiber length and a linear axial stress is built up in the fiber (Figure 7). A critical fiber length is defined such that is the fibers are shorter than the critical fiber length then the maximum normal axial stress at half the fiber length will be lower than the fiber strength and the fiber will be pulled out causing a bond failure along the fiber-matrix interface when the composite is strained under uniaxial tension. On the other hand if fibers are longer than the critical fiber length then the normal axial stress at half the fiber length will exceed the fiber strength during straining and fracture due to fiber breakage will occur.

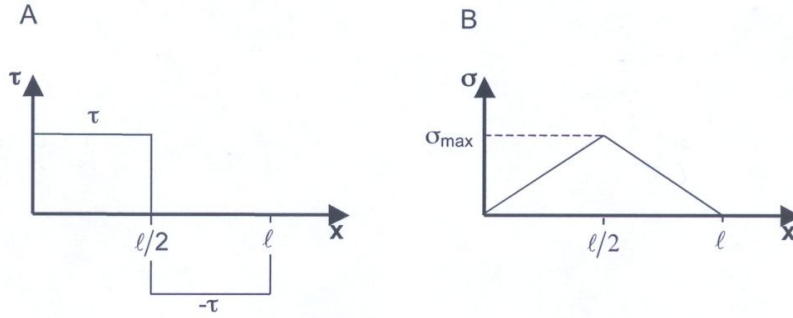


Figure 7. Axial and shear stress diagrams for short fibers (Westerlind et al. 2007).

Carlsson and Lindström (2005) arrived at the following equations when applying shear-lag theory to the paper,

$$\sigma_T^w = \frac{3}{32} \frac{\tau_b}{\rho_c} \frac{Pl}{A} RBA \quad l < l_{crit} \quad (2)$$

$$\sigma_T^w = \frac{3}{8} \frac{\sigma_f}{\rho_c} \left(1 - \frac{l_{crit}}{2l} \right) \quad l > l_{crit} \quad (3)$$

With the critical fiber length l_{crit} given by:

$$l_{crit} = \frac{2\sigma_f A}{\tau_b P(RBA)} \quad (4)$$

where σ_f and τ_b are axial fiber strength and fiber bond shear strength, respectively.

It is not a new idea to link WRV with tensile strength measurements, for example recently Westerlind et al. (2007) and Shallhorn and Gurnagul (2008) used WRV as an additional parameter in the Page equation and in the Shear Lag model. WRV and drying stresses have been observed to obtain a linear correlation (Mohlin 2005; Htun et al. 1987). The fiber slenderness ratio Pl/A present in equations of Page and shear-lag is calculated from the fiber wall thickness, fw , and fiber width, fw , by assuming a circular cross section of fiber.

$$\frac{Pl}{A} = \frac{fw \cdot l}{fw t (fw - fw t)} \quad (5)$$

In the development of the activation coefficient presented in this Thesis, WRV was used as a parameter to describe the swelling ability of the fibers.

In the activation model (Pulkkinen et al. 2010), fiber ultrastructure is ignored. However, the use of activation parameter as such has many benefits. First of all, it is easy to use and as variables requires only fiber properties that can be measured directly from the pulp suspension. Secondly, the activation parameter is designed to characterise the bonding ability of the fibers. Individual fiber strength is not included in the models, as it is not directly measurable with modern fiber analysers and its effect on tensile properties is smaller than the effect of fiber-to-fiber bonding. Even though there has been studies where fiber curl has been observed to affect zero-span strength of fibers (Mohlin and Molin 2003), it is more likely that it does not have an effect (Joutsimo et al. 2005). Therefore, factors affecting the zero-span strength are more closely associated to cellulose fibril and fibril aggregates.

4 MATERIALS AND METHODS

4.1 Pulp samples and sample preparation

(II): The four hardwood pulp samples included in reference Pulkkinen et al. (2007) were of industrial grade, and consisted of eucalypt pulps (*E. grandis*/*E. saligna*, *E. nitens*/*E. globulus*, *E. urograndis* and *E. grandis*/*E. dunnii* with different drying histories. *E. grandis*/*E. saligna* contains roughly 50/50 of each species, *E. nitens*/*E. globules* is mostly *E. nitens*, and *E. grandis*/*E. dunnii* is mostly *E. grandis*. All pulps were refined using a laboratory model Voith Sulzer refiner. The refining tackle used was a disk blade with a stock concentration of 4% at a specific edge load of 0.4 J/m with refining energies of 0, 40, 80 and 120 kWh/t. Two samples of each pulp were taken. Both of these samples were machine dried and refined. One sample was analyzed with FiberLab® analyser directly from the pulp suspension without any additional drying. The other sample was dried in a laboratory oven (105°C) before analysing it. In this study, the samples are referred to as once-dried and dried samples, respectively. In the second part of the study of paper II, only once-dried pulps were used to correlate fiber wall thickness and handsheet properties.

(III, VI): 20 *Eucalyptus grandis* clones (16 samples 4-year-old and 4 samples 8-year-old) were used in this study. Kraft pulps were produced from chips representing the whole trees. Pulps were laboratory cooked to a Kappa number of 18 ± 2 . Samples of the prepared pulps were beaten with a PFI refiner up to 2,500 revolutions according to standard ISO 5264-2. Hand sheets were made according to the standard ISO 5269-1. The laboratory sheets were dried under restraint. The drying was performed in a climate control room (23 °C and relative humidity (RH) of 50%). After drying, the handsheets were tested according to the following standards and methods:

- apparent density EN ISO 534
- tensile properties EN ISO 1924-2
- water retention value (WRV) SCAN-C62
- air resistance EN ISO 5636-5:03

Absolute dry samples were dried for 16 hours in an oven at 105°C. Handsheet conditioning to 90% RH was carried out with an OPTIDIM hygroexpansivity meter (Kajanto and Niskanen 1996).

Micro fibril angle was measured with SilviScan 2 measurement apparatus (Hatvani 1999). Samples were taken from breast height, as a bark free sample (12 mm core from bark to pith (1 radius)).

Carbohydrate composition of the pulps was determined using a method; utilizing sulphuric acid hydrolyzes at 120°C to degrade the carbohydrates into monosugars, based on Tappi standard T249-cm00. Monosugars were then analysed by ion chromatography (Metrohm 817 Bioscan system).

For the second part of the study of paper III, dynamic sheets of an *E. grandis*/*E. dunnii* commercial pulp were used. Dynamic sheets were made with a dynamic sheet former (Formette Dynamique), which had been slightly altered. The wire speed was set to 1000 m/min. The jet speed was set to ~ 920 m/min (1.6 bars) and the feed concentration was 4 g/l. The grammage of dynamic sheets was ~60 g/m². The sheets were wet- pressed according to ISO 5269-1.

(IV-V, VII, VIII): Five commercial eucalypt pulp samples from different parts of the world, accompanied by birch and acacia as reference samples were used. The samples were 1) *E. grandis*/*E. dunnii* (Uruguay), 2) *E. globulus* (Portugal), 3) *E. urograndis* (Brazil), 4) *E. urograndis*/*E. grandis* (South Africa), 5) *E. grandis*/*E. saligna* (Brazil), 6) Birch (*Betula pendula*, Finland), and 7) Acacia magnium (Indonesia). Some of the eucalypt pulp samples were mixtures of two species, 50%/50% for *E. grandis*/*E. dunnii* and 90%/10% for *E. grandis*/*E. saligna*. The ratio of fibers in *E. urograndis*/*E. grandis* was unknown. The pulp samples were obtained in mill dried form. Fibers were refined with a Voith-Sulzer disk refiner at a consistency of 4%. Fibers were refined up to 150 kWh/tonne with a specific edge load of 0.4 J/m. The handsheets were tested according to the following standards and methods:

- Apparent bulk density, ISO 534
- Tensile properties, EN ISO 1924

Isotropic handsheets of grammage 60 g/m² were made in a standard laboratory handsheet former according to the ISO 5269-1 standard. Anisotropic sheets were made with a dynamic sheet former at KCL research center. The wire speed was set to 1000 m/min. The jet speed was set to 920 m/min (1.6 bar). The feed concentration was 4 g/l. The grammage of anisotropic sheets was 60 g/m². Both the isotropic sheets and the anisotropic sheets were dried in contact with a plate to which the sheets were attached. This affected shrinkage during drying, which was done in a climate controlled room (23°C and at a relative humidity of 50%). The raw material for samples of different sizes in article V was *E.grandis/E.dunnii* (Uruguay).

4.2 Measurement of the ultra-structure of the fiber wall

4.2.1 (CP/MAS) ¹³C NMR

Solid state (CP/MAS) ¹³C NMR spectroscopy is a versatile tool for morphology studies of cellulosic materials (Atalla and VanderHart 1999; Hult et al. 2001, 2003). The supra-molecular structures of cellulose were investigated by using CP/MAS ¹³C NMR spectra along with non-linear spectral fitting, which analyzes the crystalline allomorph and disordered domains (Larsson et al. 1995, 1997; Wickholm et al. 1998; Hult et al. 2003). The line-shape spectral fitting analysis of solid state spectra allows a very detailed comparison and characterization of cellulose supra-molecular structures, and has been extensively used to investigate the structural characteristics of cellulose and its derivatives. The relative amounts of different cellulose forms in complex cellulosic materials can be determined by using spectral fitting analysis of the C4-region of (CP/MAS) ¹³C NMR spectra. The ratio of crystalline and amorphous cellulose can be characterized with a CrI (Newman and Hemmingson 1990; Liitiä et al. 2003).

It is possible to calculate the average lateral fibril dimensions from the NMR spectra if the fibrils and the fibril aggregates, as a simple approximation, are assumed to have square cross-sections (Hult et al. 2000). The fraction of the signal intensity from accessible surfaces (calculation of fibril aggregate dimension) or the fraction of the signal intensity from accessible and inaccessible surfaces (calculation of fibril dimension) are both denoted q and are given by equation (6):

$$q = \frac{(4n - 4)}{n^2} \quad (6)$$

where n is the number of cellulose polymers perpendicular to the fibril or the assumed square fibril aggregate cross-section. A conversion factor of 0.57 nm per cellulose polymer has been calculated as the mean value of the repeat distance of cellulose chains in the wide and narrow surfaces (Wickholm et al. 1998). The microfibrils in bleached chemical pulp fibers consist of two regions of cellulose: crystalline and amorphous (Bertran 1986). There is also a region between these two forms of cellulose, normally referred as para-crystalline cellulose (Larson et al. 1997). The highly ordered cellulose fibrils are poorly accessible to water molecules.

The solid-state (CP/MAS) ¹³C NMR experiments (Atalla and VanderHart 1984) were performed on a Bruker Avance-400 spectrometer operating at frequencies of 100.59 MHz for ¹³C. All the experiments were carried out at ambient temperature using a Bruker 4-mm MAS probe. The pulp samples (~45% moisture) were packed in a 4 mm ZrO rotor. CP/MAS ¹³C NMR data was acquired with 8000 scans accumulated per sample. The samples were analyzed at Georgia Institute of Technology, Atlanta, US.

The algorithm used in this study was not able to include Lorentzian lines for modeling the signals originating from the highly crystalline domain in the C (4) region (Larsson and Westlund 2005), and only Gaussian lineshapes were used. Because of this it is possible that the values for the Crystallinity Index or the relative amount of xylan were not as accurate as those obtained with the combined use of Lorentzian and Gaussian lines. However, all studied spectra were treated in the same manner, so obtained results are comparable within this thesis work.

4.2.2 SilviScan®

The basis for the measurement was SilviScan-2 X-ray diffractometer (Evans et al. 1999). The basic measurement configuration is illustrated in Figure 8. Samples were examined with the X-ray beam in the tangential direction of an increment core. The diffraction patterns were recorded with a CCD area detector and the strong (002) equatorial reflection was used for MFA analysis. Although the much weaker meridional 040 reflection can be used to obtain the microfibril orientation distribution directly, the data collection rate would be too slow for rapid examination of large numbers of increment cores.

The theory behind the measurement of MFA on SilviScan-2 is published in a publication by Evans (1999).

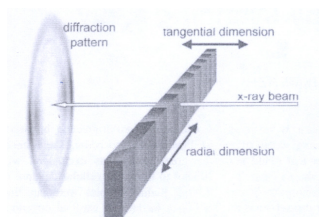


Figure 8. Instrumental configuration for scanning X-ray diffractometry (Evans et al. 1999).

4.3 Methods to characterize fiber-water interactions

In the paper industry, two of the common methods used to measure fiber swelling and its ability to retain water are WRV, water retention value (SCAN-C62), and FSP, fiber saturation point (Stone and Scallan 1968). The former measures all different types of water associated with fibers and the latter measures all water except lumen and surface water. Differential scanning calorimetry (DSC) has also been used to characterize a fiber-water system. Three types of water associated with cellulosic fibers have been identified: unbound water, freezing bound water, and non-freezing bound water (Nakamura et al., 1981; Weise et al., 1996). Bound water is considered to be located close to the fiber surface and tightly bound to it (Maloney et al., 1998a,b; Ping et al. 2001). A nuclear magnetic resonance (NMR) method has also been used for characterization of water in fibers (Tapgaard and Söderman, 2002). The non-freezing bound water was characterized by experimental free-induction-decay based on the molecular dynamics of the water molecules. These two techniques provide detailed information about the fiber-water interaction. In this thesis, WRV, FSP and DSC were used.

4.3.1 Water retention value

The measurement of water retention by centrifuging pulp fibers was first introduced by Jayme (1944). The WRV is an empiric filtration drainage test based on a convention of arbitrarily chosen parameters, of which the centrifugal field, testing time and the sample size are the most important. Several modifications were subsequently applied to the original setup. In this study, a 1700 g/m^2 fiber pad was centrifuged at 3000 g for 15 (± 30 s) minutes at a temperature of $23 \pm 1^\circ\text{C}$. The water retention value is seen as a measure of fiber swellability, including water inside (in fiber lumens) and between the fibers and on fiber surfaces. Thus the water determined with WRV will contain all the different types of water that the fiber may hold.

The compaction of the pad during centrifuging is dependent on pulp characteristics, on the mass of the sample, and on the magnitude of the gravity field applied. Therefore, a good agreement between the WRV and the FSP is only probable for centrifuging samples with extremely low basis weight (Abson and Gilbert, 1980). The swelling water determined with solute exclusion was determined equal to the water determined by WRV in a study made by Scallan and Carles 1972. Maloney et al. (1999) concluded that even though these two methods correlate well for some pulps, for some pulps it does not. Because of the large variety between the several testing conditions, it is therefore important to take this into account, when comparing WRV data from different sources. It must always be clearly stated how the WRV was obtained.

4.3.2 Fiber saturation point

FSP was measured by solute exclusion (Stone and Scallan 1968) using a 2×10^6 Dalton dextran polymer (Amersham Biosciences). In the solute exclusion method, the water-filled volume of the fiber that is inaccessible to a probe molecule of specific size is quantified by measuring the dilution of a solution of probe molecules when a wet pulp sample is added. With the largest polymers used, inaccessible to any pores, the total amount of water held by the fiber is determined. This contains all the types of water, except for lumen and surface water.

4.3.3 Differential scanning calorimetry

The thermoporosimetry measurements were carried out on a Mettler DSC 821. In the technique used in this study, the energy absorbed when water in frozen pulp fibers is melted in a stepwise manner approaching 0°C is measured. The melting energy is assumed to be directly proportional to the amount of melted water. In the form of Gibbs-Thomson equation (Maloney 1998) used, it is assumed that the pores are cylindrical. The DSC freezing and melting curves show several peaks, which depend on the size and on the water content of the sample (Yamauchi and Murakami 1991). The water remaining without transition, the non-freezing water, is understood as directly bonded water, the so-called “non-freezing bound water”. The different types of water held by a wood fiber and the techniques for determining these are schematically listed in Table 1 and Figure 9.

Table 1. Different types of water and methods for characterizing them (Salmén and Berthold 1997).

Bound “non-freezing” water	— DSC + weight	} Solute exclusion	} WRV
Freezing bound water	— DSC + weight		
Pore water	— ISEC		
Free, surface water			

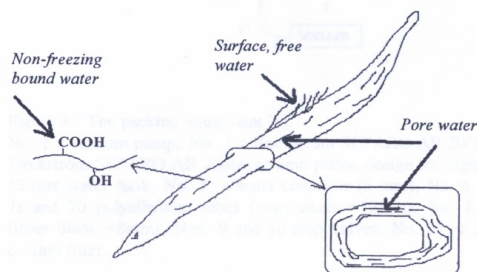


Figure 9. Different types of water held by a wood fiber (Salmén and Berthold 1997).

4.4 FiberLab® analyzer

Major part of this work was carried out by utilizing the data obtained from the FiberLab® fiber analyser at Metsä-Botnia mill in Kemi during the years 2005-2008. The data obtained was used as an input for various models used to estimate paper technical properties. The starting point for any measurement is a representative take of pictures of the fibers. These can include more information than to date has been utilized.

The apparatus measures the fiber length according to TAPPI- and ISO-standards (Anonymous 1991, 2000). The sample is diluted to a concentration of 0.02 g/l and is then sucked to a measurement capillary of size 0.5×0.5 mm. During the analysis the capillary flow is observed constantly with polarized laser and when the detector sees a fiber two 2-dimensional gray-scale pictures with a charge-coupled device (CCD) camera are taken, one for determining the fiber length and another to determine fiber width, fiber wall

thickness and the curl index (Figure 10). Fiber curl was calculated based on fiber length and its projected length. The formula used to calculate the curl was the Jordan-Page formula (Page et al. 1985).

$$\text{Curl} = (L_c/L_p - 1) * 100\% \quad (8)$$

where L_c is the fiber length along the centreline and L_p the projected length of a fiber. According to the formula straight fiber will yield a value of zero and a double folded fiber will yield a value of 0.5. The measurement ability values are presented in Table 2.

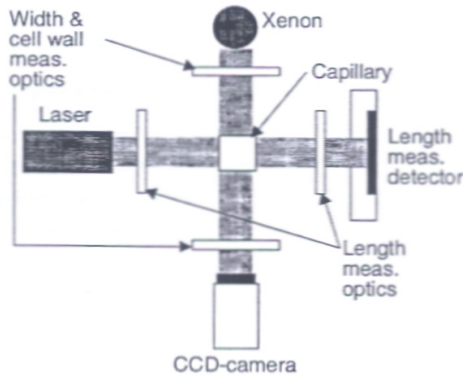


Figure 10. The measurement principle (Anonymous 2006).

The FiberLab® analyser and other Kajaani fiber analysers (such as Kajaani FS-100 and 200) have frequently been compared to other analysers in terms of pulp fiber dimensions and calculated values (Muneri and Balodis 1997; Turunen et al. 2005), or in terms of comparing wood fiber dimensions to pulp fiber dimensions (Richardson et al. 2003). The level of different analyser results between different analysers being different, they nevertheless showed good linearity (Turunen et al. 2005). One major aspect of this research project was the measurement of fiber wall thickness index. This feature is only available in the commercial FiberLab® analyser, so comparisons between the fiber wall thickness values between automated fiber analysers were not made.

FiberLab® results have been found to correlate well with certain paper technical properties. Fiber length has been found to correlate well with tensile properties (Luukkonen et al. 1990). Similar trend has been observed for fiber coarseness (and fiber wall thickness) as they correlate reasonably well with tensile- and tear strength (Paavilainen 1991; Paavilainen 1993; Pulkkinen et al. 2008). The structural properties (for example bulk density) also correlate with fiber wall thickness (Paavilainen 1993; Mörseburg et al. 1999).

The 2D CCD camera pictures (Figure 11) used to calculate fiber wall thickness are those of fiber width. Depending on the analysis, thousands of pictures can be obtained in one fiber analysis. Fiber width and fiber wall thickness index was seen not to correlate in a recent study by Pulkkinen et al. 2008b. This can be due to the assumption of circular shaped fibers with the image analysis, when fibers are “scanned” only from one side and the level of collapse cannot be seen. The calculation of fiber wall thickness index is illustrated in Figure 12.

Table 2. Measurement inaccuracies given by the manufacturer (Anonymous 2006).

Measurement inaccuracy	95 % confidence interval
Fiber length > 2,2 mm 1,8 – 2,2 mm < 1,0 mm	± 0,11 ± 0,10 ± 0,05
Projected fiber length > 2,2 mm 1,8 – 2,2 mm < 1,0 mm	± 0,11 ± 0,10 ± 0,05
Fiber width > 25,0 µm 23,5 – 24,9 µm < 20,0 µm	± 1,0 ± 0,8 ± 0,6
Fiber wall thickness > 5,0 µm < 5,0 µm	± 0,5 ± 0,3
Fiber curl > 14,0 % < 14,0 %	± 1,6 ± 1,8
Fiber coarseness > 0,165 mg/m < 0,165 mg/m	± 0,014 ± 0,009
Cross-sectional area (CSA) 360 – 510 µm ² < 280 µm ²	± 43 ± 15
Volume Index 0,600 – 1,050 · 10 ⁶ µm ³ < 0,300 · 10 ⁶ µm ³	± 0,092 ± 0,020
Arithmetic fines content > 30 % 20 – 30 % < 20 %	± 5,0 ± 3,8 ± 2,5
Length-weighted fines content > 2 % < 2 %	± 0,5 ± 0,4



Figure 11. An example 2D-picture of a fiber cross-section as seen by the fiber analyser (Anonymous 2006).

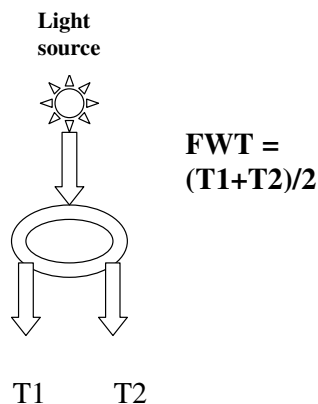


Figure 12. Calculation of the fiber wall thickness (FWT) value (Anonymous 2006).

4.5 SEM

Microscopic examinations of shrinkage-swelling behavior of pulp fibers and kraft hand sheets have previously been studied, for example, by Weise (1997), Enomae and Lepoutre (1998), as well as by Moss and Pere (2006).

Samples for SEM studies have to be dry. The dimensions of wet fibers change if the fibers are air-dried. Freeze-drying helps in preserving the wet dimensions. The sheets dried to absolute dryness were not freeze-dried, and were extracted to an exsiccator until embedded in epoxy resin (Struersin Epofix) prior to the cutting of the samples. Samples were cutted perpendicularly to the fiber direction. Grinding (Struersin

Dap-V) and polishing of the sample was done according to Reme et al. (2002). Sheet thickness was measured within each frame at 30 different locations (interval of 5 μm applied). This should smooth out the surface roughness effect in order to give us reliable results. The sheets were investigated at three different moisture contents. The pictures were taken after wet pressing, after oven drying of the sheets (~1-2% RH), and after conditioning to 50% RH and 90% RH. The corresponding moisture content (MC) of the sheets was roughly 33%, 1%, 7%, and 15%, respectively.

In this study, for the SEM images of fractionated sheets, pulp fractions were obtained by fractionating the pulp sample with a Bauer McNett Classifier (BMC). Isotropic handsheets with a standard laboratory hand sheet former were prepared for testing.

4.6 Hygroexpansivity measurements

4.6.1 OPTIDIM hygroexpansivity measurement apparatus (IV, V)

Digital correlation techniques have also been applied to hygroexpansion measurements (Kajanto and Niskanen 1996; Lif et al. 1995). A speckle pattern is created on a paper surface, either by spraying colored particles or by using natural speckles (by utilizing surface roughness or basis weight variation). In this study, a natural speckle pattern was used based on basis weight variations. Images are taken by a high-resolution CCD camera and then digitized. These techniques make it possible to obtain detailed information on two-dimensional hygrodeformation without physical contact. One disadvantage is that out-of-plane deformations such as curl and cockle (Glynn and Jones 1959; Kajanto 1992) that occur during the humidity change significantly deteriorate the accuracy of this technique.

OPTIDIM is an optical method for measuring the dimensional stability of paper under varying humidity conditions. The sample, which was placed in a humidity control cabinet, and after each humidity change and after equilibrium had been reached with the surrounding air moisture content and the moisture content of the sample, was put between weighted glass plates to prevent any out-of-plane dimensional changes and transilluminated with a bright light from the bottom, and a picture was taken from above with a CCD camera (Figure 13). By placing the weight on top of the sample just before a picture is taken, the friction between the glass and the sample was minimized. The glass weight was chosen according to ISO 8226-2:1990 based on the grammage of the handsheets. The variations in brightness level caused by the formation of the paper were measured. The dimensions of the samples at low relative humidity were compared with the dimensions at higher relative humidity. The dimensional changes as a function of relative humidity were then calculated (Kajanto et al. 1996). Six parallel square-shaped sheet samples (7 x 7 cm) were prepared for each sample. With OPTIDIM, both directions, machine and cross (MD and CD), are measured simultaneously. Relative humidity was changed linearly from standard (50% RH) to low (10% RH), then back to 50% RH, and to a higher humidities (70% RH and 90% RH) and back to standard (50% RH) humidity for 4 h per cycle from one relative humidity to another at 23 °C. The samples were also weighed at the moisture content used and thus the moisture content (%) of the paper can be measured. The hygroexpansion coefficient (β) was determined from the gradient of the linear part of the curves in the low-moisture range and is expressed as hygroexpansional strain divided by the change in moisture content of the sample (Nanri 1993).

$$\beta = \text{dimensional change (\%)} / \text{MC change (\%)} \quad (9)$$

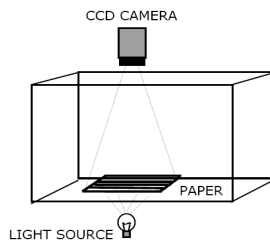


Figure 13. The measurement principle of the OPTIDIM measurement apparatus used to measure the hygroexpansivity of the sample (Kajanto and Niskanen 1996).

4.6.2 Laser measurement apparatus (V, VIII)

A non-standardized apparatus based on laser measurement of the dimensional change in the sample length was used to measure the hygroexpansion of paper strips. Hygroexpansion was measured based on ISO 8226-1 using paper-strips with 15 mm width and a span of 100 mm between the clamps. The measurements were performed on the STFI Hygroexpansivity Tester, an instrument developed at STFI-Packforsk, schematically presented in Figure 14.

It consists of pairs of rigid and freely movable clamps with a gap between the clamps of 100 mm. Even up to thirty paper strips can be measured independently in a horizontal position. A weight was placed upon the strips to eliminate any effects of buckling during registration of lengths. These clamps were placed in a chamber with regulated humidity. Movement of the clamp was measured by a laser detector.

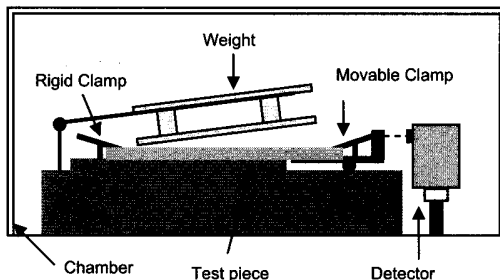


Figure 14. Schematic figure of the laser measurement device used to measure the hygroexpansivity of the paper strips (Antonsson et al. 2008).

The relative humidity was changed from $50\pm 2\%RH$ to $22\pm 3\%RH$ to $33\pm 2\%RH$ to $66\pm 2\%RH$ and the differences in lengths were measured between $33\pm 2\%RH$ and $66\pm 2\%RH$ in accordance with ISO 8226-1:1994. The hygroexpansion coefficient, β , was calculated according to (Nanri et al. 1993).

4.6.3 The Creep Measurements (VIII)

The creep measurements at both constant and with variations in relative humidity were performed on an apparatus developed by Haraldsson et al. (1994). It allows measurements with a load, both in tension and compression, during any period of time and with any humidity profile to be conducted; and the principle construction of the apparatus is shown schematically in Figure 15. The apparatus was placed in the humidity chamber that can generate conditions between 10 and 90% RH at $23^{\circ}C$.

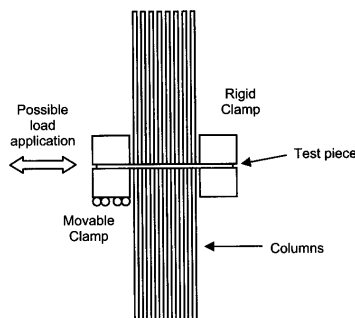


Figure 15. Schematic figure of the creep apparatus used (Haraldsson et al 1994). The function of the columns is to stabilise the test piece in compression mode measurements, hindering macroscopic buckling of the material. Strain gages measure the strain obtained between the clamps (Haraldsson et al. 1994).

In this study, the samples used were dried and bleached commercial pulp samples. The samples were cycled without load between 50% RH and 90% RH at least four times before testing to release “dried-in stresses”. Mechano-sorptive creep tests under tension were performed by changing the relative humidity between 50% RH and 90% RH. The cycle time was 7h, and three cycles, starting and ending at 50% RH

were performed. By using the strain values after three cycles and the corresponding stress values, isocyclic plots were constructed and the isocyclic creep stiffness determined, as schematically illustrated in Figure 16. It has been reported that the strain value should be limited to a maximum of 0.2% to ensure measurements within a linear region (Panek et al. 2004).

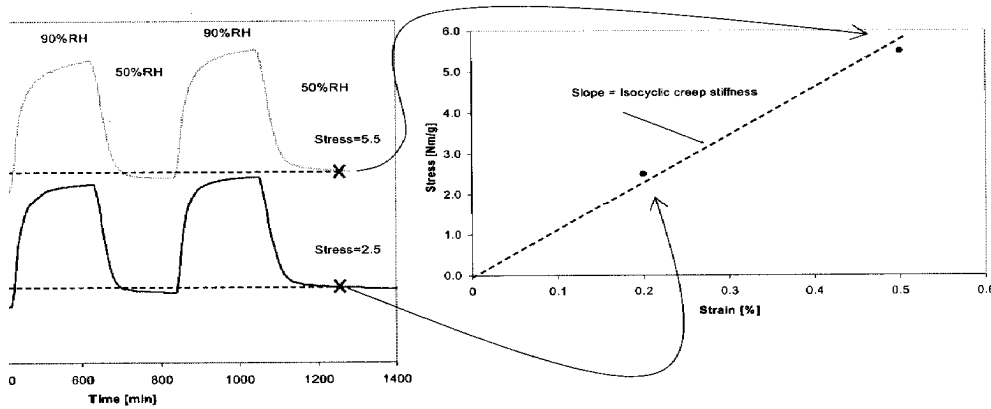


Figure 16. Schematic illustration of how isocyclic creep stiffness can be determined from the measured data (Panek et al. 2004).

5 MATHEMATICAL ANALYSIS

5.1 Calculation of distribution moments

Fiber property distributions are in many cases described only by their mean value and standard deviation, even though their shape is sometimes far from a normal distribution. To improve modeling of the tail of the distribution, higher order statistical moments, such as skewness and kurtosis, have been advocated in the literature (Randolph and Larson 1988). In particular, cubic (skewness) and quadratic polynomials (kurtosis) of Weibull distributed random variables have been proposed for preserving the first four moments of the data. It is well known that skewness and kurtosis estimated from small samples tend to be highly biased and uncertain (Pandey 2001). On the other hand, using only the first two moments can be inadequate for proper characterization, especially if the tail of the distribution is long.

The definition of an i^{th} order central statistical moment in terms of the density function, $f(x)$.

$$\mu_i = \int_0^{\infty} f(x)(x - x_0)^i dx \quad (10)$$

where x_0 is the mean of the distribution. The first two moments are the mean and standard deviation of the distribution. To improve modeling, third and fourth moments are also included. The third moment (skewness) provides a measure of the asymmetry of the density function. When distribution is skewed to the left, the skewness has negative values. The fourth moment (kurtosis) provides a measure of the “height” of the density function in relation to normal function. When the distribution peak is lower than for a corresponding normal distribution fitted to the same data, kurtosis has a negative value. Both skewness and kurtosis have a value of 0 for a normal distribution.

5.2 Weighting of distributions

Several studies have established the effect of wood fiber dimensions and morphology on certain mechanical properties of wood fiber-based products such as paper, paper board, medium-density fiberboard, hard board and wood- polymer constitutes (Paavilainen 1994a; Wangaard 1962; Vianna Doria 1991; Uesaka and Moss 1997; Pulkkinen et al. 2008b). Also, attempts have been made to link fiber distributions to in-plane hygroexpansional properties (Pulkkinen et al. 2009a). Suitable mathematical

distributions are available to accurately describe wood fiber distributions over various size regimes (Seth et al. 1997; Neagu 2006; Wathén 2006; Pulkkinen et al. 2006; Lu et al. 2007). For example fiber wall thickness data has been successfully modelled with Weibull distribution (Seth et al. 1997; Pulkkinen et al. 2006).

For fiber dimension determination, the general measurement methods include microscopy, projection, screen classification (e.g., Bauer-McNett classifier) and other particle size analyser (e.g., Kajaani FS-200) and image analysers (e.g. Kajaani FiberLab®). Particle size analysers provide the most popular automated techniques for fiber length measurement in the pulp and paper industry. Compared with other automated techniques, image analysers have high accuracy, fast speed and high reliability also for determining fiber length, fiber width and coarseness (Mark and Gillis 1983). FiberLab® fiber analyser is the only analyser today to measure the fiber wall thickness (Anonymous 2006).

The distribution of fiber lengths was found to be approximately normal when measured with Bauer-McNett classifier (Tasman 1972). It was also reported that fiber length distribution was approximately log-normal (Dodson 1992; Kropholler and Sampson 2001; Lu et al. 2007).

Failure to properly characterize an underlying distribution can lead to drastic errors in both analytical and simulation models (Law and Kelton 2000). The Weibull and lognormal families of distributions have been used with great success to model positively skewed variables (Pulkkinen et al. 2006; Lu et al. 2007). An example of two pulps that can have similar mean values for fiber length but significantly different fiber length distributions is given in Figure 17.

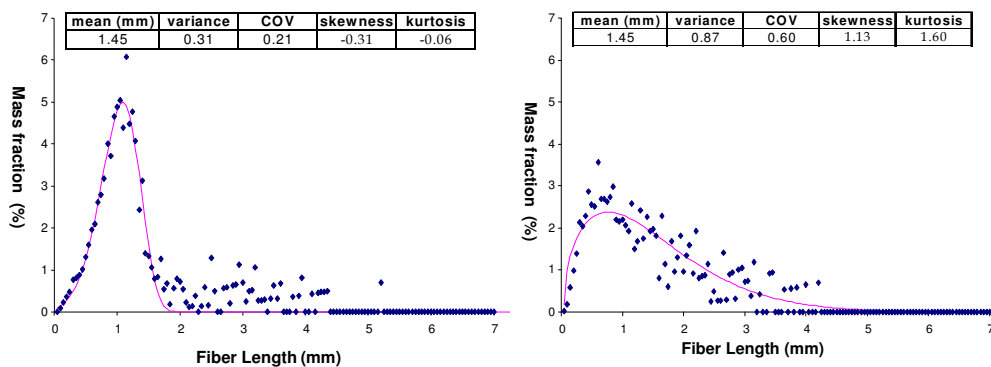


Figure 17. The weight-weighted fiber length distributions for a CTMP-mix (left) and TMP (right). Dots represent the measured data, and solid lines are the fitted Weibull distribution function (Pulkkinen et al. 2006).

This kind of approach in handling pulp fiber properties can be a significant asset in controlling the papermaking potential of pulp. When concentrating on property distributions, especially fiber dimension distributions, the heterogeneity of papermaking material can be taken in consideration. The dimensions and physical properties vary considerably between fibers and even inside an individual fiber. Depending on the physical property, the weight-weighted property distribution can be significantly different from the arithmetic or length-weighted distributions. The weight-weighted mean fiber length has been found to relate better to sheet properties than the arithmetic mean, and is considered more realistic (Clark 1985). In papermaking, fibers are used by weight. Therefore, it is more reasonable to use weight-weighted means and distributions instead of arithmetic or length-weighted means (Seth et al. 1997). Mean values, problems associated with their use and their significance in fiber physical properties are discussed for example by Seth and Jang (2004). They assess the use of population-, length-weighted- and weight-weighted mean values.

Weighting of fiber wall thickness data has been discussed for example by Richardson et al. (2003) and Pulkkinen et al. (2010). It was proposed earlier that fiber wall thickness measured with FiberLab® should be volume-weighted (Richardson et al. 2003). This was based on the better correlation with the wood tracheid wall thickness dimensions. When correlating fiber wall thickness data with paper technical

properties, the use of population weighted data for fiber wall thickness is recommended (Pulkkinen et al. 2010).

5.3 Statistical analysis

5.3.1 Correlation analysis

The dependencies between variables were screened with the help of simple correlation analysis. The basic principle was to find those variables with the most explicatory power to characterize the properties of eucalypt kraft pulp samples. The criterion was the variances between variables (R^2). The origin of each dataset was taken into consideration by grouping them depending on the laboratory which analysed the samples and that the same analyser was used for each of the datasets.

In the stage of a project, when little is known about the problem, an overview can be obtained with principal component analysis (PCA) (Eriksson et al. 1999). PCA produces a summary showing how the observations are related and if there are deviating observations or groups of observations present in the data. Principal component analysis aims to establish the number of hypothetical, independent components that account for the majority of the total variance of the variables.

5.3.2 Factor analysis

The factor analysis differs from principal component analysis since it analyses the common variance rather than the total variance of the data. The common variance represents the amount of variance that is shared among a set of items that can be explained by a set of common factors. The basic principle is the same as it tries to resolve the common variance into hypothetical common factors. Usually, the number of common factors is the same as the number of principal components.

Common factor analysis calculates a matrix that shows the relationship between the derived common factors and the variables. The elements of the matrix are termed “factor loadings”. The elements of a row in the matrix can be considered as regressions coefficients relating a variable to the factors. The factors were rotated mathematically to an orientation where they load (i.e. correlate) as strongly as possible with certain variables, whilst minimizing their loading on others exist. In this study, a “varimax” criterion (readily available in MATLAB) was used (Keiser 1958).

5.4 The wet-pressed density

In order to describe the extent of drying shrinkage potential of fiber mixtures, the concept of wet-pressed apparent density is introduced. Wet pressed apparent density for the handsheets is calculated by dividing a theoretical handsheet cross-section into rectangles of equal areas, and each grid in a sheet y-z-plane representing one oval shaped fiber cross-section and a void space between fibers. Fibers are packed in an orderly manner by using fiber length as the x-dimension of the grid (Figure 18). The fibers in the sheet are thus anisotropic. The amount of bonding between fibers is not directly included. Fiber wall thickness distribution, fiber width distribution, and fiber length distribution of un-refined fibers measured by the FiberLab®-analyser were used in the calculation of ρ_{wet} . It therefore includes the whole mass distribution of fiber material. It is calculated as

$$\rho_{wet} = \sum_{i=1}^n m_{Fi} \quad (11)$$

where $\sum_{i=1}^n m_{Fi}$ is the sum of the masses of individual oval shaped fibers in an area of a cubic meter. Each

layer in a handsheet is of a thickness of two fiber wall thicknesses. A lumen volume of 10% was included in the calculations. It is therefore assumed that most of the hardwood fibers are readily collapsed (no visible lumen space) at the beginning of drying. This is a safe argument, since most of the softwood pulp fibers are collapsed at the beginning of drying (Paavilainen 1994b). The estimate for the lumen volume

was based on our previous measurements (Pulkkinen et al. 2008a), together with evidence from SEM pictures, from where it can be seen that a major portion of eucalypt fibers are collapsed in their wet pressed state. A cell wall material density of 1.5 g/cm^3 was used to calculate the mass of the fibers. Since we are dealing with a relative measure of fiber properties, the value we choose does not make any difference. If the variations in the moisture content of the fibers would be included in the calculations, the cell wall material density varies according to the amount of moisture inside fiber wall. For example, when WRV is 1.5 g water per 1 g dry pulp, fiber wall density is approximately the used 1.5 g/cm^3 . If WRV is increased to 2.0 g water per 1 g dry pulp, fiber wall density becomes 1.9 g/cm^3 . This variation is not considered in the calculations, as only parameters that can be obtained from the FiberLab®-analyser were used. Fiber walls are assumed to be intact and there are no pores. It should be further noted that the fiber dimensions obtained and presented are for wet fibers. This is supposed to describe the swollen state of the fibers in their wet-pressed state.

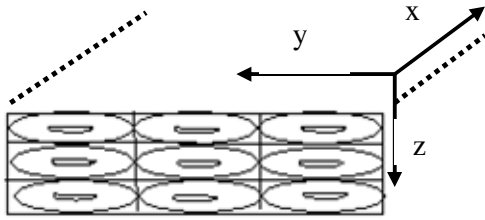


Figure 18. Cross-section of the handsheet used in calculations.

5.5 The activation parameter

Fiber segment activation modifies originally curly or otherwise deformed fiber segments, unable to carry the load, into active components of the network (Giertz 1964; Giertz and Roedland 1979; Lobben 1975). Activation of fiber network occurs during drying, when lateral shrinkage of fibers is transformed into axial shrinkage of neighbouring fibers in bonded areas. In restrained drying, the free fiber segments dry under stress and the slackness is therefore removed (Figure 19) (Giertz 1964; Giertz and Roedland 1979; Lobben 1975). Activation leads to a phenomenon called the Jentzen effect (Jentzen, 1964) where the axial elastic modulus in the fibers increases. This happens because the fiber is dried under axial load, it is straightened causing dislocations and other defects to be pulled out. This should also lead to reduced fibril angle and the rearrangement and alignment of hemicellulose and cellulose chains parallel with the external load (Figure 20). Inter-fiber bonding and shrinkage of fibers are the requisites for activation. The amount of drying stress needed to activate fiber segments depends on the morphology of the fibers (Retulainen 1997). By combining two important pulp fiber property distributions, fiber wall thickness and fiber curl distributions, the activation potential of the fiber network can be characterized (Pulkkinen et al. 2010).

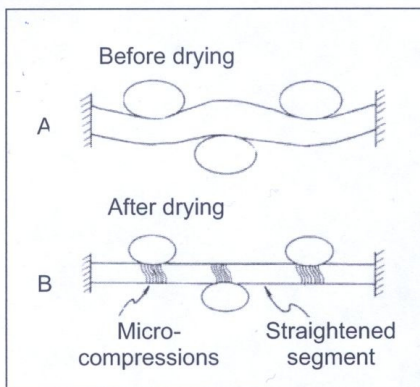


Figure 19. Schematic fiber (A) before and (B) after restrained drying (Giertz 1964).

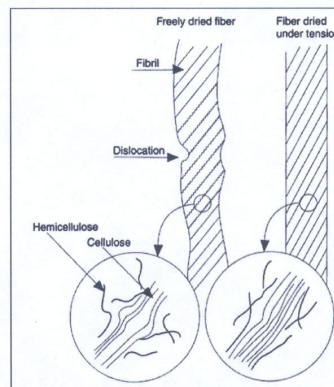


Figure 20. Schematic representation of the probable structural changes involved in the Jentzen effect (Vainio 2007).

In this Thesis, a great deal of effort is directed in investigating how fiber wall thickness can be linked to drying shrinkage, and therefore to development of paper technical properties such as tensile strength and

handsheet density. Weighting of fiber characteristic data may also be beneficial. For example, a more sophisticated evaluation of fiber analyzer data can be applied to stress the most important fractions of a given fiber property distribution with respect to the mechanical and structural properties, and this would improve the prediction accuracy of the developed model. When trying to find the best weighting for the factors of the activation coefficient model, various ways to weight fiber wall thickness has been used. The population average of fiber length has been found unsuitable for predicting the strength properties of sheets formed (Clark 1985) and therefore the use of either length-weighted values or preferably weight-weighted or volume-weighted values has been suggested by several authors (Robertson et al. 1999; Richardson et al. 2003; Jang and Seth 2004). When correlating fiber analyzer data against dimensions measured from wood, volume weighting of the data was applied by Richardson et al. (2003). However, a commonly accepted weighting procedure for fiber wall thickness data is not available. All fiber dimension measurements carried out in this study were made with a FiberLab® fiber analyser (Anonymous 2006). The correlation of volume-weighted data on fiber wall thickness and the dimensions of fibers in the wood matrix found by Richardson et al. (2003) make it worth trying to establish a parameter including volume-weighted fiber wall thickness. On the other hand, population weighted data emphasizes the importance of fines and fiber wall fragments. Therefore, the consideration of both the population weighting and volume weighting of the data is justified. Water retention value and fiber defects alone can explain majority of the differences observed in strength and stiffness, as stated by Mohlin and Hornatowska (2006).

Other properties of interest, such as hygroexpansion and mechano-sorptive creep, are also dependent on the inter-fiber bonding between fibers and the structural properties of the fiber network (Antonsson et al. 2010). Both, the tensile properties and the hygroexpansivity rely heavily on water retention value, i.e. the total water inside the fibers and fiber wall.

Equations 12 – 16 have been constructed based on the parameters found to be most important to account for fiber network. Equation (12) is based on the mean values of fiber wall thickness and curl population, and it is calculated from fiber raw data. Equation (13) takes into consideration the distribution of these parameters over the whole range of fiber space, i.e. individual fiber characteristics are multiplied before dividing them into their respective classes.

$$A(n) = \frac{\sum_{i=1}^n (fwt_i)}{n} \times \frac{\sum_{i=1}^n (curl_i)}{n} \quad (12)$$

Each population fraction has a value of $(fwt_j \times curl_j)$, and the distribution is calculated as

$$P(n_i) = \frac{(fwt_j \times curl_j)}{\sum_{j=1}^m (fwt_j \times curl_j)} * 100\% \quad (13)$$

where A is the mean activation coefficient, P is the distribution function, fwt_i and $curl_i$ are fiber wall thickness and fiber curl of an individual fiber, respectively, given by the fiber analyzer, i is the fiber index, j is the fraction index and n the number of fibers. Using equation (13) we are taking a corresponding fiber curl index and fiber wall thickness of individual fiber, therefore focusing more on the overall effect of fiber shape and size on handsheet properties.

To test whether fiber mass has significant influence on the tensile and structural properties, a second set of equations was constructed, first by using the volume-weighted data of fiber wall thickness and fiber curl mean (Equation 14), and then by utilizing the whole distributions of fiber properties by multiplying the individual characteristics and dividing them into their respective classes (Equation 15).

$$A(v) = \frac{\sum_{i=1}^n (v_i \times fwt_i)}{\sum_{i=1}^n v_i} \times \frac{\sum_{i=1}^n (v_i \times curl_i)}{\sum_{i=1}^n v_i} \quad (14)$$

Each volume fraction has a value of $(fwt_j \times curl_j \times v_j)$, and the distribution is calculated as

$$P(v_i) = \frac{fwt_j \times curl_j \times v_j}{\sum_{j=1}^m (fwt_j \times curl_j \times v_j)} * 100\% \quad (15)$$

Where the volume of an individual fiber was calculated according to

$$v = (L_c \times \pi \times fwt \times (fw - fwt)) / 1000, \mu\text{m}^3 \quad (16)$$

The first four moments of equations (12)-(15) were calculated according to equation (10) and correlated against the handsheet properties.

The water-retention value of undried eucalypt pulp samples (Pulkkinen et al. 2008b) was high for thin-walled fibers and low for thick-walled fibers. The authors assumed that the water retention value as an additional variable would be beneficial. Fiber wall thickness and curl have a similar behavior and therefore it is advisable to work with the inverse of the water retention value and doing so, the effects of fiber swelling can be emphasized. When the fiber network activation is improved, the value of activation parameter value must decrease. At the present state, the model may be valid for eucalypt fibers only. In the case of softwoods, fiber length can be of importance and should be added to the model.

WRV was calculated from a linear correlation obtained from the comparison of the mean values of fiber wall thickness against water retention values of unrefined fibers. The effect of WRV value on activity coefficient was examined by increasing fiber wall thickness and fiber curl to the power of the inverse of water retention value (WRV) by means of the Equations (12)-(15). For example, Equation (12) will take the form of

$$A(n) = \frac{\sum_{i=1}^n (fwt_i^{(1/WRV_i)})}{n} \times \frac{\sum_{i=1}^n (curl_i^{(1/WRV_i)})}{n} \quad (17)$$

There appears to be no analytical model in the literature on the role of fiber properties in the development of fiber network activation. It is known that fiber curl and micro-compressions influences tensile strength negatively (Page et al. 1985). Fibers with low fiber wall thickness influence tensile strength and handsheet density positively (Paavilainen 1991, 1993). No model pulls these observations together to explain how fiber network activation varies with changes in curl, fiber wall thickness and fiber swelling, and how to make observations on the relative importance of inter-fiber bonding and network activation based on the measured fiber properties at different handsheet densities.

The values of the activation parameter were used to describe the bonding and activation phenomena by correlating them with tensile- and structural properties. The reduced strength potential of industrially refined fibers (MacLeod et al. 1987, 2005) can be characterized using the activation coefficients introduced. The effect of fiber straightening when fibers are refined is avoided by comparing the raw data of unrefined fibers against the paper technical properties of PFI-refined fibers. The effect of the change in fiber curl as a function of refining is therefore excluded.

6 RESULTS

6.1 Changes in distributions induced by refining (II)

Low Consistency (LC) refining has long been used to improve the tensile strength of paper, but the mechanisms creating these improvements are not yet fully understood. The primary effects of refining are the creation of new surfaces, the creation of new particles and structural changes to the fibers (Hietanen and Ebeling, 1990). The major changes in fiber morphology that occur in refining have been thoroughly studied (Page 1989; Kibblewhite 1989). The refining of kraft pulp fibers affects the cross-section dimension of the fiber, fiber length and fiber coarseness. LC refining also straightens the fibers therefore making pulp stronger. The physical properties and the response to refining of never-dried and dried chemical pulps differ (Scallan and Tigerström, 1992; Laivins and Scallan, 1996; Seth, 2001). Dried and rewetted fibers are stiff, never-dried more flexible or conformable. Correspondingly, the walls of dried and rewetted fibers are stiff. The difference between the refining response of dried and never-dried fibers is mainly due to the hornification effect (Laivins and Scallan, 1996; Stone and Scallan, 1968). In this work, hornification refers to the irreversible loss of water absorption capacity in drying.

In an attempt to characterize the uniformity and quality of fibers, it has previously been suggested, that instead of focusing on the mean values, the heterogeneity of the fiber material should be taken into account (Kerekes, 2005; Jang and Seth, 2004). When relying solely on the mean values, the heterogeneous nature of the fiber property remains unclear. The dimensions, physical properties and property distributions vary considerably between fibers. It is an interesting idea to investigate whether the width or the shape of the distribution (second and third central moment of the distribution, respectively) can be used to predict the technical properties of paper. In this study, refining did not change the mean of length-weighted fiber length distributions (Table 3).

The width of once-dried eucalypt fibers either increased or remained unchanged when refining energy was applied. The response to refining for dried and rewetted fibers deviated markedly from that of once-dried fibers, where fiber width generally increased, rather than decreased.

The mean width of once-dried eucalypt pulps was slightly increased (Table 4). The results of the refining process are seen more clearly when considering the whole distribution. The relative changes in the mean values of the fiber width were minor, but changes in standard deviation and skewness were more distinctive (Table 4).

Table 3. Effect of energy loads on the mean fiber dimensions measured with FiberLab® analyzer.

Pulp	refining energy (kWh/t)	fiber length (mm)	width (µm)	wall thickness (µm)	cross-sectional area (µm ²)
<i>E.Urograndis</i> <small>un-dried</small>	0	0.82	15.9	3.3	180
	40	0.82	15.7	3.4	185
	80	0.82	16.0	3.5	190
	120	0.81	16.0	3.5	187
<i>E.Grandis/E.Dunnii</i> <small>un-dried</small>	0	0.81	15.9	3.4	182
	40	0.82	16.2	3.6	191
	80	0.82	16.0	3.7	192
	120	0.82	16.3	3.7	195
<i>E.Grandis/E.saligna</i> <small>un-dried</small>	0	0.80	16.0	3.1	174
	40	0.81	16.4	3.4	185
	80	0.82	16.3	3.4	188
	120	0.81	16.2	3.4	187
<i>E.Nitens/E.globulus</i> <small>un-dried</small>	0	0.81	16.0	3.3	189
	40	0.82	16.0	3.5	186
	80	0.81	16.4	3.6	199
	120	0.82	16.0	3.5	190
<i>E.Urograndis</i> <small>dried</small>	0	0.83	15.4	3.3	178
	40	0.81	15.3	3.3	175
	80	0.81	15.2	3.2	175
	120	0.80	15.2	3.2	173
<i>E.Grandis/E.Dunnii</i> <small>dried</small>	0	0.81	15.8	3.4	187
	40	0.81	15.7	3.4	187
	80	0.80	15.6	3.4	184
	120	0.80	15.5	3.3	181
<i>E.Grandis/E.saligna</i> <small>dried</small>	0	0.79	15.9	3.1	178
	40	0.79	15.6	3.1	177
	80	0.78	15.4	3.1	177
	120	0.78	15.4	3.1	176
<i>E.Nitens/E.globulus</i> <small>dried</small>	0	0.82	15.6	3.3	178
	40	0.82	15.6	3.3	175
	80	0.80	15.6	3.3	175
	120	0.80	15.5	3.4	173

Table 4. Characteristics of discrete fiber width distributions and their relative change in refining.

before refining	E.grandis/E.saligna _{un-dried}	E.nitens/E.globulus _{un-dried}	Eurograndis _{un-dried}	E.grandis/E.dunnii _{un-dried}	E.grandis/E.saligna _{refined}	E.nitens/E.globulus _{refined}	Eurograndis _{refined}	E.grandis/E.dunnii _{refined}
mean (μm)	16.0	16.0	15.9	15.9	15.9	15.6	15.4	15.8
variance (μm)	6.07	7.34	7.66	5.67	7.40	7.27	6.36	6.46
skewness	8.73	14.58	9.45	13.19	10.75	16.58	8.85	9.40
after refining								
mean (μm)	16.2	16.0	16.0	16.3	15.4	15.5	15.2	15.5
variance (μm)	5.93	5.77	8.21	6.15	5.80	6.88	6.12	6.70
skewness	9.03	9.02	13.80	11.98	11.99	10.12	9.04	3.14
Δ mean (%)	1.41	-0.40	0.46	2.39	-3.78	-0.47	-1.64	-2.12
Δ variance (%)	-2.44	-27.19	6.63	7.88	-27.70	-5.60	-3.82	3.50
Δ skewness (%)	3.35	-61.65	31.55	-10.06	10.36	-63.83	2.06	-199.75

The mean of the fiber wall thickness of the once-dried eucalypt fiber samples increased as refining energy was applied and the distribution of wall thickness became more heterogeneous (Figure 21) when the fiber wall swelled. As far as the relative changes in fiber characteristics are concerned, both the mean values and the standard deviations changed moderately (Table 5). However, there was no clear pattern of how fiber wall distributions behave. The standard deviation of once-dried fibers of *E. urograndis* was reduced significantly. The decrease in skewness was high for once-dried fibers. This is probably due to the detachment of fragments from the fiber wall to create new particles. This cannot be seen in length-weighted fiber length distributions, since in length-weighted distribution the influence of fines and cell fragments is compensated.

The mean of the fiber wall thickness of the dried eucalypt fibers remained practically the same. In contrast, the distributions of cell wall thickness were affected significantly. Dried fibers are more rigid than once-dried fibers and they are more susceptible to damage in refining (Seth, 2001). Drying closes most of the large pores and a substantial amount of the small pores (Park et al. 2006). Even though the pore volume of previously dried pulps can be recovered by refining (i.e., the pulp can be re-swollen), some small pores, which are closed in drying, are not re-opened by normal levels of refining. In other words, some of the negative effects of refining can be compensated, but refining does not completely reverse hornification (Laivins and Scallan 1996). The relative decrease in skewness values varied between 30-250%. It seems that dried fibers delaminate more easily than once-dried fibers. The increase in swelling of the fibers could explain the unchanged mean of fiber wall thickness.

Table 5. Characteristics of discrete fiber wall thickness distributions and their relative change in refining.

before refining	E.grandis/E.saligna _{un-dried}	E.nitens/E.globulus _{un-dried}	Eurograndis _{un-dried}	E.grandis/E.dunnii _{un-dried}	E.grandis/E.saligna _{refined}	E.nitens/E.globulus _{refined}	Eurograndis _{refined}	E.grandis/E.dunnii _{refined}
mean (μm)	3.1	3.3	3.3	3.4	3.1	3.3	3.3	3.4
variance (μm)	2.15	2.22	2.35	2.07	2.43	2.26	2.42	2.30
skewness	2.38	2.16	4.17	1.14	4.92	4.65	6.44	3.27
after refining								
mean (μm)	3.4	3.5	3.5	3.7	3.1	3.4	3.2	3.3
variance (μm)	2.23	2.25	2.16	2.14	1.96	2.22	2.08	2.42
skewness	1.73	1.67	1.26	0.61	1.44	2.52	1.99	2.32
Δ mean (%)	8.68	4.97	5.38	7.35	-1.03	1.83	-2.41	-3.02
Δ variance (%)	3.74	1.40	-8.86	2.98	-23.87	-1.56	-16.32	4.79
Δ skewness (%)	-37.52	-29.22	-230.14	-85.59	-241.71	-84.77	-224.07	-40.94

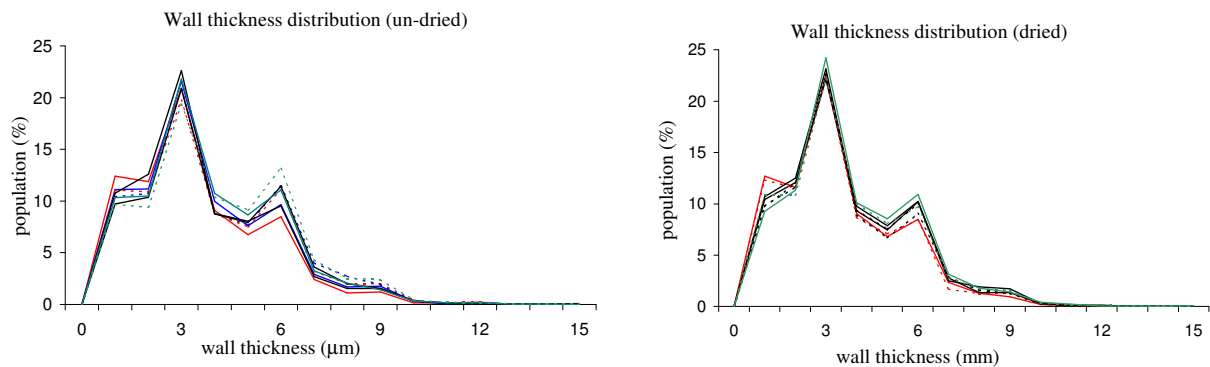


Figure 21. Fiber wall thickness distributions for once-dried and dried eucalypt fibers (refined fibers shown by dotted lines).

6.2 The drying shrinkage and cell wall thickness (III, VI)

Figure 22 shows that in the wet pressed state of the fiber network, i.e. with the assumption that fibers are mostly collapsed, the density is higher in a sheet containing more thick-walled fibers (associated with low WRV) than thin-walled fibers (associated with high WRV) for an anisotropic tightly packed network. When fiber network is dried, after which the handsheet density is measured, handsheets with higher fraction of thin-walled fibers are the ones with higher density. Based on this, it can be deduced that the difference in drying shrinkage potential is a greater force than fiber collapsibility (as the collapse degree is similar for all of the eucalypt kraft pulp fibers) in determining how handsheet properties will develop. This translates into smaller changes in the shape of thin-walled fibers in wet pressing. In this study, the drying shrinkage potential is considered as a property that keeps fibers in contact.

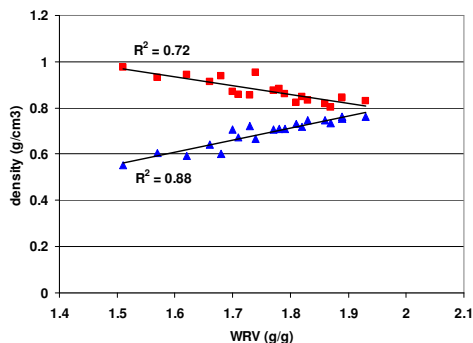


Figure 22. Measured density of the handsheets (triangles) and calculated ρ_{wet} (squares) as a function of WRV.

Fiber network consisting of thin-walled fibers have narrow drying stress distribution, especially in the case of eucalypt fibers (Mohlin and Hornatowska, 2006), therefore resulting in increased elastic modulus and tensile strength (Vainio 2007; Kärenlampi 1995) when the sheet is dried.

6.3 Correlations between variables (III)

Raw material morphological features (fiber length, fiber width, fiber wall thickness, apparent density) were used to explain the variability of physical properties of the hand sheets (bulk, tensile index, etc.). Table 6 shows the Pearson correlations (Milton and Arnold 1995) between the measured and calculated pulp fiber properties and the handsheet properties in the un-refined and refined state. The sample size was small ($n=20$), so the critical value for Pearson r to make results statistically significant ($< 1\%$) was quite high, 0.537 (the values that were not statistically significant are marked in Table 6 as n.s.). The mean value of fiber wall thickness and calculated apparent density correlated significantly with all measured properties at zero PFI revolutions and with all properties except light scattering at 500, 1000 and 2,500 revolutions. The standard deviation of fiber wall thickness correlated significantly with all properties except light scattering for both un-refined and refined pulps. Fiber wall thickness characteristics and apparent density had negative correlations with tensile index, air resistance and handsheet density, and the single greatest values found between wet pressed apparent density and handsheet properties. However, the correlations between fiber length and especially fiber width characteristics and paper technical properties were not so good. Micro fibril angle (MFA) was characterized for 12 samples. It correlated well with paper technical properties, as expected, but it also correlated well with fiber wall thickness index. This correlation is nothing new, for example Hiller (1964) and Courchene et al. (2006) observed this correlation between these two properties. However, the correlation was positive, as opposed to the results of other authors mentioned above. The reason for this could be that MFA was measured for young wood only (4-year old clones). The maceration procedure has also been seen to lower the MFA values in the S2-layer, therefore making the variability lower (Peura 2007). The values of MFA measured in this study (between $10-15^\circ$) are realistic considering the values obtained by others with X-ray diffraction, $9-18^\circ$ for *Betula pendula* (Birch)(Bonham and Barnett, 2001) and $10-20^\circ$ and $14-25^\circ$ measured for *Eucalyptus nitens* (Stuart and Evans, 1994; Evans, 1998). The MFA requires complicated measurement procedures

whereas fiber wall thickness index is simpler to measure with existing methods. For example Wimmer et al. (2002) do not give much credit to MFA as a predictor of handsheet properties of *Eucalyptus globulus*. Rather strangely, fiber width and fiber wall thickness index did not correlate. This can be due to the assumption of circular shaped fibers with the image analysis, when fibers are “scanned” only from one side and the level of collapse cannot be seen.

Table 6. Pearson correlation coefficients for the pulp properties fiber wall thickness (FWT) mean value and standard deviation and apparent density and four hand sheet properties at different PFI refining levels; coefficients are significant at $p < 1\%$, 2-tailed, $n=20$ (n.s.= not significant at $p < 1\%$).

Parameter	Fiber length _{mean} (mm)	Fiber length _{stdv.} (mm)	Fiber width _{mean} (mm)	Fiber width _{stdv.} (mm)	FWT _{mean}	FWT _{stdv.}	app. dens.	Hemicellulose	MFA
Fiber length _{mean} (mm)	1	0.94	0.61	n.s.	0.78	0.89	0.77	n.s.	0.85
Fiber length _{stdv.} (mm)	0.94	1	0.61	n.s.	0.85	0.84	0.84	n.s.	0.74
Fiber width _{mean} (mm)	0.61	0.61	1	0.67	0.61	0.84	n.s.	0.54	0.54
Fiber width _{stdv.} (mm)	n.s.	n.s.	0.67	1	n.s.	n.s.	n.s.	n.s.	0.42
FWT _{mean}	0.78	0.85	0.61	n.s.	1	0.88	0.97	n.s.	0.84
FWT _{stdv.}	0.89	0.84	0.84	n.s.	0.88	1	0.87	0.54	0.86
app. dens.	0.77	0.84	n.s.	n.s.	0.97	0.87	1	n.s.	0.92
hemicellulose	0.50	n.s.	0.54	n.s.	n.s.	0.54	n.s.	1	0.66
MFA	0.85	0.74	0.54	0.42	0.84	0.86	-0.76	0.66	1
PFI=0									
TI (Nm/g)	-0.64	-0.68	n.s.	-0.65	-0.79	-0.79	-0.83	n.s.	-0.76
density (kg/m ³)	-0.66	-0.65	n.s.	-0.65	-0.83	-0.75	-0.88	n.s.	-0.56
light scatt. (m ² /kg)	n.s.	n.s.	n.s.	n.s.	-0.77	n.s.	-0.72	n.s.	-0.52
air res. (s)	n.s.	n.s.	n.s.	n.s.	-0.75	-0.74	-0.82	n.s.	-0.72
PFI=500									
TI (Nm/g)	-0.56	-0.55	n.s.	n.s.	-0.76	-0.78	-0.79	n.s.	-0.80
density (kg/m ³)	-0.65	-0.62	n.s.	n.s.	-0.82	-0.74	-0.88	n.s.	-0.61
light scatt. (m ² /kg)	n.s.	n.s.	n.s.	n.s.	n.s.	n.s.	n.s.	n.s.	n.s.
air res. (s)	-0.66	-0.62	n.s.	n.s.	-0.69	-0.76	-0.76	n.s.	-0.64
PFI=1000									
TI (Nm/g)	-0.58	-0.61	n.s.	n.s.	-0.77	-0.70	-0.78	n.s.	-0.78
density (kg/m ³)	-0.57	-0.54	n.s.	n.s.	-0.82	-0.73	-0.87	n.s.	-0.67
light scatt. (m ² /kg)	n.s.	n.s.	-0.52	n.s.	n.s.	n.s.	n.s.	n.s.	n.s.
air res. (s)	-0.65	-0.61	n.s.	n.s.	-0.69	-0.75	-0.75	n.s.	n.s.
PFI=2500									
TI (Nm/g)	-0.58	-0.60	n.s.	n.s.	-0.74	-0.70	-0.75	n.s.	-0.76
density (kg/m ³)	-0.55	-0.53	n.s.	n.s.	-0.81	-0.74	-0.86	n.s.	-0.56
light scatt. (m ² /kg)	n.s.	n.s.	n.s.	n.s.	n.s.	n.s.	n.s.	n.s.	n.s.
air res. (s)	-0.59	-0.54	n.s.	n.s.	-0.63	-0.73	-0.68	n.s.	n.s.

6.4 Principal Component Analysis and Factor Analysis (VI)

A principal component analysis was performed using 8 variables at 5 different levels of refining (PFI 0, 250, 500, 1000, 2500 revolutions). Table 7 shows that the number of variables to describe the “metafiber” properties of eucalypt fiber network was three. Over 98% of the total variability can be accounted for by these 3 components. An additional component would increase the proportion of accounted-for variance by only less than 1%. A factor analysis was undertaken to characterize the physical meaning of these factors. The variables used in the PCA are listed in Table 8.

Table 7. Principal component analysis of data for all samples.

PRINCIPAL COMPONENT ANALYSIS OF DATA FOR ALL SAMPLES		
	Proportion of Total Variance	Cumulative proportion
COMP 1	0.810	0.810
COMP 2	0.123	0.933
COMP 3	0.051	0.984
COMP 4	0.008	0.992
COMP 5	0.005	0.997
COMP 6	0.003	1.000
COMP 7	0.000	1.000
COMP 8	0.000	1.000

Table 8. Rotated factor patterns for samples.

	Factor 1	Factor 2	Factor 3
Tensile Index (Nm/g)	0.64	0.72	0.25
Air Resistance (s)	0.90	0.52	0.05
Density (g/cm ³)	0.90	0.40	0.10
Tensile Stiffness (kN/m)	0.68	0.67	0.19
Tear Index (Nm ² /g)	0.07	0.15	0.81
Light Scattering (m ² /kg)	-0.37	-0.86	-0.25
Scott-Bond (J/m ²)	0.56	0.80	0.14
Stretch (%)	0.72	0.50	0.47

In factor analysis, a linear relationship between variables is assumed. Therefore, some initial manipulation of the raw data was required when air resistance was converted to logarithmic scale. Also, the non-linear portion of the tear index data was excluded, as for some of the samples tear index was highest at the first (250 revolutions) refining point. This was related to fiber flexibility and the ease of refining.

The rotated factor pattern revealed that the three common factors accounted for 7.8 units of variance out of a total of 8 units (8 standardized variables). Factor analysis calculates a matrix that shows the relationship between the derived common factors and the variables. The elements of a row in the matrix can be considered as regressions coefficients relating a variable to the factors. Factor 1 accounted for almost 61% of the common variance. It is strongly and positively correlated with strength properties (tensile index, tensile stiffness index, Scott-Bond), density and air resistance and stretch. It has negative loading on the light scattering coefficient. This factor was seen to represent the combined effect of inter-fiber bonding and activation of fiber network. It reflects the underlying changes in fiber properties during beating which increase fiber network activation potential (internal and external fibrillation, fiber deformations etc.). Factor 2 accounted for 24.3% of the common variance and was loaded most strongly on light scattering (-) and Scott-Bond (+), having additional high loadings on tensile index, tensile stiffness index, and stretch. A probable interpretation is that it corresponds to the degree of microcompressions formed in the fiber. As fiber length was relatively constant among the samples, and considering the strong loads in tear (+) and stretch (+), factor 3 (14.7% of the common variance) accounted for the transverse dimensions of the fibers observed with the FiberLab® analyzer. Also, fiber curl was believed to influence this parameter as it exhibited a moderate negative correlation with the tensile stiffness index.

Separating the unrefined samples from the refined samples gives us further confidence in identifying the factors as stated above. As Table 9 indicates, the loadings of factor 1 on air resistance and handsheet density are smaller for unrefined than for refined pulp, and what is more important, the light scattering coefficient is not affected negatively by this parameter. Factor 2 has the opposite effect (+) on the light scattering coefficient and a substantially lower effect on Scott-Bond when the fibers were not refined. Furthermore, the effect of stretch is lower due to the fact that more microcompressions are formed in refining.

The effect of orientation on the determined factors was not studied, since only isotropic handsheets were used to measure paper technical properties. The factors determined are therefore applicable only to isotropic fiber networks. However, it can be deduced that factors 2 and 3 are likely to be more significant after refining. The transfer of stresses in the cross-direction of the fiber network due to the alignment of fibers is more pronounced after refining. In laboratory conditions, variations in wet-pressing pressure do not affect the predictability of the model due to the easily collapsible structure of eucalypt fibers. The increase in activation (~20%) due to increased wet-pressing pressure of laboratory handsheets was observed by Vainio (2007) for spruce kraft pulp. For eucalypt fibers, a similar increase in bonded areas and the increased number of bonds resulting in decreased free fiber segment length might not be observed because of the short, homogeneous fiber length distribution, initially highly collapsed fibers, and tightly packed structure.

Table 9. Rotated factor patterns for unrefined pulp samples.

	Factor 1	Factor 2	Factor 3
Tensile Index (Nm/g)	0.94	0.33	0.08
Air Resistance (s)	0.76	0.57	0.30
Density (g/cm ³)	0.72	0.63	0.27
Tensile Stiffness (kN/m)	0.89	0.43	-0.16
Tear Index (Nm ² /g)	0.00	0.12	0.71
Light Scattering (m ² /kg)	0.26	0.52	0.16
Scott-Bond (J/m ²)	0.86	0.24	0.07
Stretch (%)	0.76	0.35	0.54

6.5 Parameters developed (III, VI)

6.5.1 Wet-pressed density and paper technical properties (III)

Figure 23 shows the hand sheet density for different refining levels as a function of ρ_{wet} . The calculated wet-pressed density describes the pulp fibers in their swollen wet-pressed state for a tightly packed oriented handsheet (fibers aligned in axial direction). Fibers with low wet-pressed apparent density are thin-walled and produce dense sheets (high apparent hand sheet density) with improved bonding and fiber segment activation (fiber straightening) that results in higher tensile index values (Figure 24). The measured values of paper technical properties of un-refined and refined samples were then compared against the wet-pressed density calculated from the FiberLab® raw data results of the un-refined fibers. This was done in order to get as reliable data for fiber dimensions as possible. The physical changes associated with refining (internal fibrillation, external fibrillation) cannot be characterized with the FiberLab® fiber analyzer (V.3.0). The changes that fiber dimensions undergo during refining are relatively small and sometimes inconsistent. This makes the prediction based on refined fiber results impractical. The dimensions of un-refined fiber, however, correlate well with paper technical properties. Thus it seems that the original fiber structure is connected to fiber network property development when fibers are refined. The correlations were found to be linear. This was seen independent of the refining level of the fibers for the handsheet density and for the tensile index. Wet-pressed density values after refining were therefore only dependent on the original mass distribution of the un-refined fibers. Also tensile index and handsheet density values after refining depend only on the original mass distribution of the fibers. The previous handsheet density models (Amiri et al. 1991; Görres et al. 1989) rely heavily on all important fiber properties, i.e. fiber coarseness, fiber width, fiber thickness, fiber curl, fiber length, and wet fiber flexibility and also to applied wet pressing pressure. The latter three become insignificant when fiber length approaches that of hardwoods. The apparent density is also dependent on average free fiber length that is a function of fiber wall thickness. The measurement of the shape and the collapse degree of the refined fibers was out

of the scope of our investigation. Therefore, how fiber shape was altered by the refining procedure is not known. In refining, the swelling and conformability of the fibers is enhanced, fines are created and bonding is improved resulting in increased density and tensile index.

Less coarse fibers are known to form more closed network structures in a sheet. Additionally, the calculated wet-pressed apparent density is therefore expected to have strong correlation with sheet porosity indicated by air resistance. The logarithmic air resistance correlated well with wet-pressed density (Figure 25).

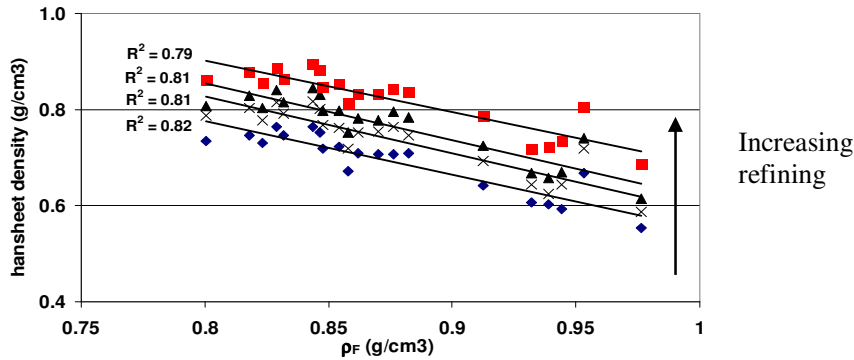


Figure 23. Hand sheet density as a function of wet-pressed density for different PFI refining levels.

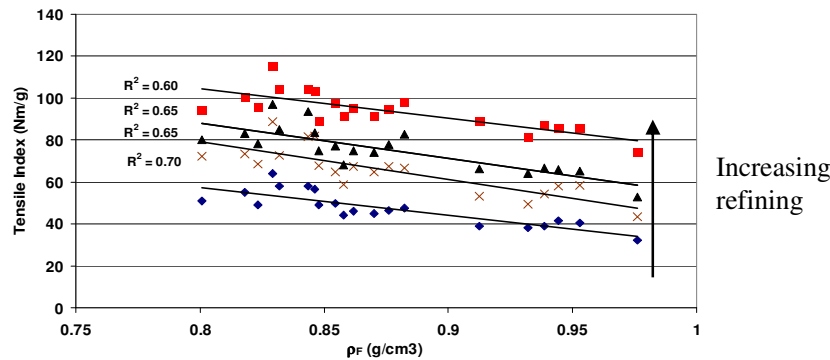


Figure 24. Tensile Index as a function of apparent density for different levels of refining.

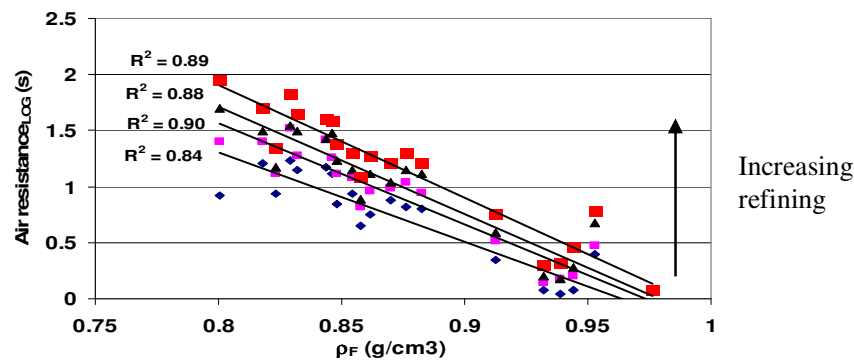


Figure 25. Logarithmic air resistance as a function of apparent density for different levels of refining.

The mass of the representative sample of fiber furnish as such appeared to be a useful parameter to predict strength-and structural properties of the handsheets made of un-dried eucalypt kraft fibers. This was enabled by the difference in the swelling behaviour of thin-walled and thick-walled fibers that surpass the effect of fiber collapse behaviour (See Chapter

6.2). All the properties can be measured directly from pulp fibers, so no additional measurements of paper technical properties are needed to make the simulations.

6.5.2 Activation parameter and paper technical properties (VI)

Generally, the fiber wall thickness distribution characteristics had positive correlation (both population weighted and weight-weighted distributions) with fiber curl, except for the kurtosis values of fiber wall thickness (negative correlation). Moreover, for the mean values, using the volume weighted fiber wall thickness improved the correlation with fiber curl. Apparently fiber curl has a better correlation with thick-walled fibers than with thin-walled fibers. The effect of beating on the increase of fiber swelling has been attributed to internal fibrillation of the fiber wall. The increased fiber swelling increases drying stresses that are beneficial to the tensile index and elastic modulus of the restraint dried fiber network (Htun and de Ruvo 1978).

Population weighting of fiber wall thickness data will be further influenced by the fines content of the samples. This is also believed to have an influence on the level of activation of the paper (Vainio et al. 2007b). Increasing fiber coarseness increases stretch potential when fibers are refined because thicker walled fibers may not flex elastically under mechanical stress in the refiner but undergo compression failure giving rise to kinks and micro-compressions (Mohlin and Hornatowska, 2006). For pulp samples refined in laboratory conditions, thin-walled fibers normally have a more angular fold, and thick-walled fibers have more kinks (Mohlin et al., 1996). Therefore a link between fiber wall thickness and curl index can be expected.

It was discovered that when weighting the wall thickness data, the correlations with the measured properties were worse than when using the population distributions. This could indicate that the amount of fines material was significant to activation behavior. The same trend was observed for other fiber characteristics calculated using the total distributions (Table 10).

Figure 26 shows the fit obtained when handsheet density and tensile strength values of unrefined and refined fibers (2,500 rev.) were plotted against the activation coefficient calculated from the mean values of the original fiber furnish dimensions (equations (12) and (14)). Refining modifies fiber properties in order to obtain the most desirable paper machine runnability and product properties. In addition to fiber morphology, inter-fiber bonding is greatly influenced by internal fibrillation introduced by refining, contributing to swelling and flexibility of fibers. The bond formation is also promoted by external fibrillation and fines formation (Retulainen et al. 1998).

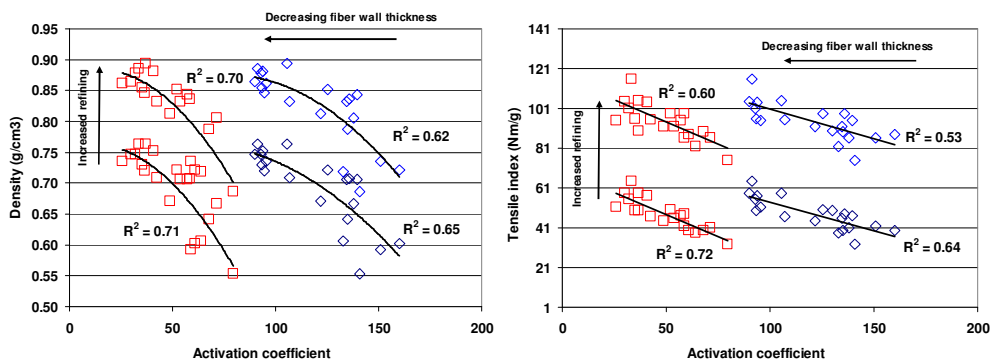


Figure 26. Comparison between the predictability of the apparent sheet density (left) and tensile index (right) based on the population- (squares) and volume-weighted (diamonds) activation coefficient for two different refining levels, PFI = 0 and 2,500 rev.

Alternative methods of implementing fiber wall thickness in the activity coefficient were investigated. By means of population weighted fiber wall thickness, more emphasis was placed on the amount of fibrils and fiber fragments in the pulp. Volume weighting of the wall thickness data underestimates the amount of small particles. Overall, activation coefficients based on the volume weighted mean had inferior correlation with the measured properties than did the activation coefficients derived from population weighted fiber wall thicknesses. The activation coefficient characteristics calculated using the total distributions again proved to be more accurate in describing the hand sheet properties (Table 10).

The inclusion of the WRV had a more pronounced impact on the correlations observed between the activation coefficient and handsheet density than on the correlations between the activation coefficient and tensile strength (Figure 27). In the case of handsheet density, the influence of water retention value on inter-fiber bonding can be seen as an improved correlation with the activation coefficient. This is understandable since thinner walled samples retain more water than thick walled samples (Figure 28), and at the same time fiber swelling affects fiber straightness by decreasing fiber curl.

The activity coefficient simulation results were less affected, when using volume-weighted values. This is an indication that fiber length and fiber width/wall thickness ratio may not be that important for the network activation coefficient of eucalypt fibers.

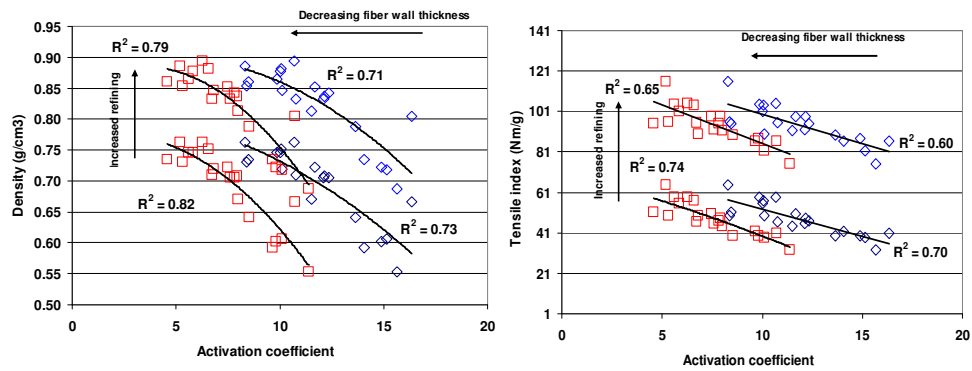


Figure 27. Comparison between the predictability of the apparent sheet density (left) and tensile index (right) based on the population- (squares) and volume-weighted (diamonds) activation coefficient with WRV for two different refining levels, PFI = 0 and PFI = 2,500.

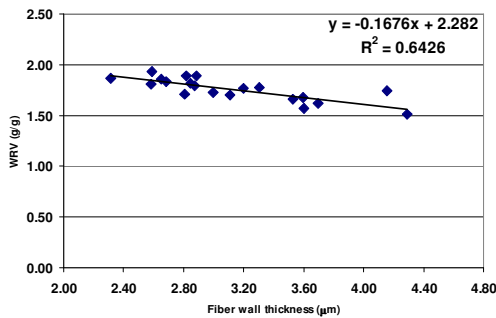


Figure 28. Water retention value as a function of fiber wall thickness.

The differences found in curve shapes for handsheet density and tensile strength can be explained by inter-fiber bonding and fiber network activation. Based on the hypothesis, the “refining response” or “activation potential” can be explained by a combination of increased inter-fiber bonding and a reduced number of incomplete active or “slack” fiber segments in

the fiber network. According to the early classification by Giertz and Roedland (1979), fiber segment activation depends on 1) fiber segment length (bond frequency), 2) fiber segment form (straight or curved), 3) bond area, and 4) degree of swelling of a crossing fiber. As fiber length was quite similar for all eucalypt fibers, bond frequency per fiber can be considered a constant. Increasing inter-fiber bonding is not the only effect of refining. Fiber segment activation is also important. This is linked to fiber morphology and fiber deformations.

As fiber wall becomes thinner and fiber curl decreases, handsheet density and tensile index experience slightly different behavior. The tensile strength increase was linear, whereas handsheet density hits a plateau at high densities. This is amplified when using WRV as a variable in the equations. Un-refined fibers experienced a slightly different behavior as highly refined fibers, where the amount of bonding can be considered to be constant for all samples (Page et al. 1979).

When the fiber walls became sufficiently thin, the change in sheet density was not linear, whereas the tensile strength increased in a linear fashion. This can be explained as follows; when the inter-fiber bonding and transverse shrinkage of the fibers is sufficient, the amount of activation mainly depends on the morphology of the fibers. Fiber length not being an important factor for the eucalypt pulp samples, the determining factor on how effectively the slack segments will straighten is the bonded area (amount of fiber contact), which is higher for thin-walled fibers. Therefore, higher shrinkage forces of thin-walled fibers will result in improved fiber network activation as more free segments are activated.

The fiber slenderness ratio used in the Page's equation (Page 1969) and in the shear-lag theory is clearly the lowest for hardwood pulps, as they possess low fiber length. In particular, eucalypt fibers have low width-wall thickness- ratio. This increases the importance of RBA in the above mentioned equations, further supporting the importance of fiber wall thickness in modeling of eucalypt fibers.

All of the factors contributing to the activation coefficient (fiber wall thickness, fiber curl, WRV) are favored by short fibers and fiber fragments. This also indicates that fiber length may not be as crucial parameter in determining eucalypt handsheet properties. Based on the study, the combined use of fiber characteristics, measurable with automated fiber analyzers, can be even more productive in interpreting handsheet properties than just concentrating on one parameter at a time.

A schematic picture (Figure 29) sums up the important elements for fiber network strength of hardwood fibers (III, VI-VII).

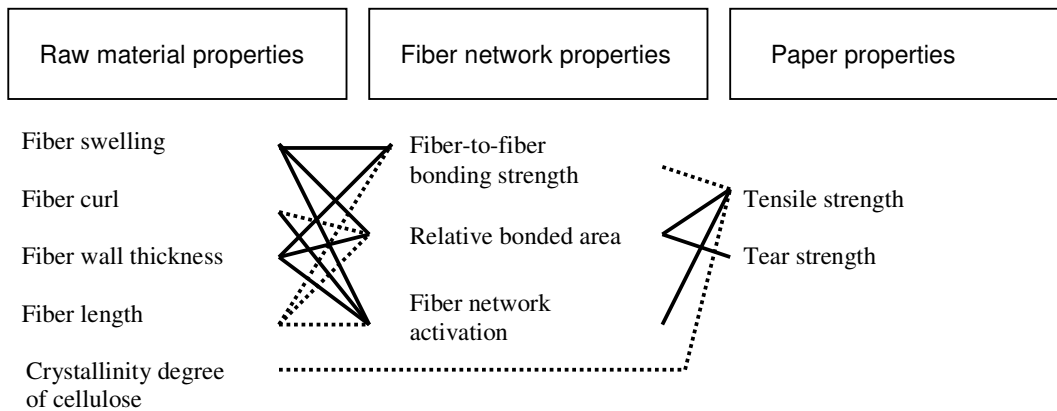


Figure 29. Effect of raw material properties on the strength properties of short-fiber pulp (significant influence = solid line, moderate effect = dashed line).

Table 10. Correlation coefficients between distribution characteristics (top - population weighted, bottom - volume weighted) and tensile index, handsheet density and air resistance.

	*) DPWM (W/RV)	PW, stdv. (W/RV)	PW, skew (W/RV)	PW, kurt.(W/RV)	DPWM	PW, stdv.	PW, skew	PW, kurt.	PWM	PWM (W/RV)	Tens. Index (Nm/g)	Density (kg/m ³)
DPWM (W/RV)	1.00											
PW, stdv. (W/RV)	0.97	1.00										
PW, skew (W/RV)	0.57	0.72	1.00									
PW, kurt.(W/RV)	0.09	-0.03	-0.41	1.00								
DPWM	0.91	0.96	0.75	1.00	1.00							
PW, stdv.	0.83	0.91	0.80	-0.29	0.97	1.00						
PW, skew	-0.17	-0.19	-0.08	0.74	-0.36	-0.32	1.00					
PW, kurt.	0.25	0.23	0.14	0.74	0.09	0.87	1.00					
PWM	0.93	0.97	0.74	-0.19	0.99	0.95	0.10	1.00				
PWM (W/RV)	0.95	0.97	0.74	-0.07	0.99	0.88	-0.20	0.17	0.95	1.00		
Tensile Index	-0.82	-0.80	-0.52	0.03	-0.84	-0.74	0.28	-0.01	-0.85	-0.85	1.00	
Density	-0.84	-0.80	-0.51	0.12	-0.80	-0.67	0.39	0.11	-0.83	-0.89	0.91	1.00
Air Resistance	-0.87	-0.82	-0.50	0.05	-0.81	-0.69	0.35	0.04	-0.83	-0.89	0.92	0.99
C/H (**)	0.28	0.39	0.46	-0.09	0.41	0.49	-0.04	0.11	0.41	0.39	-0.37	-0.17
Curl	0.55	0.62	0.55	-0.46	0.81	0.83	-0.51	-0.17	0.76	0.59	-0.64	-0.50

	*) DPWM (W/RV)	PW, stdv. (W/RV)	PW, skew (W/RV)	PW, kurt.(W/RV)	DPWM	PW, stdv.	PW, skew	PW, kurt.	PWM	PWM (W/RV)	Tens. Index (Nm/g)	Density (kg/m ³)
DVWM (W/RV)	1.00	1.00										
VW, stdv. (W/RV)	0.68	0.66	1.00									
VW, skew (W/RV)	0.35	-0.01	-0.31	1.00								
VW, kurt.(W/RV)	0.06	0.90	0.75	-0.24	1.00							
DVWM	0.81	0.90	0.80	-0.29	0.90	1.00						
VW, stdv.	0.56	0.65	0.65	0.74	0.78	0.73	1.00					
VW, skew	0.39	0.36	-0.08	0.74	0.62	0.73	0.73	1.00				
VW, kurt.	0.17	0.56	0.14	0.74	0.73	0.73	0.73	0.31	1.00			
VWM	0.75	0.84	0.77	-0.19	0.90	0.72	0.55	0.31	0.91	1.00		
VWM (W/RV)	0.66	0.91	0.74	-0.07	0.86	0.72	0.62	0.39	0.81	1.00		
Tensile Index	-0.69	-0.74	-0.23	0.02	-0.77	-0.51	-0.35	-0.09	-0.75	-0.84	1.00	
Density	-0.57	-0.69	-0.26	0.10	-0.68	-0.38	-0.28	-0.03	-0.63	-0.85	0.91	1.00
Air resistance	-0.59	-0.72	-0.33	0.04	-0.70	-0.44	-0.29	-0.10	-0.65	-0.86	0.92	0.99
C/H (**)	0.43	0.41	0.28	0.08	0.45	0.34	0.38	0.13	0.41	0.41	-0.37	-0.17
Curl	0.74	0.61	0.44	-0.45	0.85	0.50	0.37	0.05	0.86	0.60	-0.64	-0.50

*) DPWM = population weighted mean activation coefficient calculated from the distributions, equation (13), $PW_{stdv., skew \text{ and } kurt} =$ the distribution characteristics, PWM = the activation coefficient calculated according to Equation (12), DVWM = volume-weighted mean activation coefficient calculated from the distributions, equation (15), $VW_{stdv., skew, kurt} =$ the distribution characteristics, VWM= the activation coefficient calculated according to Equation (14), (W/RV) = W/RV correction used to calculate the activation coefficient.

**) C/H = the ratio between cellulose (C) and hemicelluloses (xylose, mannose and arabinose).

6.6 Dimensional stability (IV, V, VIII)

The non-linear behaviour of the pulp samples can be seen after the first absorption stage (10% → 50% RH) for measurements made with OPTIDIM (Figure 30). Therefore, the hygroexpansion coefficient throughout this study was determined as the mean value of the gradient of the first desorption stage (from 50% → 10 % RH) and the first absorption stage (from 10% → 50% RH). This is the region where there was no, or at least very little, non-linearity. The hygroexpansivity values throughout this thesis were calculated based on the moisture content of the sheet according to equation (9), as recommended by Uesaka (2002).

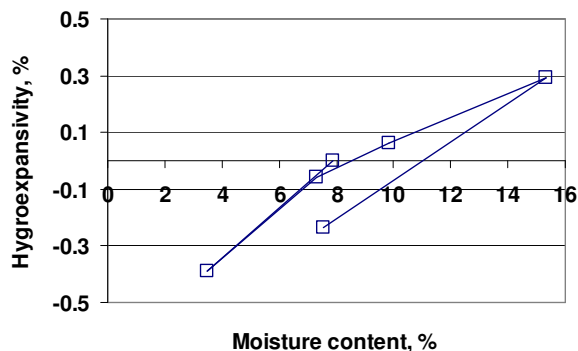


Figure 30. An example figure of a hysteresis curve of the hygroexpansion of an anisotropic sheet in the CD obtained with OPTIDIM apparatus.

6.6.1 The effect of fiber transverse dimension distributions on hygroexpansivity (IV)

The hygroexpansivity of conventional sheets measured with OPTIDIM was generally greater with increased refining. The values were roughly of the same order of magnitude, with the major differences derived from fiber morphology. The same was observed for the measurements made with laser measurement apparatus (Antonsson et al. 2010).

Figure 31 shows hygroexpansivity coefficients of anisotropic sheets as a function of refining for samples studied in the MD and CD, respectively. As the figures illustrate, refining generally had a small effect on the hygroexpansivity in the MD and a bigger effect on the hygroexpansivity in the CD (Salmén et al. 1987; Uesaka and Qi 1994).

There was no general trend for hygroexpansional behavior as a function of density for isotropic handsheets (Figure 32). This may be due to the small differences in the formation of the pulp sheet due to fiber deformations (curl etc.). Both the isotropic and the anisotropic sheets were dried in contact with a plate to which the sheets were attached.

In theory, a higher amount of fiber bonding with a fiber network consisting of thin-walled fibers should result in a higher degree of fiber segment activation (straightening of free, unbonded fiber segments) if the same amount of restraint is applied during drying.

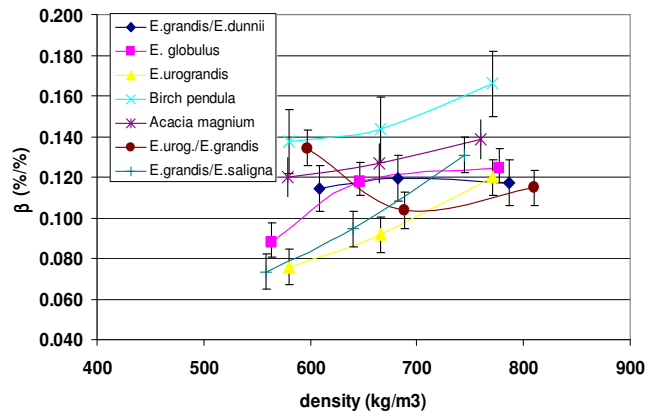
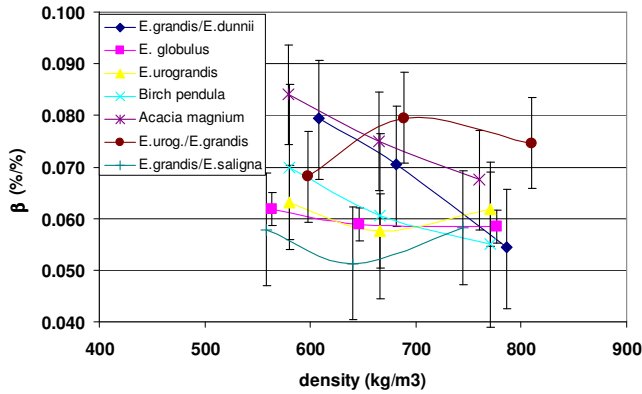


Figure 31. Hygroexpansivity coefficient as a function of sheet density in the MD (left) and CD (right) (error bars 95% confidence interval).

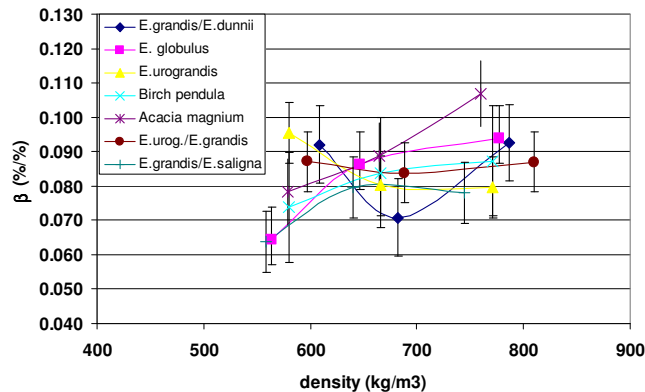


Figure 32. Hygroexpansivity coefficient as a function of sheet density of isotropic handsheets (error bars 95% confidence interval).

If we take a look at how fiber wall thickness affects the hygroexpansivity coefficient of unrefined samples, it can be seen (Figure 33) that the mean value and standard deviation of fiber wall thickness had negative correlations with the hygroexpansivity of anisotropic sheets. This is in accordance to formula presented by Uesaka (1994) for hygroexpansion of paper derived from a micromechanics analysis that provides a general framework for considering the effect of fiber-to-fiber bonding, drying restraint, and fiber dimensions. In the paper of Antonsson et al. (2010), the same results for fiber wall thickness used in this study (IV) were observed not to correlate with laser measurement apparatus hygroexpansivity measurements

of standard isotropic handsheets. In Chapter 6.6.2 reasons for the differences are discussed. In their study of the shrinkage mechanisms of paper, Nanko and Wu (1995) reported a higher amount of shrinkage for thick-walled fibers than for thin-walled fibers independent of the drying method, but they did not study the effect of fiber shrinkage to sheet hygroexpansion values. In many occasion, individual fiber hygroexpansivity has been seen to be connected to sheet hygroexpansivity for both hardwoods and softwoods (Lyne, 1994; Nanko and Tada, 1995; Nanri and Uesaka, 1993). The outlier marked as square is the birch sample. The difference in the hygroexpansional behavior of birch samples could be a result of its very different chemical and structural nature and the high amount of fines present. It is also noteworthy that birch had the highest variability in hygroexpansion measurements. The reason behind this is unknown.

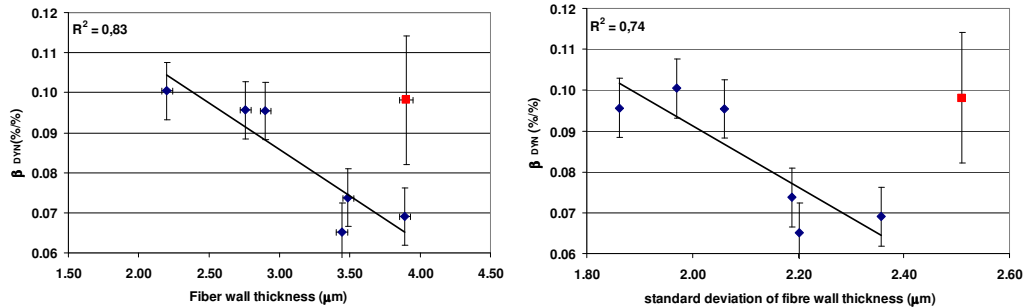


Figure 33. Geometric mean of hygroexpansivity of un-refined anisotropic sheets as a function of fiber wall thickness mean value (left) and standard deviation (right) (the outlying birch indicated as a square, acacia and eucalypt samples as diamonds).

Figure 34 shows that dynamic sheet samples with narrow fiber walls exhibited a lower overall change in sample dimensions (as the mean of CD and MD dimensional changes) than samples with thick-walled fibers when the relative humidity was changed from 10% to 90%. At higher relative humidities (between 70 and 90% relative humidity and even before that) samples exhibit non-linear behaviour due to the release of “internal stresses” (Salmén 1993; Uesaka et al. 1989; Uesaka et al. 1992) that will affect the amount of overall dimensional change observed for the humidity range used. It can be speculated, that the amount of released dried in stresses was higher for thick walled fibers.

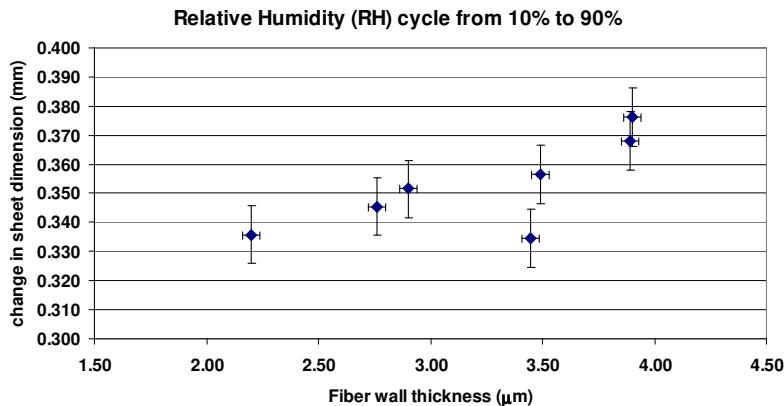


Figure 34. Overall change in sample size (dynamic sheet in the CD direction) when subjected to relative humidity between 10% to 90% as a function of fiber wall thickness (error bars 95% confidence interval).

The use of restraint-dried sheets was done in order to mimic the effects seen in the mill environment. However, one has to bear in mind that the conditions used (wet pressing, sheet making, refining, drying) were far from ideal.

For the same amount of fiber network activation potential (and the FSP values approximately at the same level) at the beginning of drying, fiber wall thickness was responsible for the differences seen in the dimensional changes of the in-plane sheet structure (Pulkkinen et al. 2009a). The orientation of these samples was approximately at the same level (characterized as the MD/CD tensile stiffness ratio of the sheet samples). Recently, there have been similar findings for isotropic handsheet hygroexpansion as well, connecting fiber wall thickness to network activation (Pulkkinen et al. 2010).

6.6.2 Laser measurement and OPTIDIM apparatus

Figure 35 shows the correlation between all OPTIDIM hygroexpansivity measurements and the laser measurement device. There seems to be a poor correlation between these two measurement methods, even though the magnitude of the results was approximately the same for a given measurement type (MD, CD, geometric mean or isotropic). The forming of hydrogen bonds at a low moisture range (Urquhart and Eckersall, 1930; Urquhart, 1958) which cannot be disrupted in re-swelling (Laivins and Scallan 1993) may have affected the results as the preconditioning of the samples differed somewhat. In the measurements with the paper strips of the laser measurement device, the samples were preconditioned at 33% RH, whereas the OPTIDIM samples were kept at +23°C and 50% RH prior to testing. It is a common practise to condition the paper first at a substantially lower humidity (e.g. at 30% or lower) before it is tested in the standard conditions in order to achieve identical moisture content at a given relative humidity (Wink, 1961).

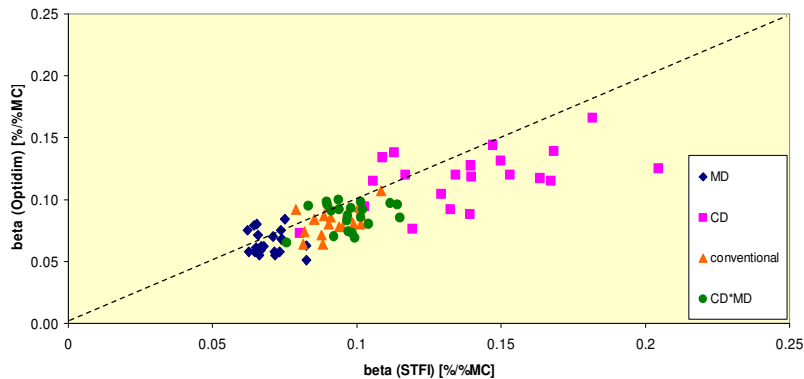


Figure 35. All data points from conventional sheets as well as the MD and CD of oriented sheets. $\sqrt{CD*MD}$ is the geometric mean of anisotropic sheets.

Another difference that may have affected on the observed differences between these two measurement methods is the low humidity used in the desorption stage of OPTIDIM (10% RH). When the relative humidity is less than 20%, the samples undergo a steep change in moisture content with increasing relative humidity and more hydrogen bonds are formed (Salmén 1993). The hygroexpansion coefficient was calculated from the linear part of the curve, which was determined to be from 10 to 50% RH for OPTIDIM and from 33 to 66% RH for the laser measurement device. For all of the samples, the dimensional changes of the samples were linear between these intervals (Figure 36). Even though in this study we did not have measurement points between relative humidities 10% and 50%, according to our earlier measurements the linearity assumption holds (unpublished data). The hygroexpansion coefficient was then calculated according to equation (9). The OPTIDIM apparatus could be adjusted to use a cycle between 33% RH and 66% RH, but as it would require a lot of additional work and, would yield no significant change in the results, the normal cycle of between 10% RH and 90% RH was used.

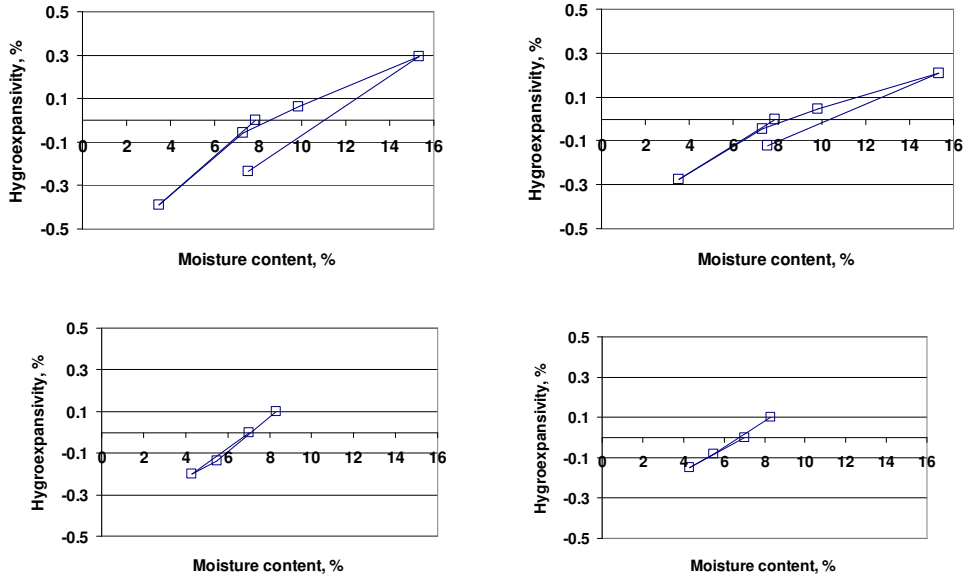


Figure 36. Dimensional changes of the OPTIDIM (above) and the laser measurement samples (bottom) for oriented sheets in the CD (left) and in the MD (right) as a function of sheet moisture content.

Figures 37 and 38 depict the hygroexpansion coefficients of isotropic handsheets as a function of the geometric mean values of machine direction and cross direction hygroexpansion coefficients for laser measurement device and OPTIDIM hygroexpansivity tester, respectively. Interestingly, some of the measurements made with the laser device (Figure 37) fall on a straight line.

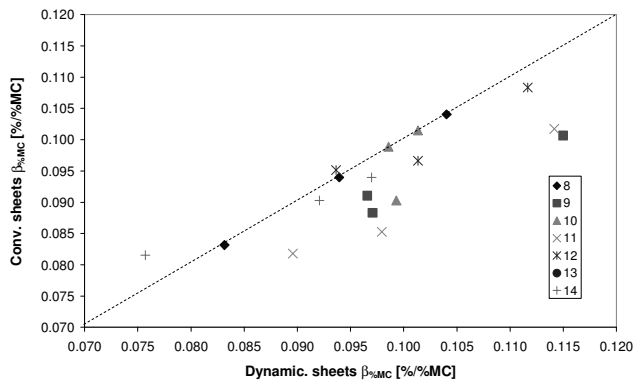


Figure 37. Comparison of the hygroexpansion of conventional and dynamic sheets with the laser measurement device.

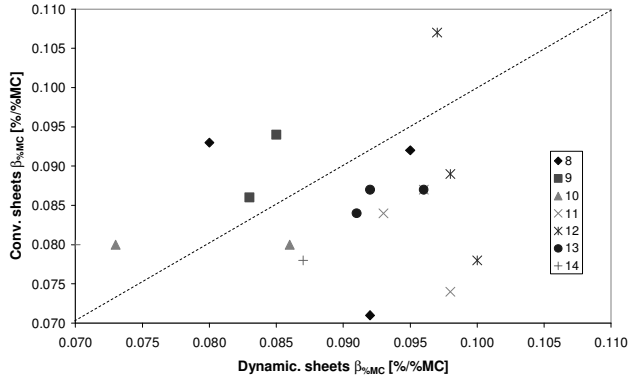


Figure 38. Comparison of the hygroexpansion of conventional and dynamic sheets with OPTIDIM.

There is no theoretical basis that these values should correlate. The measurements (made for sheets dried in restraint), as stated before, are mostly governed by the transverse hygroexpansion of the fibers. In the case of isotropic handsheets, where fibers are placed randomly to form a sheet, the hygroexpansional forces are distributed evenly in all directions therefore activating the network equally. For anisotropic sheets, depending on the amount of anisotropy, fiber network activation in the machine direction and cross direction is dependent on the morphological properties of the fibers (Uesaka 1994; Uesaka and Moss 1997). The fiber segment activation is affected by the free segment length and fiber curl, and the length of the free segment in the MD and CD is affected by the fiber orientation. The more fibers are aligned in the MD determine how many bonds there are in the CD (Lyne 1994). Relatively straight fibers together with high swelling ability at the crossing sites (good fiber-to-fiber bonding and high WRV) mean that refining has little or no effect on the hygroexpansivity of the sheets in the MD. The amount of activation depending on the shrinking ability of the fibers at the fiber bonding sites means that the results for isotropic sheets and anisotropic sheets are not necessarily comparable with each other. This may explain the differences observed for the two methods used in this thesis work and the fiber wall thickness measurements in (IV) and (VIII).

The percentual differences between the laser measurements and the OPTIDIM tester were approximately 20% for most of the measurements. The measurement accuracy of the used apparatuses was not able to explain the differences observed. The possibility exists that there could also be a significant friction force between the glass and the sample in the OPTIDIM apparatus or between the weight and the sample in the laser measurement device. To avoid this, Teflon sheets have been used to allow free shrinkage of the sample when, for example, determining stress-strain curves (Batchelor and Westerlind 2001). A similar experimental set-up could be advantageous in determining the hygroexpansivity coefficients in stress-free conditions for a set of pulps. Teflon-coated glass plates could be useful for dimensional change measurement with both types of apparatus.

A direct comparison between these two methods is impossible. However, a few possible reasons emerged to explain these differences. The use of paper strips may at least be partially responsible for the differences observed. For such a sample, local variations in thickness, fiber orientation and fiber grammage may become important. Overall, there are a lot of things that have to be taken into consideration when measuring the hygroexpansion of samples using different kinds of apparatuses, especially when dealing with samples that are relatively small in size (standard strip or smaller). It is impossible to create identical circumstances, but further studies could be executed with identical relative humidity cycles to remove uncertainties concerning either the low humidity range, or the high humidity range. The use of Teflon coated weights could also be considered.

6.6.3 The effect of sample size measured with the OPTIDIM apparatus

The samples were taken from the dynamic sheets cut both in the machine and the cross direction. The samples sizes used in this study were 100x100 mm², 60x100 mm², 36x100 mm² and 15x100 mm², so the actual number of samples of different size/orientation was eight. The normal procedure for hygroexpansion measurements was applied to all the samples with the exception of the 15x100 mm² samples, when the use of the glass weight was excluded. This may have resulted in curling of the samples (Nordström et al. 1998), making it difficult to get accurate readings of sample expansion. Therefore a large number of parallel measurements were required and the results for 15x100 mm² remain unreliable.

Table 11 shows that the difference in the shape or size of the sample was not reflected in the hygroexpansivity of the samples when using the OPTIDIM measurement apparatus. Increasing the moisture content of the sample will change the internal stress state of a fiber, and, due to the Poisson effect (Perkins 2002), the moisture-induced stresses observed in one direction will have an effect on the stresses in the other direction. Therefore, in theory, with changing aspect ratios of the MD and CD side lengths, one should see differences in the hygroexpansion values. The refining increases the bonding potential and internal and external structure of the fibers, i.e. increasing the number of fiber-to-fiber interaction. Due to the increased bonded area the paper produced is less dimensionally stable. The initial creep effect, possibly induced by the clamping of the samples in the laser measurement apparatus, can also be intensified when the samples from refined fibers are prepared, as refining lowers the stiffness of the fibers.

Table 11. The effect of shape and size of the sample on the hygroexpansivity in the MD and CD.

	100mm x 15mm	100mm x 36mm	100mm x 60mm	100mm x 100mm
Longer side cutted in MD				
β_{MD}	0.01	0.06	0.06	0.06
β_{CD}	0.07	0.08	0.08	0.08
Longer side cutted in CD				
β_{MD}	0.05	0.07	0.06	0.06
β_{CD}	0.08	0.09	0.08	0.09

Small differences can be seen with the samples of paper strips. For such a sample, local variations in sheet thickness, fiber orientation and fiber grammage may become important. Such variation may result in heterogeneous sheet hygroexpansion, causing inaccuracy during the measurement procedure when going down in sample size.

6.7 Mechanosorptive creep (VIII)

In order to isolate the effects of fiber shape and fiber distortions from the structural features of paper, only highly refined fibers (energy level of 150 kWh/t) were used to evaluate the mechano-sorptive creep. After refining fiber-to-fiber bonding can be considered to be constant (Page et al. 1979).

Both, the tensile stiffness index and hygroexpansion are related to network structure, i.e. handsheet structural density (Panek et al. 2005; Uesaka 2002). When plotting the hygroexpansion coefficient against the isocyclic creep stiffness a statistically significant correlation (Table 12) was found. To the best of the authors' knowledge, this correlation has not previously been reported in the literature. This indicates that fiber-to-fiber bonding is also important to mechano-sorptive creep.

Table 12. Correlation coefficients between hygroexpansion, tensile stiffness index, isocyclic creep stiffness and fiber characteristics (2-tailed test, statistically significant ($p < 0.05$). Level of significance > 0.74 (7 samples).

	Refined to 150 kWh/t			Un-refined mean dimensions				Un-refined		Refined		
	β_{150} (%%)	TSI ₁₅₀ (kNm/g)	IC ₁₅₀ (kNm/g)	Wall (μm)	Width (μm)	Length (mm)	Curl (%)	Xylose (%)	WRV (g/g)	β TSI	WRV ₁₅₀ (g/g)	β TSI _{150}}
β_{150} (%%)	1.00											
TSI ₁₅₀ (kNm/g)	0.37	1.00										
IC ₁₅₀ (kNm/g)	-0.86	-0.19	1.00									
Wall (μm)	0.49	0.59	-0.59	1.00								
Width (μm)	0.15	0.75	-0.07	0.82	1.00							
Length (mm)	0.14	0.70	-0.27	0.86	0.83	1.00						
Curl (%)	-0.74	0.03	0.82	-0.43	0.07	-0.21	1.00					
Xylose (%)	0.37	0.36	-0.10	0.43	0.58	0.12	0.10	1.00				
WRV (g/g)	-0.75	-0.57	0.57	-0.36	-0.20	-0.27	0.56	-0.30	1.00			
β TSI [†]	-0.29	-0.90	0.31	-0.69	-0.74	-0.77	-0.04	-0.35	0.49	1.00		
WRV (g/g) ₁₅₀	0.91	0.59	-0.82	0.76	0.50	0.44	-0.57	0.55	-0.69	-0.58	1.00	
β TSI _{150}} [†]	0.84	-0.20	-0.79	0.18	-0.28	-0.26	-0.79	0.19	-0.47	0.22	0.62	1.0

[†] hygroexpansivity divided by the tensile stiffness index

Morphological factors may also account for higher hygroexpansion, as fiber wall thickness was seen to correlate moderately with the hygroexpansion coefficient (Pulkkinen et al. 2009a). A correlation analysis was applied for strength properties, hygroexpansivity coefficient, mechano-sorptive creep and fiber properties to investigate the correlations between these characteristics.

Both isocyclic creep stiffness and hygroexpansivity of the handsheet were strongly connected to fiber deformations (curl) of the original furnish, so it is obvious that fiber network activation influences hygroexpansivity and mechano-sorptive creep. The effect of raw material size and shape disappeared when fibers were refined (Table 13). This indicated that fiber swelling degree (measured as WRV) determined the development of hygroexpansivity and tensile stiffness of the handsheets. This hides the factors that surge when fiber wall is modified through refining (including for example internal and external fibrillation).

The tensile stiffness index development was, in addition to fiber-to-fiber bonding, also influenced by the dimensions of the original fiber furnish. When the inter-fiber bonding and transverse shrinkage of the fibers is sufficient, the amount of activation mainly depends on the morphology of the fibers. Fiber length not being an important factor for the eucalypt pulp samples, the determining factor on how effectively the slack segments will straighten is the bonded area (amount of fiber contact), which is higher for thin-walled fibers. Therefore, it can be speculated that higher shrinkage forces of thin-walled fibers will result in improved fiber network activation as more free segments are activated.

Table 13. Correlation coefficients between hygroexpansion, tensile stiffness index, and fiber characteristics (2-tailed test, statistically significant ($p < 0.05$). Level of significance > 0.43 (21 samples).

	β (%%)	TSI (kNm/g)	density (kg/m ³)	wall (μm)	wall _{stdv.} (μm)	WRV (g/g)	curl (%)
β (%%)	1.00						
TSI (kNm/g)	0.82	1.00					
density (kg/m ³)	0.86	0.97	1.00				
wall (μm)	0.22	0.25	0.17	1.00			
wall _{stdv.} (μm)	0.11	0.35	0.31	0.70	1.00		
WRV (g/g)	0.92	0.96	0.97	0.27	0.31	1.00	
curl (%)	-0.24	0.00	0.08	-0.34	-0.02	-0.06	1.00

To include both, the effect of fiber-to-fiber bonding and structural properties of the handsheets in the evaluation of mechano-sorptive creep, a ratio between the hygroexpansion coefficient and tensile stiffness index (Figure 39) was used to describe the impact of the swelling of fibers, fiber dimensions and fiber shape (curl) on isocyclic creep data in a qualitative manner. This is the same Figure presented in article (VIII), except that for the fitting of the data a third degree polynomial has been used to improve the precision of the fit.

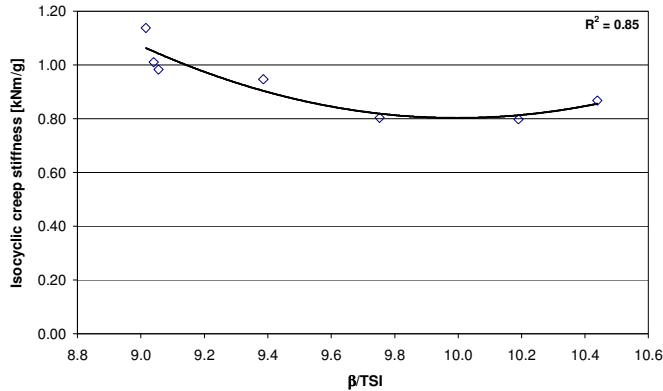


Figure 39. Isocyclic creep stiffness as a function of the hygroexpansivity/tensile stiffness index-ratio.

The hardwood samples can be ranked in terms of their mechano-sorptive creep properties by measuring their tensile stiffness and hygroexpansion values. The difference in hygroexpansion between pulp samples compared at similar densities was a result of the combined effect of fiber distortions and fiber swelling which determine the level of bonding in a fiber network. Tensile properties of un-dried fiber networks can be seen to be more dependent on the morphology of the fibers (Pulkkinen et al. 2010). In the case of once-dried fibers, as were used in this study, the loss in relative bonded area when the fibers are dried (Gurnagul et al. 2001) may interfere with the observed tensile stiffness- hygroexpansion relationship. The nearly exponential left part of the curve in Figure 39 can be explained by the increased activation of the samples resulting in higher tensile stiffness values (lower β/TSI -ratio).

6.8 Raw material and fiber network parameters affecting hygroexpansivity and mechano-sorptive creep

The tensile stiffness index of handsheets prepared from once-dried un-refined fibers (IV-V, VII-VIII) did not correlate with the activation coefficient calculated with equation (12) (Figure 40) that was fitted to a third degree polynomial. When fibers were refined, the correlation improved markedly, thus implying that the improvements in bonding and changes in fiber wall structure due to refining were the major contributors to observed increased strength of the hand sheets. This was further backed up by a multiple regression analysis (combined R^2 value of 0.92), revealing that WRV (R^2 of 0.8) was mostly responsible for the goodness-of-fit. This was believed to be also partly due to the difficulty of fiber analyzers to measure refined fibers. Both, the measurement of fiber wall thickness and the measurement of fiber curl produce difficulties (Mohlin 2005).

Mohlin (2005) has shown that tensile strength property development in commercial, dried bleached softwood kraft pulp samples could be explained entirely by two fiber properties: fiber swelling and fiber straightness (curl). Based on the correlation observed in Figure 41 for tensile stiffness index and the activation coefficient, this seems to be the case for commercial eucalypt pulp samples as well.

In the light of observed results in Articles IV-V and VII-VIII some observations about the behaviour of eucalypt fibers in an environment where changes in relative humidity occur can be made. These are gathered and presented in Figure 41, that presents the most important moisture dependent raw material parameters influencing network properties and, therefore, eventually the hygroexpansional and creep properties of paper.

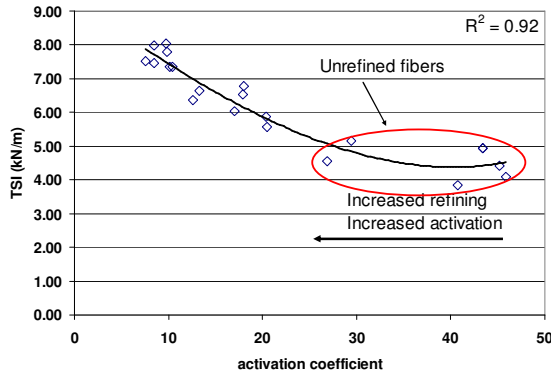


Figure 40. The influence of refining on the tensile stiffness index and activation coefficient.

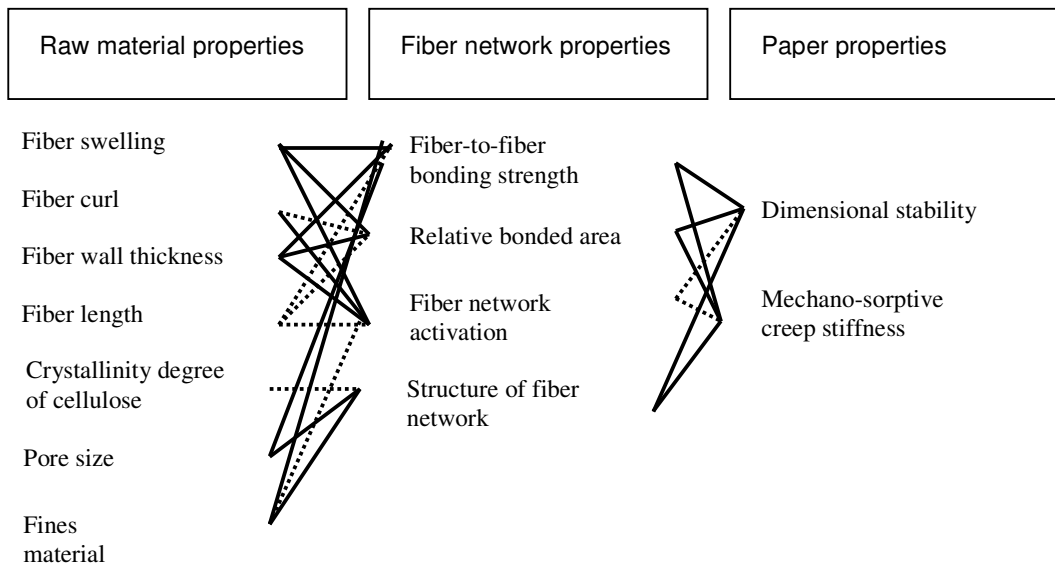


Figure 41. Effect of raw material properties on the hydroexpansional properties of short-fiber pulp (significant influence = solid line, moderate effect = dashed line).

6.9 Changes in fiber wall thickness distributions due to moisture

The changes in fiber wall thickness distributions were investigated based on SEM images of 100% *E. grandis* bleached chemical pulp isotropic handsheets. For samples of un-fractionated pulp, changes were clearly seen in the fiber wall thickness mean values (Figure 42). However, this is not directly a result of fiber swelling behaviour as fiber wall thickness mainly decreased with increasing moisture. This would imply that fiber wall does not actually swell under sheet moistures of 16% (90% RH). The phenomenon seen could be the combined result of loss in inter-fiber bonding and structural recovery of individual fibers when fibers are oven dried. The absence of hydrogen bonding between fibers (and therefore the absence of inter-fiber forces mainly keeping fibers in contact) would result in recovery of fiber shape, the extent of it depending on fiber wall thickness. According to Retulainen (1997), the main part of fiber shrinkage takes place when the dry matter content of fibers is between 80-90%. It is, however, also possible that the changes in fiber wall thickness were so small they cannot be detected with SEM. The size of the pixel obtained in the image analysis was 0.14 μm . This is fairly big compared to measured fiber wall thickness values. With fiber wall thickness of 3 μm this would mean that less than 5% change in the fiber wall thickness were not detected for individual fibers. The relative resolution in the measurement of fiber wall area, diameter and perimeter is better than with the wall thickness measurement. Drying in situ has been seen to

reduce fiber reswelling. This change cannot be observed for dry fibers, even though these fibers might be solvent-exchanged or freeze-dried (Bawden and Kibblewhite 1997). This means that the degree of reswelling may not be fully revealed when observing dry fiber cross-sections, like for example when investigating fiber dimensional changes from SEM images (Weise and Paulapuro 1999). However, this does not affect the comparisons made for the fiber wall thicknesses calculated with Euclidian distance map (EDM) algorithm, and by assuming that eucalypt fiber are on average rectangular shaped (Figure 42).

Furthermore, as Figure 43 depicts, fiber wall thickness distributions calculated from the raw data of all 1000 fibers by assuming rectangular shape and the values obtained from Euclidian distance map (EDM) measurements were similar for fibers dried to absolute dryness and for the wet-pressed fibers. Therefore it is quite safe to assume that fibers are on average rectangular shaped. The underestimation of fiber wall thickness value when we use only the un-collapsed fibers to calculate wall thickness arises from the fact that fibers seen by the algorithm, i.e. those with visible lumen are more likely to have more round shape, and fibers have their smallest diameter when their cross sections are circular. If eucalypt fibers are readily collapsed after wet pressing, the collapsibility of fibers does not play a significant role in determining the properties of the hand sheets. This we have deduced earlier (Pulkkinen et al., 2008b) by examining the fiber wall thickness data against water retention value. It was also a topic of conversation by Mohlin and Hornatowska (2006). In order to visualize differences between distributions more clearly 3-parameter Weibull distributions were fitted to data. Figure 44 presents fiber wall thickness distribution of fitted un-fractionated pulp handsheet calculated by the algorithm and by calculating the fiber wall thickness by assuming rectangular shape of the fibers.

The 3-parameter Weibull distribution was calculated as

$$f(x) = \alpha \cdot \beta \cdot (x - \gamma)^{\beta-1} \exp(-\alpha \cdot (x - \gamma)^\beta) \quad (18)$$

where α is the scale parameter, β is the shape parameter, and γ the location parameter. The Weibull distribution parameters of the distributions of this study are presented in Table 14. The results illustrate, that the mean value and spread of the distribution was relatively unchanged for both the un-fractionated and fractionated samples. The skewness and kurtosis values, notorius for their sensitivity towards large deviations from the mean value, were observed (Pandey 2001).

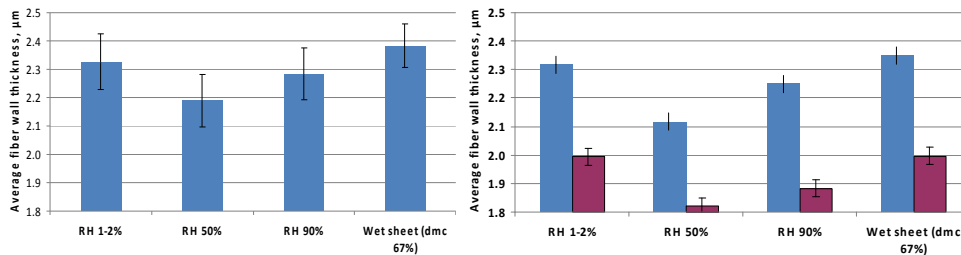


Figure 42. Fiber wall thickness for un-fractionated sample calculated from the results of un-collapsed fibers only by EDM (left) and by assuming a rectangle shape (right). In the right hand side left bar represent value calculated from all measurements and right bar the value calculated from the uncollapsed fibers only.

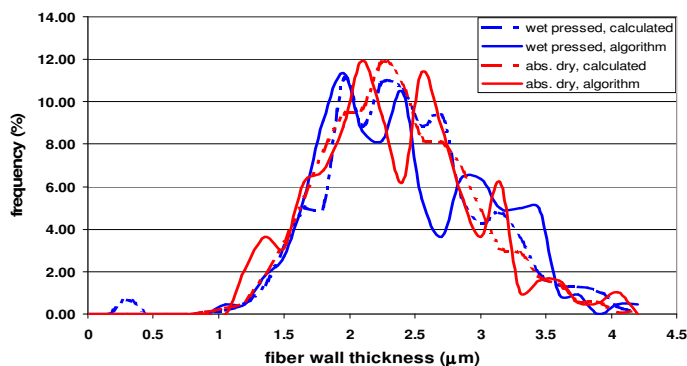


Figure 43. Distributions of fiber wall thickness of un-fractionated sample calculated from the results of 1000 fibers assuming rectangles and by using the algorithm (only un-collapsed fibers calculated).

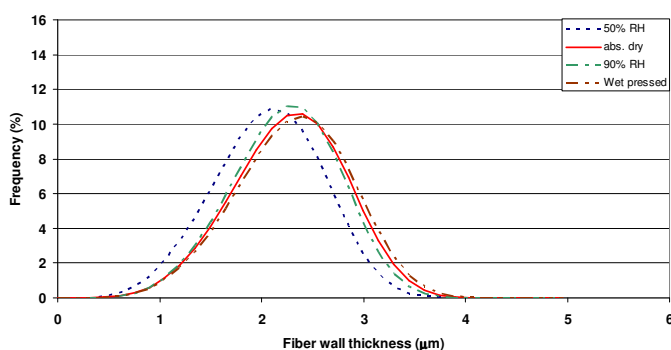


Figure 44. The fitted Weibull distributions of fiber wall thickness of un-fractionated sheets in different relative humidity conditions and at the wet pressed state.

Table 14. Distribution moments of the samples of fractionated and whole pulp sheets.

	μ (μm)	σ (μm)	skew	kurt
+28				
- abs. dry	2,71	0,77	0,32	0,98
- 50% RH	2,75	0,76	0,18	1,20
- 90% RH	2,68	0,73	0,21	1,14
-100 + 200				
- abs. dry	2,21	0,56	0,14	1,76
- 50% RH	2,17	0,58	0,26	1,30
- 90% RH	2,22	0,58	0,22	1,29
whole pulp				
- abs. dry	2,32	0,60	0,88	2,38
- 50% RH	2,12	0,58	0,62	0,26
- 90% RH	2,25	0,62	0,43	2,13
- wet pressed	2,35	0,63	0,26	1,37

6.10 The degree of crystallinity and handsheet properties (VII)

The Crystallinity Index (CrI) has been considered an important factor for monitoring the structural features of the cellulosic substrate. The calculated Crystallinity Index (CrI) values are presented in Table 15 along with the rest of the results of the spectral fitting. CrI was calculated as a percentage of the sum of crystalline and para-crystalline cellulose fraction in the C-4 signal cluster (Lennholm, 1994). The correlation between the values determined by ion chromatography and those determined by CP/MAS ^{13}C NMR was good (Figure 45), implying that there is a certain fraction of xylan that is intimately associated with the

cellulose, as has been suggested for bleached birch kraft pulp (Liitiä et al. 2003). The same has been suggested earlier by Newman et al. (1993) in a study made with pine kraft pulp. Similar to our study, the amount of hemicelluloses was inferior when determined with NMR. Comparison between chemical and NMR results provide implication for a distinction between disordered hemicelluloses and hemicelluloses associated with ordered domains (observed with NMR). The correlation between the results of carbohydrate analysis and the relative amount of xylan observed from the spectral analysis also support the validity of using NMR for quantitative analysis of pulp components. Recent evidence of the association between xylan and cellulose based on dynamic FT-IR has also been presented by Dammström et al. (2009).

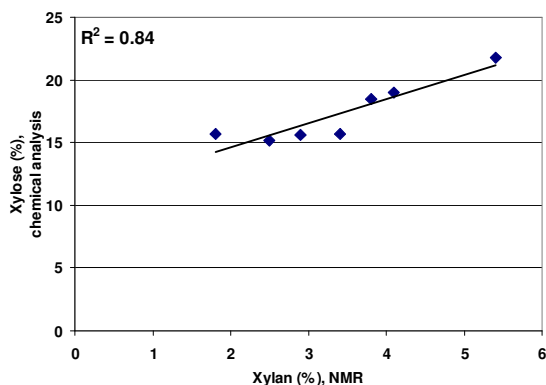


Figure 45. The correlation between the total xylan content and xylan measured with NMR.

Table 16 presents the results of the correlation analysis performed between the measured and calculated pulp fiber properties, handsheet properties of un-refined fibers and the NMR data. Table 17 shows the correlations between the NMR data and the hygroexpansivity measurements.

Table 15. The line-fitting results of C-4 region of CP/MAS ^{13}C NMR spectrum of pulp sample (values are relative intensity in percent, %).

Sample	Crystalline cellulose (L_{11})	Para-crystalline cellulose	Accessible fibril surface	Inaccessible fibril surface	CrI (%)	Xylan (%)
<i>Eucalyptus grandis/E. dunnii</i>	15.0	31.5	2.6	49.0	48.5	1.8
<i>Betula pendula/B. pubescens</i>	13.2	29.3	2.6	49.6	44.5	5.4
<i>Acacia magnium</i>	13.0	35.4	3.1	46.0	49.6	2.5
<i>E. Globulus</i>	12.8	33.6	2.6	46.8	47.0	4.1
<i>E. Urograndis/E. grandis</i>	13.2	34.8	2.8	45.4	47.3	3.8
<i>E. grandis/E. Saligna</i>	14.3	35.6	3.3	43.1	48.5	3.4
<i>E. Urograndis</i>	15.1	40.5	3.7	37.8	49.4	2.9

Table 16. Correlations of NMR data, handsheet strength properties and fiber dimensions (2-tailed test, statistically significant ($p < 0.05$)). Level of significance > 0.74 (7 samples).

	1	2	3	4	5	6	7	8	9	10	11
CrI%	1.00										
Xylan% (NMR)	-0.88	1.00									
Tensile stiffness index (kNm g^{-1}) (MD)	0.06	0.01	1.00								
Tensile stiffness index (kNm g^{-1}) (CD)	-0.76	0.47	0.47	1.00							
Elastic modulus (Mpa)	-0.45	0.20	0.23	0.70	1.00						
Tensile index (Nm g^{-1}) (MD)	-0.05	0.14	0.94	0.58	0.40	1.00					
Tensile index (Nm g^{-1}) (CD)	-0.77	0.74	0.46	0.99	0.73	0.61	1.00				
Fibre wall thickness (m)	-0.68	0.76	0.59	0.90	0.49	0.57	0.84	1.00			
Fibre width (m)	-0.66	0.64	0.08	0.84	0.64	0.14	0.79	0.84	1.00		
Fibre length (m)	-0.13	0.10	0.21	0.58	0.65	0.21	0.52	0.67	0.74	1.00	
Curl (%)	-0.09	-0.12	-0.86	-0.39	-0.08	-0.88	-0.14	-0.42	0.07	-0.14	1.00

A correlation analysis on the crystallinity index and xylan content (relative amount in percent), strength properties of dynamic handsheets in machine and cross direction and fibre characteristics (fibre length, width, wall thickness and fibre curl). 1: CrI%, 2: Xylan% (NMR), 3: Tensile stiffness index (kNm g^{-1}) (MD) 4: Tensile stiffness index (kNm g^{-1}) (CD), 5: Elastic modulus (Mpa), 6: Tensile index (Nm g^{-1}) (MD), 7: Tensile index (Nm g^{-1}), (CD), 8: Fibre wall thickness (m), 9: Fibre width (m), 10: Fibre length (m), 11: Curl (%)

Table 17. Correlations of NMR data and the hygroexpansivity measurements (2-tailed test, statistically significant ($p < 0.05$). Level of significance > 0.74 (7 samples).

	CrI (%)	Xylan % (NMR)	Isotropic handsheet	Dynamic sheet, goern, mean	Dynamic sheet, CD	Dynamic sheet, MD
CrI (%)	1.00					
Xylan % (NMR)	-0.88	1.00				
Isotropic handsheet	0.77	0.90	1.00			
Dynamic sheet, goern, mean	0.10	0.05	-0.16	1.00		
Dynamic sheet, CD	-0.16	0.23	-0.22	0.92	1.00	
Dynamic sheet, MD	-0.17	0.16	-0.04	0.43	0.40	1.00
Fibre wall thickness (μm)	-0.68	0.76	-0.66	0.10	0.17	-0.57
Standard dev. (μm)	-0.50	0.58	-0.58	0.22	0.29	-0.41
Fibre width (μm)	-0.66	0.64	-0.57	0.07	0.12	-0.29
Standard dev. (μm)	-0.26	0.28	-0.24	0.32	0.23	-0.08

A correlation analysis on the crystallinity index and xylan (measured with NMR in relative amount in percent), the hygroexpansional properties of isotropic and dynamic handsheets and the mean and standard deviation of fiber width and fiber wall thickness. The hygroexpansivities obtained from Pulkkinen *et al.* (2009b)

Based on Tables 16 and 17, the crystallinity index (CrI) and xylan content of the samples had good correlations with tensile strength properties in the cross direction and moderate correlations with the fiber wall thickness index and fiber width. With an increasing cellulose crystallinity, tensile strength in the cross-direction decreases, probably due to the lower amount of xylan in the cellulose-xylan matrix of fiber wall. Bergander and Salmén (2002) have shown that hemicellulose plays a much more important role than the cellulose for transverse properties of fibers. The crystallinity index determined may reflect all carbohydrates associated with ordered domains, not just cellulose (Newman 1993), which explains the strong correlation between crystallinity index and ordered xylan content. Ordered xylan closely associated to crystallite surfaces will contribute to the diffraction signal of the amorphous region either by broadening the peak or by increasing its intensity. The relationship between strength properties and crystallinity has been confirmed earlier (Annergren *et al.*, 1963; Kettunen *et al.* 1982; Kibblewhite and Bawden 1989), as samples with a higher amount of crystalline cellulose produce sheets with lower tensile strength.

The only significant correlation observed for the hygroexpansional data and NMR results was between the hygroexpansivity of the isotropic handsheets and the xylan content of the fiber wall. This could have been anticipated due to the higher moisture absorbing capacity of hemicelluloses (Salmén 2004). Corte and Kallmes (1962) provided a mathematical description of fiber orientation in 2-D fiber networks where the average free fiber segment length is shorter for isotropic fiber networks. Therefore the amount of fiber crossings is higher for isotropic sheets. This can make the distinction of the hygroexpansion of isotropic samples easier.

The moderate correlation between fiber wall thickness, fiber width, and CrI is interesting. Based on the results obtained the crystallinity of the fiber wall decreases as the fiber wall thickness increases (Figure 46). This implies that fiber wall thickness value may be partly influenced by the fiber detection procedure, as earlier speculated by Jordan and O'Neill (1994). This is consistent with the fact that only crystalline cellulose is detected with polarized light used in fiber detection (Pirainen 1985; Olson *et al.* 1995). As fiber analyzer can only detect the birefringent (double refracting) part of the fibers, i.e. cellulose (Pirainen 1985; Olson *et al.* 1995), the fiber wall thickness value can be partly influenced by the fiber detection procedure (Jordan and O'Neill 1994).

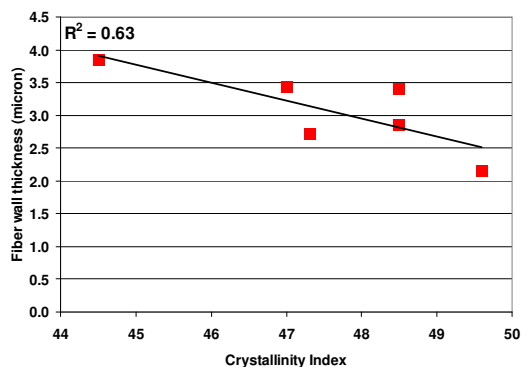


Figure 46. Fiber wall thickness as a function of the crystallinity index (Pulkkinen et al. 2009c).

Some aspects of interest still remained untouched. For example, the effects of fiber drying-rewetting cycle and fiber refining have in some studies, e.g. Wormald et al. (1996), seen to affect the molecular ordering of cellulose. This has to be taken into account when considering the possible effects of cellulose crystallinity on hygroexpansional or strength properties. The distortions formed in the cellulose fibrils probably are not totally released, due to the presence of fully amorphous cellulose or of a lower accessibility of some regions in the fibrils to the water. The effect of refining on cellulose crystallinity, especially in the surface layers would be of great scientific interest. The amount of hydrogen bonds formed between fibrils (internal strength), and between fibers (bonding ability) affect both, the strength properties and the hygroexpansional properties. On the other hand, Liitiä et al. (2000) did not observe any differences in the relative amount of cellulose crystallinity before and after refining for TCF bleached spruce kraft pulps.

To conclude, the hygroexpansional behavior of the handsheets and the crystallinity index of the cellulose in the samples were not inter-correlated. The findings of this study together with earlier publications led us to speculate that the differences seen between the strength properties of the unrefined samples used in this study were mainly dependent on the crystallinity degree of the cellulose. Some implications were also seen that crystallinity index is influenced by the structured hemicelluloses, and not solely by the structured cellulose.

6.11 Pore size distribution measurements: links to hygroexpansion and activation (VII)

The water absorbability of pulp fibers due to the amount of amorphous regions of the fibers was indirectly detected with the DSC. The results from the thermoporosimetry are shown in Table 18 for the pulp samples studied. The amount of non-freezing water and micropore water obtained with DSC should be rather similar for never-dried and dried samples (Salmén and Berthold 1997; Maloney and Paulapuro 1999). Therefore, the differences in drying of the pulp samples were not assumed to cause any differences in the measurements with DSC (Salmén, 1993; Maloney and Paulapuro, 1999).

The amount of lignin and hemicelluloses varies between samples. This will affect the amount of bound water measured with DSC (Salmén and Berthold 1997) as pore sizes develop into larger ones as removal of lignin and hemicelluloses is processed further. As Figure 47 shows, the mean pore size measured with DSC is a function of both the crystallinity index and the amount of xylan measured with NMR therefore correlating with the ordered structures of cellulose and xylan. It seems that fibers with low xylan content had slightly lower mean pore size independent of the amount of water contained in the amorphous regions of the fiber wall (Table 18). The same has been observed by Wan et al. (2010) with atomic force microscopy. This is also consistent with the observations made by Duchesne et al. (2001). They observed

that the fibril aggregates (macrofibrils) with high hemicellulose content were well organised with porous structure. Fibril aggregates with low hemicellulose content had a smoother, flatted and more compact surface structure. This implies that the more ordered structures and presumably more tight organization of fibril aggregates for low xylan content samples influences the pore size observed. The calculated fibril aggregate dimension did not, however, back up this hypothesis, as they did not correlate with the xylan content determined. The calculated fibril aggregate sizes were smaller (6.5-8.0 nm) than those published in the literature (Hult et al. 2001; Wan et al. 2010). The signal from the hemicelluloses could have affected the determination of accessible surfaces therefore making the calculated fibril aggregate size smaller.

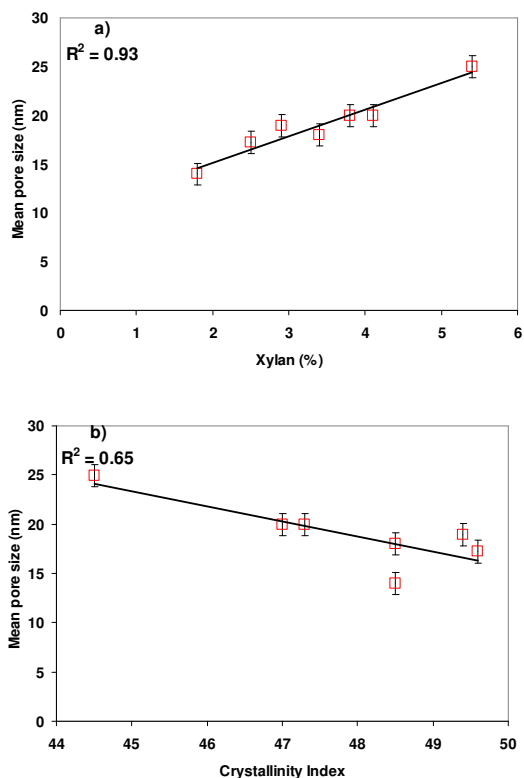


Figure 47. The mean pore size as a function of the (a) Crystallinity Index (CrI) and as a function of (b) xylan measured with the NMR (error bars present 95% confidence interval).

Table 18. Results of the DSC analysis.

Sample #	Crystallinity Index (%)	DSC (NFW)	DSC (FBW)	DSC (TBW)	Average pore size (nm)	Stdv. of pore size (nm)
<i>Eucalyptus grandis/E. dunnii</i>	48,5	0,30	0,441	0,741	14	1
<i>Betula pendula/B. pubescens</i>	44,5	0,29	0,431	0,721	25	3
<i>Acacia magnium</i>	49,6	0,27	0,402	0,672	17	2
<i>E. globulus</i>	47	0,29	0,473	0,763	20	2
<i>E. urograndis/E. grandis</i>	47,3	0,30	0,477	0,777	20	2
<i>E. grandis/E. saligna</i>	48,5	0,32	0,418	0,738	18	2
<i>E. urograndis</i>	49,4	0,30	0,500	0,800	19	2

FBW: Free bound water (mL g⁻¹), TBW: Total bound water (mL g⁻¹)

The small average pore size probably affected the moisture absorbance of the fibers, enabling them to absorb lots of moisture at the linear part of the hysteresis cycle resulting in high

hydroexpansion coefficient (Pulkkinen et al. 2009a). Further evidence is given by Figure 48 that shows the hydroexpansivity of the isotropic handsheet plotted against the average pore size.

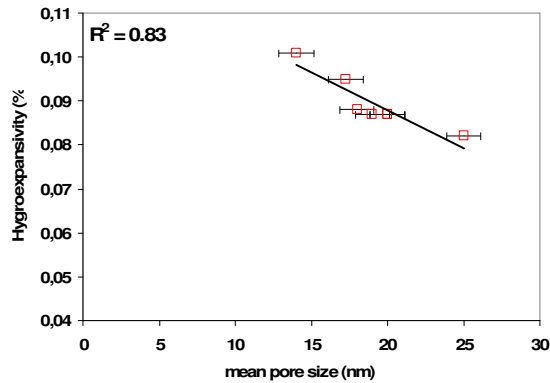


Figure 48. Hydroexpansivity as a function of mean pore size measured with DSC.

Forsström et al. (2005) studied the influence of pore structure and water retaining ability of unbleached kraft pulp fibers on different paper strength properties. The pore structure was determined with NMR relaxation measurements and the water retaining ability with WRV and FSP measurements. Larger pore radii led to higher tensile index of pulp handsheets. However, increased yield led to smaller pores and an increase in tensile index.

7 OPTIMAL FIBER DISTRIBUTION AND PAPER PROPERTIES (I-VIII)

For a given end-use, an optimal distribution of a given property can be totally different, whether good bulk, tensile or hygroexpansional properties are desired. In addition, the combination of various fiber property distributions and their inter-correlations has to be known before any conclusions can be made of the effects of individual distributions on paper properties.

No universally accepted distribution model has been proposed for predicting paper properties based on various fiber characteristics. The distributions formed when the original wood is chipped, cooked and bleached, depend on numerous processing steps that alter the distribution of fiber properties and even the distributions inside a single fiber in terms of its chemical and physical properties.

Changes in the fiber structure of wood fibers are not always easy to measure. Often a good understanding is obtained when several methods are combined. In this work, CP/MAS ^{13}C -NMR was used to characterize the ultrastructure of fibers, differential scanning calorimetry, water retention value, fiber saturation point measurements. Scanning electron microscopy was used to characterize fiber swelling and dimensional changes of the fibers due to variations in moisture content. Fiber length and other fiber dimension distribution measurements were used to investigate changes in fiber network structural parameters and resulting strength and hygroexpansional properties.

The results of the CP/MAS ^{13}C -NMR indicated that crystallinity of cellulose influences the strength properties in the cross-direction negatively. This is in accordance with the earlier findings of Bergander and Salmén (2002) where they have shown that hemicellulose plays a much more important role than the cellulose for transverse properties of fibers. Based on the observed correlation between the crystallinity index and fiber wall thickness measured with FiberLab®, it is possible that the crystallinity of cellulose can also affect the fiber detection process with fiber analysers (VII). The fiber analysers based on using polarized light detect only crystalline cellulose. The link between crystallinity and analyzer results was first speculated by Jordan and O'Neill (1994). This has to be remembered when dealing for example with fibers that contain high amounts of hemicellulose.

Based on the differences observed in fiber swelling ability, indications were found that WRV was the most important single factor contributing to fiber-to-fiber bonding potential of fibers. This was consistent with the findings of Mohlin and Hornatowska (2006).

The packing of the sheet is important to apparent density, air resistance and tensile properties of the sheets. Based on the study made by Pulkkinen et al. 2008b (III), by assuming a certain collapsibility degree (the same for all fibers), an anisotropic packing of fibers to a sheet of given grammage alone gives us reasonable results to estimate some of the most important paper technical properties. The main uncertainty of the model probably comes from neglecting fiber network activation (VI) which is especially seen as inaccuracy in predicting tensile strength of the handsheets. After a certain density is achieved at sufficiently low wall thickness values, and the inter-fiber bonding development is decaying, tensile index continues to improve. This is caused by low fiber wall thickness and low fiber curl together with WRV improve the fiber network activation (Pulkkinen et al. 2010)(VI). Together with fiber curl (Joutsimo et al. 2005; Mohlin et al. 1996; Page et al. 1979) WRV is the most important parameter determining the amount of activation potential. The use of activation coefficient distributions did not give any improvement over the use of mean value in the activation model predictions. However, it was obvious that the population distribution mean values were more sensitive to distribution width and skewness than the volume weighted distributions.

A schematic picture (Figure 49) sums up the most important elements needed for an optimum distribution of properties in terms of strength, structure and hygroexpansion. The effect of fiber length distribution for short-fiber raw material properties due to its homogeneous nature is insignificant. The differences in other dimension distributions determine the differences observed in sheet properties. Some of the fiber properties, e.g. fiber wall thickness, affected a range of paper properties. Where as, some fiber properties were seen to have only a minor effect on the measured properties, e.g. hemicellulose content and crystallinity degree of cellulose. This also means that some of the paper technical properties are more easily influenced by a proper choice of easily measurable distribution parameters than the others. For example, tensile strength for eucalypt is easily predictable, due to its strong dependence on fiber wall thickness measurements, with off-line analysers.

The models developed (III, VI) can be applied directly to random fiber networks. The effect of fiber orientation on the measured paper properties is significant. The increased amount of fiber-to-fiber contact surfaces affect the bonding ability and therefore to hygroexpansional properties and, via network activation to strength development.

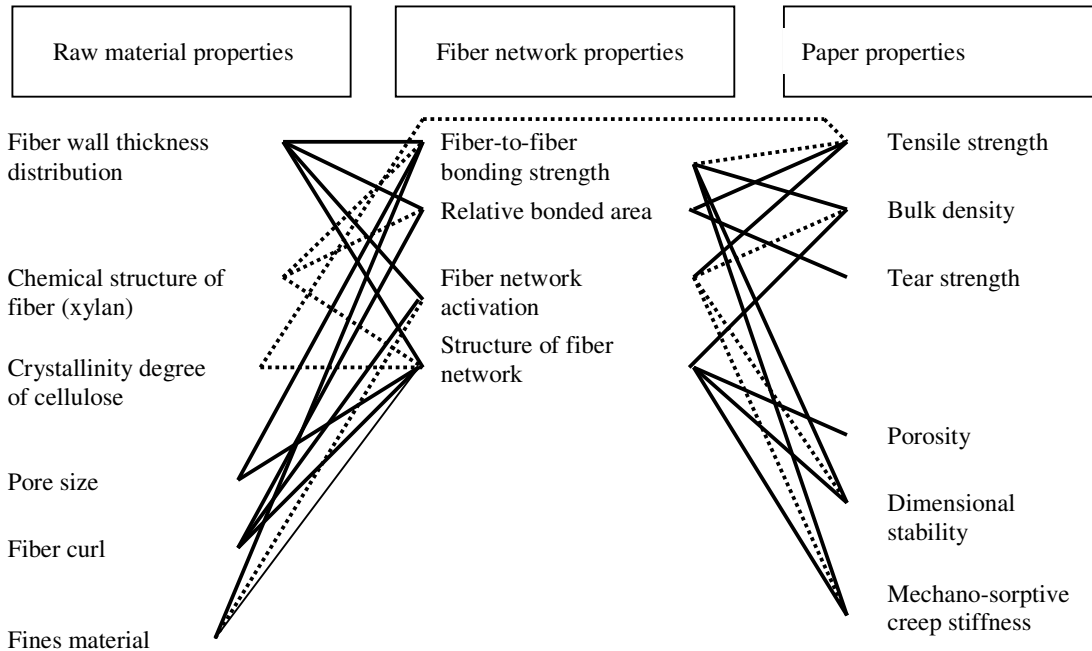


Figure 49. Effect of raw material properties on the papermaking properties of short-fiber pulp (significant influence = solid line, moderate effect = dashed line).

8 CONCLUSIONS

Fiber wall thickness, fiber curl, WRV, and crystallinity of the cellulose were seen as the most important factors connected to network strength properties of eucalypt fiber networks through network activation and fiber-to-fiber bonding. Both, the effect of bonding and activation also significantly affect the structure of forming fiber network through fiber property distributions. Especially fiber wall thickness distribution influenced the packing of eucalypt fibers to a great extent, making fiber wall thickness the most important parameter for bulk density.

Hygroexpansivity of oriented fiber network is connected to fiber dimension distributions. Both, hygroexpansivity and mechano-sorptive creep stiffness were relatively unaffected by activation of isotropic fiber network, and were mainly determined by the bonding potential of the fibers. The effect of activation was seen to influence mechano-sorptive creep stiffness only at high refining levels, where the effects of different morphological parameters were impossible to differentiate due to the used measurement equipment.

The parameters developed during this study strongly indicate that fiber curl, fiber wall thickness and WRV are the most important parameters for eucalypt paper tensile strength and structural parameters; high WRV and low curl and wall thickness enhancing these properties. On the other hand, fiber width and fiber length had smaller impacts on measured properties than rest of the morphological properties. Here are few properties that should be measured in order to obtain a reliable general view of the end-use product.

The properties that should be measured are:

Hardwood chemical pulp properties in the order of importance:

- Fiber wall thickness distribution
- Fiber curl distribution
- Fiber swelling degree (WRV)
- The crystallinity degree of cellulose

The handsheet properties of the hardwood chemical pulp:

- Tensile strength and tensile stiffness
- Dimensional stability with laser measurement

The paper properties that should be measured:

- Formation
- Fiber orientation
- Density

FiberLab® analyzer gives tools to a rapid assessment of fiber properties and produce results that correlate well with paper technical properties. Different weighting procedures were investigated, but no method did prove to be superior. In the end, no single representation of the particle size can be claimed to be more accurate than another. Instead, what is most important is that the measured parameter best relates to the application being developed.

Today's goal in fiber property development is to develop fibers with small perimeter and relatively high fiber wall thickness. In terms of wood properties the aim is met when high basic density is combined with low coarseness. In terms of paper technical properties the low coarseness and high density fiber combines the advantages of high density and high amount of fibers per gram, i.e. high bulk potential at a certain strength level, good formation and optical properties. Low coarseness also enables fibers to have better runnability related

properties such as drainage and tensile strength than high coarseness fibers. Through a proper analysis of fiber analyzer data, an increasing number of observations can be made regarding strength, structural and hygroexpansional properties. In this Thesis, common nominators were found to model these properties by using the distributions of fiber properties.

Overall, through proper modeling of fiber properties, significant savings in laboratory measurement costs can be obtained. The strength, structural and hygroexpansional properties all are functions of inter-fiber bonding and fiber network activation. With the development of modeling parameters which include the most important fiber properties, the need for laboratory experiments can be reduced. One interesting new application field for the developed parameters is the research and breeding programs of eucalypt clones, wherein after maceration process wet fiber dimensions can be easily measured with FiberLab® analyzer and the strength potential and structural properties estimated based on fiber dimensions only.

LIST OF ABBREVIATIONS AND SYMBOLS

A	Fiber cross-sectional area (μm^2)
A(n)	Arithmetic activation coefficient mean value
A(v)	Volume-weighted activation coefficient mean value
B	Shear bond strength per unit bonded area (MPa)
BMC	Bauer McNett Classifier
CCD	Charge-coupled device
CD	Cross direction
(CP/MAS) ^{13}C NMR resonance	Cross-polarization/magic angle spinning nuclear magnetic
CrI	Crystallinity Index (dimensionless)
DP	Degree of polymerization
DSC	Differential scanning calorimetry
FA	Factor analysis
FSP	Fiber saturation point (ml/g)
fw	Fiber width (μm)
fwt	Fiber wall thickness (μm)
FTIR	Fourier transform infra red
Kurt	Kurtosis
L_c	Contour fiber length (mm)
L_{crit}	Critical fiber length (mm)
L_p	Projected fiber length (mm)
LC	Low consistency
m_{Fi}	Mass of fiber (g)
MC	Moisture content (%)
MD	Machine direction
MFA	Micro fibril angle ($^\circ$)
n	Number of cellulose polymers in Equation (6)
P	Perimeter of the fiber cross-section (μm)
P(a)	Arithmetic activation coefficient distribution function
P(v) function	Volume-weighted activation coefficient distribution
PCA	Principal Component Analysis
q Equation (6)	Fraction of the signal intensity from accessible surfaces in
RBA	Relative Bonded Area (%)
RH	Relative humidity (%)
SEM	Scanning Electron Microscope
Skew	Skewness (dimensionless)
T	Tensile index (Nm/g)
v	Volume of fiber (μm^3)
WRV	Water retention value (g/g)
Z	Zero-Span tensile strength (Nm/g)
β	Coefficient of hygroexpansion (%/%)
ρ	Density of fiber wall (g/cm^3)
ρ_{wet}	Wet-pressed density (g/cm^3)
σ_f	Axial fiber strength (MPa)
τ_b	Fiber bond shear strength (MPa)

REFERENCES

- Abson, D. and Gilbert, R. D. (1980).** Observations on water retention values. *Tappi J.* 63(9):146-147.
- Alfthan, J.; Gudmundson, R.; Östlund, S. (2002).** A micromechanical model for mechanosorptive creep in paper, *Journal of Pulp and Paper Sci.* 28(3):98-104.
- Amiri, R.; Wood, J.R.; Karnis, A. (1991).** The apparent density of paper. *International Paper Physics Conference, Kona, Hawaii*, pp.11-18.
- Anagnost, S.E.; Mark, R.E.; Hanna, R.B. (2000).** Utilization of soft-rot cavity orientation for the determination of microfibril angle. Part I. *Wood Fiber Sci.* 32(1):81-87.
- Annergren G; Rydholm S; Vardheim S. (1963).** Influence of raw material and pulping process on the chemical composition and physical properties of paper pulps. *Svensk Papperstidning* 66(6):196-210.
- Anonymous (1991).** Fiber length of pulp paper by automated optical analyzer. *Tappi standard T 271 pm-91*.
- Anonymous (2000).** Determination of fiber length by automated optical analysis. *ISO standard 16065-1*.
- Anonymous (2006).** Kajaani FiberLab®. Käyttäjän käsikirja K02642 V1.0 FI Metso Automation 3/2006.
- Antonsson, S. (2008).** Strategies for improving kraftliner pulp properties, Ph.D. Thesis, Royal University of Technology, Stockholm, Sweden, 43 p.
- Antonsson, S.; Pulkkinen, I.; Fiskari, J.; Lindström, M.E.; Karlström, K. (2010).** The relationship between hygroexpansion, tensile stiffness, and mechano-sorptive creep in bleached hardwood kraft pulp samples. *Appita J.* 63(3):225,231-234.
- Atalla, R.H. and VanderHart, D.L. (1984a).** Native cellulose: A composite of two distinct crystalline forms. *Science* 223(4633):283-285.
- Atalla, R.H. and VanderHart, D.L. (1984b).** Studies of macromolecules in native cellulose using solid-state ¹³C NMR. *Macromolecules* 17:1465-1472.
- Atalla, R.H. and VanderHart, D.L. (1999).** The role of solid state ¹³C NMR spectroscopy in studies of the nature of native celluloses. *Solid State Nuclear Magnetic Resonance* 15(1):1-19.
- Bardage, S.; Donaldson, L.; Tokoh, C.; Daniel, G. (2004).** Ultrastructure of the wood cell wall of unbeaten Norway spruce pulp fibre surfaces. *Nordic Pulp Paper Res. J.* 19(4):448-452.
- Batchelor, W.J. and Westerlind, B.S. (2003).** Measurement of short span stress-strain curves of paper. *Nordic Pulp & Paper Research Journal* 18(1):44-50.
- Bawden, A.D. and Kibblewhite, R.P. (1997).** Effects of multiple drying treatments on kraft fiber walls. *J. Pulp Paper Sci.* 23(7): 340-346.
- Bergander, A. and Salmén, L. (2002).** Cell wall mechanical properties and their effects on the mechanical properties of fibers. *J. of Materials Science* 37(1):151-156.
- Bertran, M.S. and Dale, B.E. (1986).** Determination of cellulose accessibility by differential scanning calorimetry. *J Appl Polym. Sci.* 32(3): 4241-4253.
- Bichard, W. and Scudamore, P. (1988).** An evaluation of the comparative performance of the Kajaani FS-100 and FS-200 fiber length analysers. *Tappi J.* 71(12): 149-155.
- Bonham, V.A. and Barnett, J.R. (2001).** Fiber length and microfibril angle in silver birch. *Holzforchung* 55(2):159-162.
- Boutelje, J. (1968).** Juvenile wood with particular reference to Norway spruce. *Svensk Papperstidning* 71(17): 581-585.
- Brecht, W.; Arrazola, X.; Wunderbaum, F.T.; Mah, Y.M. (1974).** Die Dimensions-Instabilität von Papier aus dem Blickwinkel der Prüftechnik [Dimension Instability of Paper with Perspective of the Testing Technique]. *Wochenbl. Papierfabr* (6):185-192.
- Brändström, J.; Bardage, S.L.; Daniel, G.; Nilsson, D. (2003).** The structural organization of the S-1 cell wall layer of Norway spruce tracheids. *IAWA J.* 24(1):27-40.
- Byrd, V.L. (1972).** Effect of relative humidity changes during creep on handsheet paper properties. *Tappi* 55(2):247-252.
- Carlsson, L.A. and Lindström, T. (2005).** A shear-lag approach to the tensile strength of paper. *Composites Science and Technology* 65(2):183-189.
- Clark, J. d' A. (1985).** *Pulp Technology and Treatment for Paper*, Second Edition, Miller Freeman Publications Inc, San Francisco, pp.452-502.
- Claudio da Silva, E. (1983).** The flexibility of pulp fibers- A structural approach. In: *Proceedings of 1983 TAPPI/CPPA International Paper Physics Conference, Cape Cod*, pp.13-15.
- Corte, H. and Kallmes, O.J. (1962).** Formation and structure of paper, Bolam F. (ed), *Transactions of the 2nd fundamental research symposium, BPBMA, London, UK*, pp. 13 - 46.

- Courchene, C. E.; Peter, G. F.; and Litvay, J. (2006).** Cellulose microfibril angle as a determinant of paper strength and hygroexpansivity in *Pinus taeda* L. *Wood and Fiber Science* 38(1): 112-120.
- Cox, H.L. (1952).** The elasticity and strength of paper and other fibrous materials, *British J. Applied Physics*. 3(3):372.
- Dadswell, H. E. (1958).** Wood structure variations occurring during tree growth and their influence on properties. *J. Inst. Wood Sci.* 1(1): 2-24.
- Dahlman, O.; Jacobs, A.; Sjöberg, J. (2003).** Molecular properties of hemicelluloses located in the surface and inner layers of hardwood and softwood pulps. *Cellulose* 36(10):325-334.
- Dammström, S.; Salmén, L.; Gatenholm, P. (2009).** On the interaction between cellulose and xylan, a biomimetic simulation of the hardwood cell wall. *BioResources*. 4(1):3-14.
- De Ruvo, A.; Fellers, C.; Kolseth, P. (1986).** *Paper Structure and Properties*, (Bristow, J.A.; Kolseth, P. ed.): Marcel Dekker, New York, pp. 267-279.
- Downes, G.; Evans, R.; Wimmer, R.; French, J.; Farrington, A; Lock, P (2003).** Wood, pulp and handsheet relationships in plantation grown *Eucalyptus globulus*. *Appita Journal* 56(3): 221-228.
- Duchesne, I. and Daniel, G. (1999).** The ultrastructure of wood fiber surfaces as shown by a variety of microscopical methods- A review. *Nord. Pulp Paper Res. J.* 14(2):129-139.
- Duchesne, I.; Hult, E.-L.; Molin, U.; Daniel, G.; Iversen, T.; Lennholm, H. (2001).** The influence of hemicellulose on fibril aggregation of kraft pulp fibers as revealed by FE-SEM and CP/MAS ¹³C NMR. *Cellulose* 8(2):103-111.
- Duffy, G.G. and Kibblewhite, R.P. (1989).** A new method of relating wood density, pulp quality, and paper properties. *Appita J.* 42(3): 209–214.
- Earl, W.I. and VanderHart, D.L. (1981).** Observations by High-Resolution Carbon-13 Nuclear Magnetic Resonance of Cellulose I Related to Morphology and Crystal Structure. *Macromolecules* 14(3):570-574.
- Enomae, T. and Lepoutre, P. (1998).** Observation of the swelling behaviour of kraft fibers and sheets in the environmental scanning electron microscope. *Nord. Pulp Paper Res. J.* 13(4):280-284.
- Eriksson, L.; Johansson, E.; Kettaneh-Wold, N.; Wold, S. (1999).** *Introduction to Multi- and Megavariate Data Analysis using Projection Methods (PCA & PLS)*, Umetrics, Umeå, Sweden, 492 p.
- Evans, R.; Newman, R.H.; Roick, U.C.; Suckling, I.D.; Wallis, A.F.A. (1995).** Changes in cellulose crystallinity during kraft pulping. Comparison of infrared, X-ray diffraction and solid-state NMR results. *Holzforchung* 49(8): 498-504.
- Evans, R. (1998).** Rapid scanning of microfibril angle in increment cores by X-ray diffractometry. In microfibril angle in wood: Proceedings of the IAWA/IUFRO International Workshop on the significance of microfibril angle to wood quality, ed. B.G. Butterfield, Westport, New Zealand, Canterbury, NZ, pp. 116-139.
- Evans, R. (1999).** A variance approach to the X-ray diffractometric estimation of microfibril angle in wood. *Appita J.* 52(4):283, 294.
- Evans, R.; Hughes, M.; Menz, D. (1999a).** Microfibril angle variation by scanning X-ray diffractometry. *Appita J.* 52(5):363-367.
- Evans, R.; Kibblewhite, R.P.; Lausberg, M. (1999b).** Relationships between wood and pulp properties of twenty-five 13-year-old radiata pine trees. *Appita J.* 52(2):132-139.
- Evans, R.; Stringer, S.; Kibblewhite, P. (2000).** Variation of microfibril angle, density and fibre orientation in twenty-nine *Eucalyptus nitens* trees. *Appita J.* 53(5): 450-457.
- Kibblewhite, R.P.; Evans, R.; Riddell, M.J.C. (2003).** Kraft handsheet, wood tracheid and chemical property interrelationships for 50 individual radiata pine trees. *Appita J.* 56(3):229-233.
- Fengel, D. and Wegener, G. (1984).** *Wood: Chemistry, Ultrastructure, Reactions*. Walter de Gruyter, New York, 613 p.
- Foelkel, C. (2007).** The eucalyptus fibers and the kraft pulp quality requirements for paper manufacturing. http://www.eucalyptus.com.br/capitulos/ENG03_fibers.pdf. 30.8.2009.
- Forsström, J.; Andreasson, B.; Wågberg, L. (2005).** Influence of pore structure and water retaining ability of fibers on the strength of papers from unbleached kraft fibers. *Nordic Pulp Paper Res. J.* 20(2):176-185.
- French, J.; Conn, A.B.; Batchelor, W.; Parker, I. (2000).** The effect of fibril angle on some handsheet mechanical properties. *Appita J.* 53(3):210-226.
- George, H.O. (1958).** Methods of affecting the dimensional stability of paper. *Tappi J.* 41(1):31–33.
- Giertz, H. W. (1964).** Contribution to the theory of tensile strength. EUCEPA/ European TAPPI Conference on Beating, Proceedings, Venice, Italy, 1964, pp. 39-47.
- Giertz, H. W. and Roedland, H. (1979).** Elongation of segments- bonds in the secondary regime of the load/elongation curve. International Paper Physics Conference, Harrison Hot Springs, British Columbia, Canada, September 17-19, 1979, CPPA/TAPPI, Montreal, Canada, pp. 129-136.

- Glynn, P. and Jones, W.H. (1959).** The fundamentals of curl in paper. *Pulp Pap. Mag. Can.* 60(10):T316-T323.
- Gümüşkaya, E.; Mustafa, U.; Hüseyin, K. (2003).** The effect of various pulping conditions on crystalline structure of cellulose in cotton linters. *Polymer degradation and stability* 81(6):559-564.
- Gorres, J.; Sinclair, A.; Tallentire, A. (1989).** An Interactive Multi-Planar Model of Paper Structure. *Paperi ja Puu* 71(11):54-59.
- Gurnagul, N.; Page, D.H.; Seth, R.S. (1990).** Dry Sheet Properties of Canadian Hardwood Kraft Pulps. *J. Pulp Paper Sci.* 12(1):J36-J41.
- Hartler, N. (1995).** Aspects of curled and microcompressed fibers. *Nord. Pulp Paper Res. J* 10(1): 4-7.
- Haslach, H.W. (2002).** Moisture-accelerated creep. In: *Handbook of Physical Testing of Paper*, Vol. 1, Dekker, New York, pp. 174-231.
- Hatakeyama, T.; Nakamura, K.; Tajima, T.; Hatakeyama, H. (1987).** The effect of beating on the interaction between cellulose and water. *CPPA International Paper Physics Conference*, Quebec, Canada, pp.87-91.
- Hatvani, T.S. G.; Evans, R.; Kibblewhite, R.P.; Parker, I.H. (1999).** Relationships between tracheid and kraft pulp fiber transverse dimensions. *Appita Annual General Conference Proceedings*, 53rd (Vol. 1), pp. 87-94.
- Haraldsson, T.; Fellers, C.; Kolseth, P. (1994).** A Method for Measuring the Creep and Stress-Strain Properties of Paperboard in Compression. *J. Pulp. Pap. Sci.* 20(1): J14-J20.
- Hietanen, S. and Ebeling, K. (1990):** Fundamental aspects of the refining process. *Paperi ja Puu* 72(2): 158-163
- Hiller, C.H. (1964).** Correlation of fibril angle with wall thickness of tracheids in summerwood of slash and loblolly pine. *Tappi J.* 47(2):125-128.
- Hiltunen, E. (2005).** Refining of softwood kraft- fiber length distribution and fiber wall thickness. *Proceedings, PIRA Refining & Mechanical Pulping Conference*, 2nd and 3rd of March, Barcelona, Spain.
- Horton, R.H.; Moran, L.A.; Ochs, R.S; Rawn, D.J.; Scrimgeour, K.G. (2001).** *Principles of Biochemistry*, 3rd Ed, Prentice Hall, 460 p.
- Htun, M. and de Ruvo, A. (1978).** The implication of the fines fraction for the properties of bleached kraft sheet. *Svensk Papperstidn.* 81(16): 507-513.
- Htun, M.; Hanson, T.; Fellers, C. (1987).** Torkningens inverkan på papperets mekaniska egenskaper, STFI-Meddelande D281, Stockholm, Sweden (in Swedish).
- Hult, E.-L.; Larsson, P.T.; Iversen, T. (2000).** A comparative CP/MAS 13C NMR study of cellulose structure in spruce wood and kraft pulp. *Cellulose.* 7(1): 35-55.
- Hult, E.-L.; Larsson, P.T.; Iversen, T. (2001).** Cellulose fibril aggregation- an inherent property of kraft pulps. *Cellulose* 42(8):3309-3314.
- Hult, E.-L.; Iversen, T.; Sugiyama, J. (2003).** Characterization of the supermolecular structure of cellulose in wood pulp fibers. *Cellulose* 10(2):103-110.
- Jang, H.F. and Seth, R.S. (2004).** Determining the mean values for fiber physical properties. *Nord. Pulp Paper Res. J.* 19(3): 372-378.
- Jayme, G. (1944).** Mikro-Quellungsmessungen an Zellstoffen. *Der Papier-Fabrikant/ Wochenblatt für papierfabrikation.*(6):187-194.
- Jentzen, C.A. (1964).** The effect of stress applied during drying on some of the properties of individual pulp fibres. *Tappi* 47(7):412-418.
- Johansson K.; Thuvander F.; Germgård U. (2001).** Single fiber fragmentation: a new measure of fiber strength loss during brown stock washing and oxygen delignification. *Appita J.* 54(3): 276-280.
- Johnson, B.; Kibblewhite, R.B.; Badger, M. (2004).** Kraft Pulp Refining and Reinforcement Potential in Fiber-cement Composites. 58th Appita Annual Conference and Exhibition Incorporating the Pan Pacific Conference. Canberra, Australia, 19-21 April, 2004.
- Jordan, B.D. and Page, D.H. (1983).** The role of fundamental research in papermaking. Ed. J.Brandner, Technical Section, BPBMA, London, UK, pp.745.
- Jordan, B.D. and O'Neill, M.A. (1994).** The birefringence of softwood mechanical pulp fines. *Journal of Pulp Paper Sci.* 20(6): J172-J174.
- Joutsimo, O.; Wathen, R.; Tamminen, T. (2005).** Effects of fiber deformations on pulp sheet properties and fiber strength. *Paperi ja Puu* 87(6): 392-397.
- Kaiser, H.F. (1958).** The Varimax Criterion for Analytic Rotation in Factor Analysis. *Psych.* 23(3):187-200.
- Kajanto, I. (1992).** Analysis of paper cockling with an optical scanner. *Proceedings of 1992 Paper Physics Seminar*, Otaniemi, Finland, pp. 45-47.
- Kajanto, I., and Niskanen, K. (1996).** Optical measurement of dimensional stability. *Progress in*

- Paper Physics - A seminar proceedings, Stockholm, Sweden, 1996, pp. 75-77.
- Kallmes, O.; Corte, H.; Bernier, G. (1963).** The structure of paper V: The bonding states of fibers in randomly formed papers. *Tappi J.* 46(8):493-501.
- Kerekes, R.J. (2005).** Characterizing refining action in PFI mills. *Tappi J.* 4(3): 9-13.
- Kettunen J; Laine JE; Yrjölä I; Virkola N-E. (1982).** Aspects of strength development in fibers produced by different pulping methods. *Paperi ja puu* 64(4):205-211.
- Kibblewhite, R.P. and Brooks, D. (1975).** Factors which influence the wet-web strength of commercial pulps. *Appita J.* 28(4):227-231.
- Kibblewhite, R.P. (1989).** Effects of pulp drying and refining on softwood fiber wall structural organisations. In: Baker's Fundamentals of Papermaking. Transactions of the 9th Fundamental Research Symposium, Cambridge, UK, pp. 121-152.
- Kibblewhite P and Bawden D. (1989).** Structural organizations and papermaking qualities of kraft, soda AQ, neutral sulfite AQ, polysulfide and polysulfide-AQ pulps. *Appita J.* 42(4): 275-281.
- Kibblewhite, R.P. (1993).** Effects of refined softwood/Eucalypt pulp mixtures on paper properties. Transactions of the 10th Fundamental Research Symposium Products of Papermaking, Oxford, September 1993.
- Kibblewhite, R.P.; Evans, R.; Shelbourne, CJA; Riddell, M.J.C. (2003).** Changes in Density and Wood-fiber Properties with Height Position in 15/16-year-old *Eucalyptus nitens* and *E. Fastigata*. 57th Appita Annual General Conference Proceedings, Carlton, Victoria, Australia, pp. 111-118.
- Kim, C.Y.; Page, D.H.; El-Hosseiny, F.; Lancaster, A.P.S. (1975).** The mechanical properties of single wood pulp fibers. III. The effect of drying stress on strength. *Journal of Applied Polymer Sci.* 19(6):1549-1562.
- Kärenlampi, P. (1995).** Effect of Distributions of Fiber Properties on Tensile Strength of Paper: A closed-Form Theory. *Journal of Pulp Paper Sci.* 21(4):J138.
- Laiwins, G.V and Scallan, A.M. (1996).** The influence of drying and beating on the swelling of fines. *Journal of Pulp Paper Sci.* 22(5): 178-182.
- Larsson, P.T.; Westermark, U.; Iversen, T. (1995).** Determination of the cellulose Ia allomorph content in a tunicate cellulose by CP/MAS ¹³C-NMR spectroscopy. *Carbohydrate Res.* 278(2):339-343.
- Larsson, P.T.; Wickholm, K.; Iversen, T. (1997).** A CP/MAS ¹³C NMR investigation of molecular ordering in celluloses. *Carbohydrate Res.* 302(1-2): 19-25.
- Larsson, P.T. and Westlund, P-O. (2005).** Line shapes in CP/MAS ¹³C NMR spectra of cellulose I. *Spectrochimica Acta Part A* 62: 539-546.
- Law, A.M. and Kelton, W.D. (2000).** Simulation modelling and analysis, 3rd edition, McGraw-Hill, Inc. Boston, MA, 338 p.
- Lichtegger, H.; Reiterer, A.; Tchegg, S.E.; Fratzl, P. (1999).** Variation of cellulose microfibril angles in softwoods and hardwoods- A possible strategy of mechanical optimization. *J. Struct. Biol.* 128(3): 257-269.
- Lichtegger, H.; Reiterer, A.; Tchegg, S.E.; Fratzl, P. (2000).** Microfibril angle in the wood cell wall: mechanical optimization through structural variation? COST Action E20, Proceedings of Workshop Fiber Wall & Microfibril Angle, May 11-13, 2000, Athens, Greece, pp.1-4.
- Lif, J.O.; Fellers, C.; Söremark, C.; Sjodahl, M. (1995).** Characterizing the in-plane hygroexpansivity of paper by electronic speckle microscope. *J. Pulp Paper Sci.* 21(9):J302-J309.
- Lindström, T. (1980).** Der Einflu. chemischer Faktoren auf Faserquellung und Papierfestigkeit. *Das Papier* 34(12):561-568.
- Lindström, T. and Carlsson, G. (1982).** The effect of carboxyl groups and their ionic form during drying on the hornification of cellulose fibers. *Svensk Papperstidning* 85(15):R146-R151.
- Lindström, T. (1986).** The concept and measurement of fiber swelling. In: Bristow, J.A.; Kolseth, P. Paper. Structure and Properties. Marcel Decker Inc., New York, pp.75-97.
- Lennholm, H.; Larsson, T.; Iversen, T. (1994).** Determination of cellulose I α and I β in lignocellulosic materials. *Carbohydr. Res.* 261(1): 119-131.
- Lütiä, T; Maunu, S-L.; Hortling, B. (2001).** Solid state NMR studies on inhomogeneous structure of fiber wall in kraft pulp. *Holzforschung* 55(5):503-510.
- Lütiä, T.; Maunu, S-L.; Hortling, B.; Tamminen, T.; Pekkala, O.; Varhimo, A. (2003).** Cellulose crystallinity and ordering of hemicelluloses in pine and birch pulps as revealed by solid-state NMR spectroscopic methods. *Cellulose* 10(4): 307-316.
- Lima, J.T.; Breese, M.C.; Cahalan, C.M. (2004).** Variation in microfibril angle in Eucalyptus clones. *Holzforschung* 58(2):160-166.
- Lobben, T.H. (1975).** The tensile stiffness of paper. Part 1. A model based on activation. *Norsk Skogindustri* 29(12):311-315.

- Lu, J.Z.; Monlezun, C.J.; Wu, Q.; Cao, Q.V. (2007).** Fitting Weibull and Lognormal distributions to medium-density fiberboard fiber and wood particle length. *Wood and Fiber Sci.* 39(1):82-94.
- Luukkonen, M.; Suutari, H.; Paavilainen, L. (1990).** Utilization of pulp drainage and fiber length measurements. *Appita J.* 43(2): 213-216.
- Lyne, A.L. (1994).** The hygroexpansivity of unfilled and filled laboratory made fine papers. Ph.D. Thesis, Stockholm, Sweden, Royal Institute of Technology.
- Maloney, T.C. and Paulapuro, H. (1998).** Hydration and swelling of pulp fibers measured with differential scanning calorimetry. *Nordic Pulp Paper Res. J.* 13(11):31-36.
- Maloney, T.C.; Laine, J.E.; Paulapuro, H. (1999).** Comments on the measurement of cell wall water. *Tappi J.* 82(9):125-127.
- Mark, R.E. and Gillis, P.P. (1983).** Structure and structural anisotropy. Pages 283 and 371 in R.E. Mark, K. Murakami, eds. *Handbook of physical and mechanical testing of paper and paperboard.* Marcel Dekker, Inc., New York, NY.
- Mark, R.E. (2002).** Mechanical properties of fibers. Chapter 14 in *Handbook of Physical Testing of Paper*, 2nd Ed., Marcel Dekker, New York, NY, USA, Vol.1, pp.727-869.
- McLeod, J.M.; Cyr, M.; Embley, D.; Savage, P. (1987).** Where strength is lost in kraft pulping of softwoods? *Journal of Pulp Paper Sci.* 13(3):J87-J92.
- McLeod, J.M. (2005).** Making and losing pulp strength in bleached kraft mills. *International Pulp Bleaching Conference*, June 14-16, Stockholm, Sweden, pp. 31-46.
- McMillin, C. W. (1973).** Fibril angle of loblolly pine wood as related to specific gravity, growth rate, and distance from pith, *Wood Sci. Technol.* 7(4):251-255.
- McGraw, R. A. (1997).** The influence of tree age, position in tree, and cultural practices on wood specific gravity, fiber length, and microfibril angle, In: *Wood quality factors in loblolly pine*, Tappi Press, Atlanta, GA. 96 p.
- Milton, J.S. and Arnold, J.C. (1995).** *Introduction to probability and statistics*, McGraw-Hill, New York, 811 p.
- Mohlin, U.-B. and Alfredsson, C. (1990).** Fiber deformation and its implications in pulp characterization. *Nordic Pulp Paper Res. J.* 5(4):172-179.
- Mohlin, U.-B. (1991).** Low consistency beating - laboratory evaluation contra industrial experience. *Current and future technologies of refining*, Conference Proceedings. 10-12 December 1991. Pira, Leatherhead, UK. Volume 1, Paper 01, 14 pages. In *Current and Future Technologies of Refining*. PIRA, Leatherhead, UK, pp.1-14.
- Mohlin, U.B.; Dahlbom, J.; Hornatowska, J. (1996).** Fiber deformation and sheet strength. *Tappi J.* 79(6): 105-111.
- Mohlin, U.-B., Molin, U., Waubert de Puiseau, M. (2003).** Some aspects of using zero-span tensile index as a measure of fiber strength, *International Paper Physics Conference*, 7 -11 September, Victoria, BC, Canada, pp. 107-113.
- Mohlin, U.-B. (2005).** Which are the important fiber properties. *Proceedings*. In *SPCI International Conference*, Stockholm, Sweden, pp.1-5.
- Mohlin, U.-B. and Hornatowska, J. (2006).** Fiber and sheet properties of Acacia and Eucalyptus. *Appita J.* 59(3):225-230.
- Moss, P.A. and Pere, J. (2006).** Microscopical study on the effects of partial removal of xylan on the swelling properties of birch kraft pulp fibers. *Nordic Pulp Paper Res. J.* 21(1):8-12.
- Muneri, A. and Balodis, V. (1997).** Determining fiber coarseness of small wood samples from acacia mearnsii and Eucalyptus grandis by Kajaani FS 200 fiber analyser. *Appita J.* 50(5): 405-408.
- Mörseburg, K.; Hultholm, T.; Lundin, T.; Lönnberg, B. (1999).** Experiences with the Kajaani FiberLab Analyzer in determining morphological characteristics of mechanical and chemical pulps. 5th PTS-Symposium, April 14-15, Dresden, Germany, pp.13/1-13/11.
- Nanko, H.; Ohsawa, J.; Okagawa, A. (1989).** How to see interfiber bonding in paper sheets. *J. Pulp Pap. Sci.* 15(1): 17-19.
- Nanko, H. and Tada, Y. (1995).** Mechanisms of hygroexpansion of paper. *International Paper Physics Conference*, September 11-14, Niagara-on-the-Lake, Ontario, US, pp.159-171.
- Nanko, H. and Wu, J. (1995).** Mechanisms of paper shrinkage during drying. *Proceedings: 1995 International Paper Physics Conference*, TAPPI, Atlanta, GA, US, pp.159-171.
- Nanri, Y. and Uesaka, T. (1993).** Dimensional stability of mechanical pulps: drying shrinkage and hygroexpansivity. *Tappi J.* 76(6):62-66.
- Nazhad, M.M.; Karnchanapoo, W.; Palokangas, A. (2003).** Some effects of fiber properties on formation and strength of paper. *Appita J.* 56(1): 61-65.
- Neagu, R.C.; Gamstedt, E.K.; Lindström, M. (2006).** Characterization methods for elastic properties of wood fibers from mats for composite materials. *Wood and Fiber Science.* 38(1):95-111.

Nelson, M.L. and O'Connor, R.T. (1964). Relation of certain infrared bands to cellulose crystallinity and crystal lattice type. Part I. Spectra of lattice types I, II, III and of amorphous cellulose. Part II. A new infrared ratio for estimation of crystallinity of cellulose I and II. *J. Appl. Pol. Sci.* 8(3):1311-1341.

Newman, R.H. and Hemmingson, J.A. (1990). Determination of the degree of cellulose crystallinity in wood by carbon-13 nuclear magnetic resonance spectroscopy. *Holzforschung* 44(5):351-355.

Newman, R.H.; Hemmingson, J.A.; Suckling, I.D. (1993). Carbon-13 Nuclear Magnetic Resonance Studies of Kraft Pulping. *Holzforschung* 47(3): 234-238.

Newman, R.H. (1994). Crystalline forms in softwoods and hardwoods. *J. Wood Chem. Science* 14(3):451-466.

Newman, R.G. and Hemmingson, J.A. (1994). Carbon-13 NMR distinction between categories of molecular order and disorder in cellulose. *Cellulose* 2(2):95-110.

Nordström, A.; Gudmundson, P.; Carlson, L.A. (1998). Influence of Sheet Dimensions on Curl of Paper. *Journal of Pulp Paper Sci.* 24(1): 18-25.

Olson, J.A.; Robertson, A.G.; Finnigan, T.D.; Turner, R.R.H. (1995). An analyzer for fiber shape and length. *Journal of Pulp Paper Sci.* 21(11): J367-J373.

Paavilainen, L. (2000). Quality-competitiveness of Asian short-fiber raw materials in different paper grades. *Paperi ja Puu* 82(3):156-160.

Paavilainen, L. (1989). Effect of sulphate cooking parameters on the papermaking potential of pulp fibers. *Paperi Puu* 72(4): 356-363.

Paavilainen, L. (1991). Influence of morphological properties of wood fibers on sulphate pulp fiber and paper properties. *Proceedings of International Paper Physics Conference, Kona, Hawaii*, p.383-395.

Paavilainen, L. (1993). Importance of cross-dimensional fiber properties and coarseness for the characterization of softwood sulphate pulp. *Paperi ja Puu* 75(5): 343-351.

Paavilainen, L. (1994b). Bonding potential of softwood sulphate pulp fibers. *Paperi ja Puu* 76(3):162-173.

Paavilainen, L. (1994a). Influence of fiber morphology and processing on the papermaking potential of softwood sulfate pulp fibers. *TAPPI Pulping Conference, San Diego, CA, USA, Nov. 6-10, 1994*, pp.857-868.

Paakkari, T. and Serimaa, R. (1984). A study of the structure of wood cells by X-ray diffraction. *Wood Sci. Technol.* 18(2): 79-85.

Page, D.H. (1969). A theory for the tensile strength of paper. *Tappi J.* 52(4): 674-681.

Page, D.H.; Seth, R.S.; De Grace, J.H. (1979). The elastic modulus of paper I. The controlling mechanisms. *Tappi J.* 62(9): 99-102.

Page D.H. and El-Hosseiny, F. (1983). The mechanical properties of single wood pulp fibers. Part VI. Fibril angle and the shape of the stress-strain curve. *Pulp Pap. Can.* 84(9)TR99-00.

Page, D.H.; Seth, R.S. Jordan, B.D., Barbe, M.C. (1985). Curl, crimps, kinks and microcompressions in pulp fibers- their origin, measurements and significance. *Paper making raw materials: their interactions with the production process and their effect on paper properties. Transactions of the 8th Fundamental Research Symposium held in Oxford September 1985*, ed. V. Punton. Vol. 1, Mechanical Engineering Publications Limited, London, pp. 183-227.

Page, D.H. (1989). The beating of chemical pulps- The action and the effects. *Transactions of the ninth fundamental research symposium, Cambridge, UK*, pp.1-37.

Pandey, M.D. (2001). Extreme quantile estimation using order statistics with minimum cross-entropy principle. *J. Prob. Eng. Mech.* 16(1): 31-42.

Panek, J.; Fellers, C.; Haraldsson, T. (2004). Principles of evaluation for the creep of paperboard in constant and cyclic humidity. *Nord. Pul Pap. Res. J.* 19(2): 155-163.

Panek, J.; Fellers, C.; Haraldson, T.; Mohlin, U.B. (2005). Effect of fiber shape and fiber distortions on creep properties of kraft paper in constant and cyclic humidity. *Advances in Paper Science and Technology*, vol. 2, pp. 777-796, The Pulp and Paper Fundamental Research Society, Bury.

Park, S.; Venditti, R.; Jameel, H.; Pawlak, J. (2006). Changes in pore size distribution during the drying of cellulose fibers as measured by differential scanning calorimetry. *Carbohydrate Polymers* 66(1): 97-103.

Park, S.; Johnson, D.K.; Ishizawa, C.I.; Parilla, P.A.; Davis, M.F. (2009). Measuring the crystallinity index of cellulose by solid state ¹³C nuclear magnetic resonance. *Cellulose* 16(4):641-647.

Perkins, R.W. (2002). Models for describing the elastic, viscoelastic, and inelastic mechanical behaviour of paper and board. In: *Handbook of Physical Testing of Paper*, Vol. 1, Dekker, New York, pp. 1-75.

Peura, M. (2007). Studies on the cell wall structure and on the mechanical properties of Norway spruce. Ph.D. Thesis, University of Helsinki, Finland.

- Piirainen, R. (1985).** Optical method provides quick and accurate analysis of fiber length. *Pulp and Paper* 59(11): 69-74.
- Pikulik, I.I. (1997).** Wet-web properties and their effect on picking and machine runnability. *Pulp and Paper Canada* 98(12): 161-165.
- Pikulik, I.I.; Sparker, D.G.; Poirier, N.A.; Crotofino, R.H. (1995).** Dewatering and consolidation of wet webs. 81st PAPTAC Annual Meeting, Montreal, Canada, January 1995. Preprints A, Canadian Pulp and Paper Association, Montreal, Canada, pp. A123-A136.
- Preston, R. D. (1934).** The organisation of the walls of conifer tracheids. *Phil. Trans. Roy. Soc.* B224:131-174.
- Pulkkinen, I.; Ala-Kaila, K.; Aittamaa, J. (2006).** Characterization of wood fibers using fiber property distributions. *Chemical Engineering and Processing* 45(7): 546-554.
- Pulkkinen, I.; Fiskari, J.; Aittamaa, J. (2007).** The effect of refining on fiber transverse dimension distributions of eucalyptus pulp species. *O Papel* 68(5):58-66.
- Pulkkinen, I.; Fiskari, J.; Alopaeus, V. (2008a).** Observation of the swelling behaviour of fractionated kraft handsheets in the scanning electron microscope, *Progress in Paper Physics Seminar-A seminar proceedings*, Helsinki, Finland, pp.251-254.
- Pulkkinen, I.; Fiskari, J.; Alopaeus, V. (2008b).** The use of fiber wall thickness data to predict handsheet properties of eucalypt pulp fibers. *O Papel* 69(10): 71-85.
- Pulkkinen, I.; Fiskari, J.; Alopaeus, V. (2009a).** The effect of hardwood fiber morphology on the hygroexpansivity of paper. *BioResources* 4(1):126-141.
- Pulkkinen, I.; Fiskari, J.; Alopaeus, V. (2009b).** The effect of sample size and shape on the hygroexpansion coefficient - A study made with advanced methods for hygroexpansion measurement. *Tappsa J. March*: 26-33.
- Pulkkinen, I.; Fiskari, J.; Alopaeus, V. (2009c).** CPMA^S ¹³C NMR Analysis and Differential Scanning Calorimetry of Fully Bleached Eucalypt Pulp Samples: Links to hand sheet hygroexpansivity and strength properties. *J. of Applied Sciences* 9(22):1-8.
- Pulkkinen, I.; Fiskari, J.; Alopaeus, V. (2010).** New model for tensile strength and density of eucalyptus hand sheets - An activation parameter based on fiber distribution characteristics. *Holzforschung*. 64(2):201-209.
- Randolph, A.D. and Larson, M.A. (1988).** *Theory of particulate processes*, Academic Press, San Diego, 1988, 369 p.
- Reme, P.A.; Johnsen, P.O.; Helle, T. (2002).** Assessment of Fiber Transverse Dimensions using SEM and Image Analysis. *Journal Pulp Paper Sci.* 28(4):122-128.
- Retulainen, E. (1997).** *The Role of Fiber Bonding in Paper Properties*, Ph.D. Thesis, Helsinki University of Technology, Finland.
- Retulainen, E.; Niskanen, K.; Nilsen, N. (1998)** Fibers and bonds. In: Niskanen, K. (ed.), *Paper Physics, Papermaking Science and Technology Book 16*, Fapet Oy, Jyväskylä, pp. 55-87.
- Richardson, J.D.; Riddell, M.J.C.; Burrell, P. (2003).** Experience with the FiberLab® V3.0 analyser for measuring fiber cross-section dimensions. *Proceedings of 57th Appita Annual Conference and Exhibition*, Melbourne, Australia, 5-7 May, 2003, pp.315-322.
- Rowland, S.P. and Roberts, E.J. (1972).** Disposition of D-glucopyranosyl units on the surfaces of crystalline elementary fibrils of cotton cellulose. *J. Polym. Science. Part A-1: Polymer Chemistry* 10(3): 867-879.
- Ruel, K.; Chevalier, V.; Guillemain, F.; Berrio-Sierra, J.; Joseleau, J-P. (2006).** The wood cell wall at the ultrastructure scale- Formation and topochemical organization. *Maderas, ciencia y tecnología* 8(2):107-116.
- Salmén, L.; Fellers, C.; and Htun, M. (1985).** The in-plane and out-of-plane hygroexpansional properties of paper. In: *Papermaking Raw Materials, Vol 2.*, V. Punton (ed.), Mechanical Engineering Pub., London, UK, pp. 511-527.
- Salmén, L.; Fellers, C.; Htun, M. (1987).** The development and release of dried-in stresses in paper. *Nordic Pulp Paper Res. J.* 2(2):44-48.
- Salmén, L.; Boman, R.; Fellers, C.; and Htun, M. (1987).** The implications of fiber and sheet structure for the hygroexpansivity of paper. *Nord. Pulp Paper Res. J.* 2(4):127-131.
- Salmén, L. (1993).** Responses of paper properties to changes in moisture content and temperature. in: *Products of papermaking, Vol. 1.* C.F. Baker, ed. Pira Int., Cambridge, UK, pp.369-430.
- Salmén, L. and Berthold, J. (1997).** The swelling ability of fibers. *Fundamentals of Papermaking Materials- 11th Fundamental Research Symposium*, Cambridge, UK, 21-26 Sept. 1997, pp.683-701.
- Salmén, L. (2004).** Micromechanical understanding of the cell-wall structure. *C.R. Biologies* 327(9-10):873-880.

Salmén, L. and Burgert, I. (2009). Cell wall features with regard to mechanical performance. A review. *Holzforschung* 63(2):121-129.

Santos, A.; Anjos, O.; Simões, R. (2006). Papermaking potential of *Acacia dealbata* and *Acacia melamoxylon*. *Appita J.* 59(1):58-64.

Santos, A.; Amaral, M.E.; Vaz, A.; Anjos, O.; Simões, R. (2008). Effect of *Eucalyptus globulus* wood density on papermaking potential. *Tappi J.* 7(5):25-32.

Scallan, A.M. and Carles, J.E. (1972). The correlation of the water retention value with the fiber saturation point. *Svensk Papperstidning.* 75(17):699-703.

Scallan, A.M. and Tigerström, A.C. (1992): Swelling and elasticity of the cell walls of pulp fibers. *J. Pulp Paper Sci.* 18(5) 188-193

Schönberg, C.; Oksanen, T.; Suurnäkki, A.; Kettunen, H.; Buchert, J. (2001). The importance of xylan for the strength properties of spruce kraft pulp fibers. *Holzforschung.* 55(6):639-644.

Segal, L.; Creely, J.J.; Martin Jr, A.E.; Conrad, C.M. (1959). An empirical method of estimating the degree of crystallinity of native cellulose using the X-ray diffractometer. *Textile Res. J.* 29:786-794.

Seth, R.S.; Barbe, M.; Williams, J.A.; Page, D.H. (1982). The strength of wet webs: A new approach. *Tappi J.* 65(3): 135-138.

Seth, R.S.; Page, D.; Barbe, M.C.; Jordan, B.D. (1984). The mechanism of the strength and extensibility of wet webs, *Svensk Papperstidn.* 87(6):R36-R43.

Seth, R.S., Jang, H.F., Chan, B.K., Wu, C.B. (1997). Transverse Dimensions of Wood Pulp Fibers and Their Implications for End Use,” *Fundamentals of Papermaking Materials, Transactions of the Fundamental Research Symposium, 11 th*, pp. 473-503.

Seth, R.S. (1990). Fiber Quality Factors in Papermaking- I. The importance of Fiber Length and Strength. In: *Proceedings Materials Research Society Symposium, San Francisco, CA April 18-20, Vol. 197*, pp 125-141.

Seth, R.S. (1990). Fiber Quality Factors in Papermaking- II. The importance of Fiber Coarseness. In: *Proceedings Materials Research Society Symposium, San Francisco, CA April 18-20, Vol. 197*, p 143-146.

Seth, R.S. (2001): The difference between never-dried and dried chemical pulps. *TAPPI Pulping Conference, Seattle, WA , United States, Nov. 4- 7*, pp.296-311.

Seth, R.S. and Jang, H.F. (2004). Determining the mean values for fiber physical properties. *Nordic Pulp Paper Res. J.* 19(3): 372-378.

Shallhorn, P. and Gurnagul, N. (2008). A semi-empirical model of the tensile energy absorption of sack kraft paper, *Progress in Paper Physics Seminar, June 2-5, Otaniemi, Finland*, pp.177-180.

Sisson, W.A. (1943). Cellulose fibers, X-ray examination, In: E. Ott, editor, *Cellulose and cellulose derivatives, Chapter III-A (b)*, pages 256-266. Interscience Publisher, New York.

Sjöberg, J.; Kleen, M.; Dahlman, O.; Agnemo, R.; Sundvall, H. (2004). Fiber surface composition and its relations to papermaking properties of soda-anthraquinone and kraft pulps. *Nord. Pulp. Pap. Res. J.* 19(3):392-396.

Somwang, K.; Enomae, T.; Isogai, A.; Onabe, F. (2002). Changes in crystallinity and re-swelling capability of pulp fibers by recycling treatment. *Tappi J.* 56(6):863-869.

Spiegelberg, H.L. (1966). The effect of hemicelluloses on the mechanical properties of individual pulp fibers. *Tappi* 49(9):388-396.

Stone, J.E. and Scallan, A.M. (1965a). Effect of component removal upon the porous structure of the cell wall of wood, *J. Polym. Sci. Part C.* 11:13-25.

Stone, J.E. and Scallan, A.M. (1965b). Influence of drying on the pore structure of the cell wall. *Consolidation of the Paper Web, Transactions of the Symposium (ed. F. Bolam), September 1965, Cambridge, UK, Vol. 1*, pp. 145-166.

Stone, J.E. and Scallan, A.M. (1968). A structural model for the cell wall of water-swollen wood pulp fibres based on their accessibility to macromolecules. *Cellul. Chem. Technol.* 2(3):343-358.

Stuart, S. and Evans, R. (1994). X-ray diffraction estimation of the microfibril angle variation in eucalyptus wood. *Appita J.* 48(3):197-200.

Taiz, L. and Zeiger, E. (2002). *Plant Physiology.* Sinauer Associates, Inc. Publisher, Sunderland, USA, 690 p.

Thygesen, A.; Oddershede, J.; Lilholt, H.; Thomsen, A.B.; Ståhl, K. (2005). On the determination of crystallinity and cellulose content in plant fibers. *Cellulose* 12(14):563-576.

Trepanier, R. (1998). Automatic fiber length and shape measurement by image analysis. *Tappi J.* 81(6):152-154.

Turunen, M.; Le Ny, C.; Tienvieri, T.; Niinimäki, J. (2005). Comparison of fiber morphology analysers. *Appita J.* 58(1):28-32.

- Uesaka, T.; Kodaka, I.; Okushima, S., Fukuchi, R. (1989).** History-dependent dimensional stability of paper. *Rheol. Acta* 28(3):238-245.
- Uesaka, T.; Moss, C.; Nanri, Y. (1992).** The characterization of hygroexpansivity of paper. *Journal of Pulp Paper Sci.* 18(1):J11-J16.
- Uesaka, T. (1994).** General formula for the hygroexpansion of paper. *J. Materials Sci.* 29:2373-2377.
- Uesaka, T., and Qi, D. (1994b).** Hygroexpansivity of paper - Effects of fiber-to-fiber Bonding. *J. Pulp Paper Sci.* 20(6):J175-J179.
- Uesaka, T., and Moss, C. (1997).** Effects of fiber morphology on hygroexpansivity of paper- A micromechanics approach, In: *Fundamentals of Papermaking Materials, Transactions of the Fundamental Research Symposium, 11th, Cambridge, UK, Sept. 1997, Vol. 1, pp. 663-679.*
- Uesaka, T. (2002).** Dimensional stability and environmental effects on paper Properties. In: *Handbook of Physical Testing of Paper, Vol. 1, Dekker, New York, pp. 115-171.*
- Urquhart, A.R. and Eckersall, N. (1930).** The moisture relations of cotton. VII: A study of hysteresis. *J. Textile Inst.* 21(10):T499-T510.
- Urquhart, A.R. (1958).** The reactivity of cellulose. *Textile Res. J.* 28(2):159-169.
- Vainio, A. (2007).** Interfiber Bonding and Fiber Segment Activation in Paper- Observations on the Phenomena and Their Influence on Paper Strength Properties, Ph.D. Thesis, Helsinki University of Technology, Finland.
- Vainio, A.; Sirviö, M.; Paulapuro, H. (2007a).** Observation on the microfibril angle of Finnish papermaking fibers, *Proceedings. 2007 International Paper Physics Conference, Appita, May 6-10, 2007, Gold Coast, Australia, pp. 397-403.*
- Vainio, A.; Kangas, J.; Paulapuro, H. (2007b).** The role of TMP fines in interfiber bonding and fiber-segment activation. *Journal of Pulp and Paper Sci.* 33(1): 29-34.
- Van Den Akker, J.A.; Lathrop, A.L.; Voelker, M.H.; Dearth, L.R. (1958).** Importance of fiber strength to sheet strength. *Tappi J.* 41(8): 416-425.
- Vianna Doria, B.D.; Claudio-da Silva, E.; Manfred, V. (1991).** Influence of eucalyptus fiber characteristics on paper properties. *Proceedings of International Paper Physics Conference, Kona, Hawaii, pp.185-196.*
- Wakelin, R.F.; Blackwell, B.G.; Corson, S.R. (1994).** The influence of equipment and process variables on mechanical pulp fractionation in pressures screens. *Proc. 48th Appita Annual Conference, Melbourne, Australia, pp.611-615.*
- Wan, J.; Wang, Y.; Xiao, Q. (2010).** Effects of hemicellulose removal on cellulose fiber structure and recycling characteristics of eucalyptus pulp. *Bioresource Technology* 101(12):4577-4583.
- Wang, X. (2006).** Improving the papermaking properties of kraft pulp by controlling hornification and internal fibrillation. Ph.D. Thesis, Helsinki University of Technology, Finland.
- Wangaard, F.F. (1962).** Contributions of hardwood fibers on the properties of kraft pulps. *Tappi J.* 45(7): 548-556.
- Wathén, R. (2006).** Studies on fiber strength and its effect on paper properties. Ph.D. Thesis, Helsinki, Finland.
- Watson, A. J. and Dadswell, H. E. (1964).** Influence of fiber morphology on paper properties. 4. Micellar spiral angle. *Appita J.* 17(6):151-157.
- Weise, U. (1997).** Characterization and Mechanisms of Changes in Wood Pulp Fibers Caused by Water Removal, Ph.D. Thesis, Helsinki University of Technology, Finland.
- Westerlind, B.; Amesson, P.; Sandström, P.; Gradin, P. (2007).** Engineering approach to Page and Shear-lag theory for predicting tensile strength of paper. 61st Appita Annual Conference and Exhibition: *Proceedings, Gold Coast, Australia, May 6-9th, pp.123-131.*
- Wickholm, K.; Larsson, P.T.; Iversen, T. (1998).** Assignment of non-crystalline forms in cellulose I by CP/MAS ¹³C NMR spectroscopy. *Carbohydrate Res.* 312(3):123-129.
- Williams, M.F. (1994).** Matching wood fiber characteristics to pulp and paper process and products, *Tappi J.* 77(3):221-227.
- Wimmer, R.; Downes, G.M.; Evans, R.; Rasmussen, G.; French, J. (2002).** Direct effects of wood characteristics on pulp and handsheet properties of *Eucalyptus globulus*. *Holzforschung* 56(3): 244-252.
- Wink, W.A. (1961).** The effect of relative humidity and temperature on paper properties. *Tappi J.* 44(6):171A-180A.
- Wormald, P.; Wickholm, K.; Larson, P.; Iversen, T. (1996).** Conversion between ordered and disordered cellulose. Effects of mechanical treatment followed by cyclic wetting and drying. *Cellulose* 3(1):141-152.
- Yamauchi, T. and Murakami, K. (1991).** Differential scanning calorimetry as an aid for investigating the wet state of pulp. *J. Pulp Paper Sci.* 17(6): J223-J226.

Åkerholm, M. (2003). Ultrastructural aspects of pulp fibers as studied by dynamic FT-IR spectroscopy. Doctoral Thesis, Royal Institute of Technology, Department of fiber and Polymer Technology, Stockholm, Sweden.